IMAGING CALCINEURIN DYNAMICS IN YEAST: DEVELOPMENT AND APPLICATION OF A NOVEL PROBE OF CALCINEURIN ACTIVITY

by

Tovah Honor Aronin

A dissertation submitted to Johns Hopkins University in conformity with the requirements for the degree of Doctor of Philosophy

Baltimore, Maryland

January, 2016

ABSTRACT

Calcineurin (Cn) is a highly conserved calcium-responsive phosphatase that is crucial for many cellular pathways, especially those that control the response to outside stimuli. Misregulation of Cn has been associated with pathological conditions including cardiac hypertrophy, Down Syndrome, and Alzheimer's Disease. Previous studies of Cn and its downstream effectors have largely relied on assays that lack single-cell or temporal resolution. Herein, I describe my efforts to develop a fluorescent probe based on a truncated version of the Cn-responsive transcription factor Crz1 and use it to investigate Cn-Crz1 activation dynamics in single cells in real time. Crz1 activates its own transcription as well as transcription of Cn regulators, thus participating in multiple feedback loops. The truncated version of Crz1 used for the probe does not bind DNA and is therefore inert with regards to feedback. Using this probe, I reveal a new phenomenon of Cn activity in the absence of stimulation named "flickering." Flickering is a low level of Cn activation that stimulates brief probe translocation in steady-state conditions. I also use the probe to investigate feedback loops involved in Cn regulation. The vacuolar calcium transporters Pmc1 and Vcx1 are both necessary to maintain cytosolic calcium concentration and prevent hyperactivation of Cn in both stimulating and non-stimulating conditions. The putative Cn chaperone Rcn1p is needed for normal Cn activity both before and after signaling. My studies present a new way to measure Cn activation which can be applied to clinical and basic study of this crucial signaling factor.

Advisor and Primary Reader: Kyle W. Cunningham, Dept. of Biology, Johns Hopkins University, Baltimore, MD

Secondary Reader: Haiqing Zhao, Dept. of Biology, Johns Hopkins University, Baltimore, MD

DEDICATION

To my parents for their endless support.

To my husband for his constant encouragement.

To my advisor for his infectious enthusiasm.

TABLE OF CONTENTS

INDEX OF TABLES

INDEX OF FIGURES

CHAPTER ONE: INTRODUCTION

Calcium signaling and calcineurin regulation

CALCIUM SIGNALING

In order to survive, cells must be able to respond to their environment. Living cells do not exist in a vacuum, and external conditions dictate much of what goes on inside a cell. Cells need to sense the availability of nutrients, the presence of neighbors, stimulation by growth factors, and many other environmental cues. These extracellular stimuli need a way in which to signal inside the cell in order to affect cell function as a whole. Furthermore, extracellular stimuli need to be coupled to intracellular responses such as metabolic changes or gene transcription. This is accomplished by the use of second messengers, small molecules that activate signaling cascades. One of the most important of these is calcium (Ca^{2+}).

Concentration and localization of Ca^{2+} are the most tightly regulated of any ion (Clapham, 2007). Ca^{2+} is essential to many cellular functions. It is used as a second messenger by many different cell types in organisms from fungi to mammals to regulate functions from cell division to cell death (Karlstad et al., 2012).

Fungi use Ca^{2+} signals to respond to outside stimuli such as mating pheromones, endoplasmic reticulum (ER) stress induced by anti-fungal drugs, and changes in environmental conditions including pH level and nutrient availability (Iida et al., 1990; Bonilla et al., 2002; Tisi et al., 2002; Heath et al., 2004). In plants, Ca^{2+} regulates the activity of ion transporters; the response to stresses from cold, excess salt, and insufficient water; the response to light; and the circadian rhythm (White and Broadley, 2003; Drerup et al., 2013).

In mammals, Ca^{2+} signaling controls a vast array of processes. In neuronal synaptic spines, changes in cytosolic free Ca^{2+} concentration ($[Ca^{2+}]_{cyt}$) control the formation or erasure of temporary memories by means of reversible, Ca^{2+}-dependent changes in protein phosphorylation, cytoskeleton remodeling, and the trafficking and localization of AMPA receptors (Berridge et al., 2000; Berridge, 2011). High, short increases in $[Ca^{2+}]_{cyt}$, caused by the opening of Ca^{2+} channels in the plasma membrane (PM) during an action potential, trigger neurotransmitter release. Low, longer-term increases, caused by trains of action potentials without time to return to resting $[Ca^{2+}]_{cyt}$ between them, accelerate the recruitment of vesicles to the membrane so that they are ready to be released (Neher and Sakaba, 2008). Both exocytosis and endocytosis at synaptic membranes require slightly elevated $[Ca^{2+}]_{cyt}$ (Igarashi and Watanabe, 2007). In addition, neuronal cell survival after ischemic injury requires the action of both kinases and phosphatases that are activated by Ca^{2+} signaling (Sasaki et al., 2011).

Ca^{2+} is required for muscle contraction in response to stimulation in a process known as excitation-contraction coupling. An action potential causes the opening of voltage-gated Ca^{2+} channels (VGCCs) in the PM, allowing a small influx of Ca^{2+} to enter the cell from outside. The rise of $[Ca^{2+}]_{cyt}$ in the space near the membrane induces a larger influx from intracellular stores in the nearby sarcoplasmic reticulum (SR) by opening the Ca^{2+}-activated ryanodine receptor (RyR) (Brochet et al., 2012). This Ca^{2+}-induced Ca^{2+} release allows spatial amplification of the signal that starts at the PM. The Ca^{2+} released from the SR binds troponin C, which binds troponin I, allowing myosin to bind to actin and thereby activating myosin-actin contraction (Bers, 2008; Nakamura et al., 2011).

Lysosomes are the organelles responsible for degradation of cellular material sent for removal through endocytosis, phagocytosis, or autophagy. They are also responsible for cellular processes such as PM repair, pathogen defense, signaling, and cell death (Saftig and Klumperman, 2009). In order to perform these and other functions, lysosomes must be able to fuse with one another as well as with phagosomes and other vesicles containing material for degradation (Coen et al., 2012). This fusion is triggered by Ca^{2+}, and does not happen when lysosomal Ca^{2+} homeostasis is disturbed, leading to loss of lysosomal function (Bakker et al., 1997; Coen et al., 2012).

In the circulatory system, resistance to blood flow is determined by properties of red blood cells, especially deformability and aggregation. Deformability is the property of red blood cells that allows them to pass through narrow capillaries without fragmenting. Ca^{2+} signaling is the main pathway red blood cells use to regulate these properties. Mechanical stress causes Ca^{2+} influx, which eventually leads to decreased deformability and an increase in aggregation (Muravyov and Tikhomirova, 2012).

Cell cycle progression is dependent on Ca^{2+} oscillations at the G1/S transition. These oscillations originate mainly in intracellular Ca^{2+} stores, with some contribution from extracellular Ca^{2+}. Blocking the channels that allow Ca^{2+} exit from stores, inositol 1,4,5,-trisphophate (IP_3) receptors (IP_3Rs) and RyRs, slows cell proliferation and reduces the number of cells that progress to G2/M phase in both embryonal carcinoma and adult stem cells (Resende et al., 2010).

In the mammalian oocyte, oscillations of $[Ca^{2+}]_{cyt}$ occur at fertilization. These oscillations are necessary and sufficient to allow embryo development;

microinjection of Ca^{2+} into an unfertilized oocyte induces cell division. Unfertilized oocytes are arrested in meiosis II, and the arrest is maintained by the cytostatic factor complex. Ca^{2+} oscillations activate calmodulin-dependent kinase (CaMK) II, which inhibits the cytostatic factor complex and allows meiosis to be completed. The oscillations also inhibit the activity of mitogen-activated protein kinase (MAPK) signaling, which allows the pronucleus to form (Kashir et al., 2012).

Changes in $[Ca^{2+}]_{cyt}$ regulate transcriptional changes in myocytes, neurons, and many other cell types (Schwaller, 2012). In neurons, over 300 genes have been identified that are regulated by changes in $[Ca^{2+}]_{cyt}$. These genes are regulated by a group of approximately thirty transcription factors (TFs), including cyclic adenosine 3′,5′-monophosphate (cAMP)-responsive element binding protein (CREB), Elk-1, nuclear factor of activated T-cells (NFAT), and nuclear factor kappa B (NF-κB). These TFs are all activated in the cytoplasm by rapid increases in $[Ca^{2+}]_{cyt}$. They then translocate to the nucleus, where elevated nuclear free Ca^{2+} concentration ($[Ca^{2+}]_{nuc}$), caused by long-term increases in $[Ca^{2+}]_{cyt}$, maintains them in the activated state. The transcriptional repressor downstream regulatory element antagonistic modulator (DREAM) can bind Ca^{2+} directly. When $[Ca^{2+}]_{nuc}$ rises, DREAM binds Ca^{2+} and releases the DNA, allowing transcription to proceed (Dolmetsch, 2003; Zaidi et al., 2004). These and other mechanisms allow cells to alter their transcriptional profile in response to stimulation.

These are only a few of the myriad of uses that cells have for Ca^{2+} signaling. Ca^{2+} is an extremely versatile messenger and fundamental to nearly

every cellular process. One of the enduring mysteries in the field that I will address experimentally in this work is how Ca^{2+} signals are regulated in cells. Some general background on $[Ca^{2+}]_{cyt}$ control follows.

CALCIUM HOMEOSTASIS

Ca^{2+} is such an effective regulator of cellular processes because of how tightly it is regulated. Cells can very precisely set the resting concentration of Ca^{2+} in various compartments such that very small changes can be sensed and responded to in different ways in each cellular location. Resting $[Ca^{2+}]_{cyt}$ is kept very low, in the range of 10-100 nM, which is up to 20,000-fold lower than the extracellular concentration (Gennaro et al., 1984; Ingwall and Balschi, 2006; Clapham, 2007). This gradient is maintained by buffering of the cytosol, sequestration of Ca^{2+} in intracellular stores, and removal of Ca^{2+} through the PM, along with control of flow into the cytosol (Gilabert, 2012).

Only one to five percent of Ca^{2+} ions entering the cytosol remain as free Ca^{2+} ions contributing to $[Ca^{2+}]_{cyt}$. This is due to the rapid action of Ca^{2+} buffers, which include ATP and other polyanions as well as Ca^{2+}-binding proteins with high capacity for Ca^{2+}. These Ca^{2+} buffers also restrict the diffusion of Ca^{2+} ions, reducing the spatial range as well as the amplitude of changes in $[Ca^{2+}]_{cyt}$ (Gilabert, 2012).

There are four major proteins that buffer cytosolic Ca^{2+}: parvalbumin (α and β), calbindin-D9k, calbindin-D28k, and calretenin. They are small proteins containing multiple EF hand Ca^{2+}-binding domains. These buffers have no Ca^{2+} bound at basal $[Ca^{2+}]_{cyt}$ and are ready to bind Ca^{2+} whenever $[Ca^{2+}]_{cyt}$ rises

(Schwaller, 2010). They all have multiple sites for Ca^{2+} binding and some show cooperativity. They undergo little or no conformational change upon binding of Ca^{2+} and most have no known interaction partners (Schwaller, 2012). The different buffers show varying Ca^{2+} affinities and binding kinetics, allowing a cell to fine-tune its cytosolic response to Ca^{2+} influx by expressing different amounts of each buffer. The buffers are not redundant; each has its own distribution, and $[Ca^{2+}]_{cyt}$ dynamics will be disrupted if any one is absent (Schwaller, 2010). Along with these proteins, small molecules can act as cytosolic Ca^{2+} buffers. The most important is adenosine triphosphate (ATP), which rapidly binds Ca^{2+} and can control its diffusion (Michailova and McCulloch, 2001; Montalvo et al., 2006).

While cytosolic Ca^{2+} buffers act quickly, their effects are limited. They cannot remove Ca^{2+} from the cytosol and eventually saturate. In order to end Ca^{2+} signals, Ca^{2+} is pumped out of the cytosol. Due to the fact that Ca^{2+} removal from the cytosol moves Ca^{2+} against its concentration gradient, energy is required for this process. P-type ATPase Ca^{2+} pumps use ATP as an energy source to move Ca^{2+} ions across membranes (Brini and Carafoli, 2009). Ca^{2+} pumps act on a timescale of tens of seconds to move Ca^{2+} into intracellular organelles, where it is stored for release in later signaling events (Gilabert, 2012).

The main sites of Ca^{2+} storage are the SR in muscle cells and the ER in all other cells. The three-member family of pumps that operate in SR and ER membranes is known as the sarco/endoplasmic reticulum Ca^{2+} ATPases (SERCA). The action of SERCA is critical in maintaining proper ER and SR function. SERCA is also found in the membrane of the Golgi along with another two-member family of Ca^{2+} pumps, the secretory pathway Ca^{2+} ATPases (SPCA).

SERCA and SPCA are both subtype IIa P-type ATPases. SPCA has higher Ca^{2+} affinity than SERCA, allowing it to operate at even lower $[Ca^{2+}]_{cyt}$, but lower capacity (Brini and Carafoli, 2009). Together these pumps maintain low basal $[Ca^{2+}]_{cyt}$ and protect against small fluctuations. They remove Ca^{2+} that is released by the cytosolic buffers as $[Ca^{2+}]_{cyt}$ returns to baseline after a signaling event.

The ER and SR regulate $[Ca^{2+}]_{cyt}$ by acting as both a sink of excess Ca^{2+} and a store of Ca^{2+} to be released when needed for signaling. Organellar Ca^{2+} buffers, along with regulating protein folding and other ER/SR pathways, bind Ca^{2+} with low affinity and high capacity, allowing the ER and SR to store Ca^{2+} and release it quickly (Prins and Michalak, 2011; Gilabert, 2012; Schwaller, 2012). The total $[Ca^{2+}]$ of these compartments is in the millimolar range, but the free Ca^{2+} concentration of the ER ($[Ca^{2+}]_{ER}$) is around 200-500 μM, which is still 1,000 times higher than $[Ca^{2+}]_{cyt}$ (Prins and Michalak, 2011; Gilabert, 2012). This allows for quick mobilization of large amounts of Ca^{2+} when needed while maintaining relatively constant $[Ca^{2+}]_{ER}$.

The most important buffer in the ER is calreticulin, which buffers up to half of ER Ca^{2+} in non-muscle cells. Immunoglobulin binding protein (BiP) is another ER Ca^{2+} buffer, responsible for about one quarter of the buffering capacity of the ER. Calreticulin and BiP are also protein chaperones that ensure the correct folding of proteins in the ER and require the high $[Ca^{2+}]_{ER}$ for maximal chaperone activity. The depletion of Ca^{2+} from the ER can lead to accumulation of misfolded proteins and activation of the unfolded protein response (Prins and Michalak, 2011).

The SR is a specialized form of the ER found in muscle cells. Its primary function is the storage and release of Ca^{2+} to regulate muscle contraction and relaxation. The primary Ca^{2+} buffer in the SR is calsequestrin, which has a high capacity for Ca^{2+} ions. In addition to controlling $[Ca^{2+}]_{SR}$ by binding Ca^{2+} directly, calsequestrin regulates Ca^{2+} release through the RyR Ca^{2+} channel in response to changes in $[Ca^{2+}]_{SR}$. Another high-capacity SR Ca^{2+} buffer, the histidine-rich Ca^{2+} binding protein (HRC), also regulates RyR activity. In addition, it regulates SERCA, thereby controlling Ca^{2+} transport both into and out of the SR (Prins and Michalak, 2011).

Another organelle that can serve as both a sink and a source for large amounts of Ca^{2+} is the mitochondria (Boyman et al., 2013). For small changes in $[Ca^{2+}]_{cyt}$, efflux to the ER/SR and out of the cell is sufficient and mitochondrial Ca^{2+} uptake accounts for approximately one percent of Ca^{2+} efflux, but when $[Ca^{2+}]_{cyt}$ rises to the micromolar range, the mitochondria play a major role in buffering $[Ca^{2+}]_{cyt}$ (Bers, 2008; Gilabert, 2012). Ca^{2+} enters the mitochondria through a channel in the inner mitochondrial membrane known as the mitochondrial Ca^{2+} uniporter which is highly selective for Ca^{2+} but has low affinity, so little Ca^{2+} is passed at basal $[Ca^{2+}]_{cyt}$ (De Stefani et al., 2011; Palty and Sekler, 2012). Mitochondria are poised to take up large amounts of Ca^{2+} after a signaling event by their close proximity to ER Ca^{2+} release sites (Saris and Carafoli, 2005). When the Ca^{2+} concentration of the mitochondria rises, many of the key enzymes of the mitochondrial matrix are activated. In this way, processes of the mitochondria and the rest of the cell are linked, especially supply and demand of ATP (Bers, 2008). To prevent mitochondrial Ca^{2+}

overload, which can lead to the activation of the mitochondrial permeability transition pore and cell death, Ca^{2+} is extruded from the mitochondria by a cation exchanger in the inner mitochondrial membrane that transports sodium (Na^{+}) in exchange for Ca^{2+} (NCLX) (Palty et al., 2012; Boyman et al., 2013).

Along with the organelles just discussed, other subcellular compartments maintain luminal Ca^{2+} concentrations higher than the cytoplasm. These include the Golgi apparatus, peroxisomes, lysosomes, and endosomes. For the latter three of these, it is not known how or why these organelles maintain such high luminal Ca^{2+} concentrations (Prins and Michalak, 2011). The Golgi, however, has both Ca^{2+} pumps (SERCA and SPCA) and Ca^{2+} channels (RyR and IP_3R) in the membranes of various subcompartments, indicating that it participates in Ca^{2+} uptake and regulated release (Lissandron et al., 2010). The Golgi also has its own set of Ca^{2+}-binding proteins to regulate luminal Ca^{2+} concentration as well as Ca^{2+}-dependent enzymes such as the kexin family of proteases (Oda, 1992; Prins and Michalak, 2011).

In addition to storing Ca^{2+} in the many organelles discussed above, cells are able to remove excess Ca^{2+} entirely. There is another four-member family of subtype IIb P-type Ca^{2+} ATPases in the PM, the plasma membrane Ca^{2+} ATPases (PMCA), which has slightly lower affinity for Ca^{2+} than SPCA and operates as a fine tuner of $[Ca^{2+}]_{cyt}$ (Brini and Carafoli, 2009). In general, the pumps have high affinity and low capacity for Ca^{2+}. This means that they are important in maintaining low $[Ca^{2+}]_{cyt}$ in unstimulated cells but are quickly overwhelmed when $[Ca^{2+}]_{cyt}$ rises above baseline during a signaling event. When this happens,

a variety of Ca^{2+}/cation antiporters (CaCAs) become active (Carafoli and Brini, 2000; Lytton, 2007)

CaCAs have a low affinity for Ca^{2+} compared to the pumps, so they operate mainly when $[Ca^{2+}]_{cyt}$ is high. CaCAs can transport a large number of ions rapidly, however, so they can make quick adjustments to $[Ca^{2+}]_{cyt}$. The requirement for energy to move Ca^{2+} against its concentration gradient is overcome by coupling this energetically unfavorable process to the energetically favorable movement of another ion down its concentration gradient into the cytosol. In mammals, there are three families of CaCAs, two of which are found in the PM: the three-member Na^+/Ca^{2+} exchanger (NCX) family and the five-member potassium (K^+)-dependent Na^+/Ca^{2+} exchanger (NCKX) family. The single member of the Ca^{2+}/cation exchanger (CCX) family is NCLX, which is in the inner mitochondrial membrane and was discussed above. Along with Ca^{2+} pumps, PM CaCAs are critical in the maintenance of $[Ca^{2+}]_{cyt}$ homeostasis and recovery from perturbations (Clapham, 2007; Lytton, 2007; Palty et al., 2012). Regulation of some of these important Ca^{2+} efflux pathways will be explored in Chapter 4.

CALCIUM INFLUX

Cells maintain low $[Ca^{2+}]_{cyt}$ for two reasons. The first is the cytotoxicity of large amounts of free Ca^{2+} ions; if cells allow Ca^{2+} to accumulate in the cytoplasm, they will die due to sustained activation of proteases, nucleases, and other detrimental enzymes (Brini and Carafoli, 2009; Gilabert, 2012). The second

reason is to be able to use controlled changes in $[Ca^{2+}]_{cyt}$ to communicate internally and regulate cellular processes.

A Ca^{2+} signaling event occurs when $[Ca^{2+}]_{cyt}$ is allowed to rise locally or transiently. Signaling is stimulated by triggers such as action potentials, neurotransmitters, and growth hormones (Dolmetsch, 2003). In response to these and other triggers, Ca^{2+} is allowed to passively flow down its concentration gradient into the cytoplasm through Ca^{2+} channels in the PM and organellar membranes. These channels are gated to allow Ca^{2+} to pass only under conditions specific to each cell type.

As mentioned earlier, Ca^{2+} release from internal stores is a major contributor to Ca^{2+} signaling events (Clapham, 2007). Signaling from the PM to intracellular stores is accomplished by means of second messengers generated by enzymatic modification of small molecules such as phosphotidylinositol 4,5-bisphosphate (PIP_2) and nicotinamide adenine dinucleotide (NAD) (Galione and Chuang, 2012). Many cell types mainly use IP_3-induced Ca^{2+} release from the ER to generate Ca^{2+} signals (Thurley et al., 2012). The IP_3R is activated by a signaling cascade that begins with binding of any of a multitude of ligands to a G-protein-coupled receptor in the PM. The subunits of the receptor separate, and the Gα subunit activates phospholipase C, which cleaves PIP_2 into diacyl glycerol (DAG) and IP_3. IP_3 then diffuses into the cytoplasm and activates the IP_3R at low $[Ca^{2+}]_{cyt}$ and high $[Ca^{2+}]_{ER}$ (Skupin and Thurley, 2012). IP_3 has a greater diffusion range than Ca^{2+}, allowing it to act as a global messenger beyond the limited spatial area of $[Ca^{2+}]_{cyt}$ elevation (Parys and De Smedt, 2012).

Large-scale release of Ca^{2+} from the ER and SR is also induced by small increases in $[Ca^{2+}]_{cyt}$ caused by influx from either an intracellular store or outside the cell. As mentioned above, this mechanism of Ca^{2+}-induced Ca^{2+} release (CICR) is important for amplification of small, local signals. While the IP_3R is sometimes involved, CICR relies mainly on the RyR, which is activated by micromolar $[Ca^{2+}]_{cyt}$ and cyclic adenosine diphosphate ribose, a metabolite of NAD. A small rise of $[Ca^{2+}]_{cyt}$ will cause the nearest RyRs to open, allowing Ca^{2+} to flow into the cytoplasm and increasing the amplitude and range of the $[Ca^{2+}]_{cyt}$ rise. This will cause more RyRs to open, thus generating a larger signal (Mackrill, 2012). Another mechanism for activation of RyRs is direct interaction with VGCCs. Some VGCCs sense changes in PM voltage and instead of opening to let Ca^{2+} flow through the PM they cause RyRs to open and allow Ca^{2+} into the cytoplasm from internal stores (Berridge et al., 2000). RyRs close when $[Ca^{2+}]_{cyt}$ rises into the millimolar range (Lanner, 2012).

The most potent Ca^{2+}-releasing messenger is nicotinic acid adenine dinucleotide phosphate (NAADP), another metabolite of NAD. NAADP activates two-pore channels (TPCs) in the membranes of acidic organelles such as lysosomes. Like IP_3Rs, TPCs are more sensitive to ligand activation from the cytosol at high luminal $[Ca^{2+}]$. TPCs are not targets of CICR, though they may induce CICR by releasing Ca^{2+} to activate IP_3Rs and RyRs. NAADP-stimulated Ca^{2+} release may also regulate fission, fusion, and trafficking of lysosomes and endosomes (Galione and Chuang, 2012).

Intracellular Ca^{2+} stores are limited, and they may not be sufficient to generate the signals required in some cell types or they may run low in

conditions of high signaling. To counter this, cells need a way to augment and refill intracellular stores. This is controlled by a mechanism known as store-operated Ca^{2+} entry (Gwack et al., 2007). When $[Ca^{2+}]_{ER}$ is low, the transmembrane proteins stromal interacting molecule (STIM) 1 and 2 form aggregates in the ER membrane. These aggregates collect in the portion of the ER membrane that is very close to the PM, where they stimulate Ca^{2+} influx through the Orai Ca^{2+} channel, allowing for refilling of the ER Ca^{2+} store (Karlstad et al., 2012). There is some evidence that another PM cation channel, the canonical transient receptor potential (TRPC) channel, interacts with STIM and Orai to participate in store-operate Ca^{2+} entry (Berna-Erro et al., 2012). TRPC or other TRP channels in the PM may also interact with IP_3Rs, providing yet another mechanism to regulate this Ca^{2+} influx pathway (Ramsey et al., 2006).

TRP channels are a large, diverse group of cation channels found in both the PM and intracellular membranes (Ramsey et al., 2006). They are permeable to mono- and divalent cations, especially Na^+ and Ca^{2+}. Different channels have different permeability ratios; some allow almost exclusively one ion through, others are non-selective (Berna-Erro et al., 2012). Their modes of activation are as diverse as their ion selectivities. They can be receptor-gated – activated by G-protein-coupled receptors, receptor tyrosine kinases, and other ligand-activated transmembrane proteins; ligand-gated – activated directly by the binding of a ligand such as capsaicin, DAG, or inorganic ions; or activated by changes in cellular conditions such as temperature or mechanical pressure (Ramsey et al., 2006). Many are responsive to changes in $[Ca^{2+}]_{cyt}$ (Su et al., 2009).

Like TRP channels, other channels in the PM generate signals directly, rather than through stimulation or refilling of intracellular Ca^{2+} stores. VGCCs in the PM respond immediately to membrane depolarization by opening and allowing very fast, high-capacity Ca^{2+} influx (Clapham, 2007). VGCCs are made up of the pore-forming α_1 subunit with some combination of β, $\alpha_2\delta$, and γ subunits. There are multiple versions of each subunit, creating channels with a variety of functional and regulatory properties (Siwek et al., 2012). The channels open when a change in membrane potential causes a conformational change of a positively-charged region that blocks the Ca^{2+} pore in the closed state (Karlstad et al., 2012).

There are also a variety of other ligand-gated and receptor-activated channels in the PM that play minor roles in Ca^{2+} influx in response to a variety of stimuli (Berna-Erro et al., 2012). The effect of all of these Ca^{2+} influx pathways, so varied in their localization and modes of activation, is a system for generating Ca^{2+} signals that can be precisely regulated both spatially and temporally. This gives cells the ability to use just one molecule, Ca^{2+}, to code for a wide variety of cellular responses (Siwek et al., 2012). In later chapters, I will experimentally determine some parameters of this signal encoding.

CALCIUM SENSORS

Ca^{2+} in the cytosol affects cellular processes by interacting with thousands of Ca^{2+}-binding proteins (Clapham, 2007). One group of Ca^{2+}-binding proteins that is very important for effecting downstream responses is the cytosolic Ca^{2+} sensors. Like the cytosolic Ca^{2+} buffers, Ca^{2+} sensors bind Ca^{2+} rapidly and with

high affinity (Yáñez et al., 2012). Unlike buffers, however, sensors are present at lower total concentrations in the cell, undergo larger conformational changes on Ca^{2+} binding, and participate in Ca^{2+}-dependent interactions with other proteins (Gilabert, 2012; Schwaller, 2012).

Ca^{2+} sensors expand the effect of spatially and temporally restricted Ca^{2+} elevation by facilitating diffusion and remaining activated after a signal has ended. There are four families of these cytosolic Ca^{2+} sensors: S100, neuronal calcium sensor (NCS) proteins, calmodulin (CaM), and calcineurin (Cn) (Clapham, 2007; Yáñez et al., 2012). The S100 and NCS families are important in regulation of Ca^{2+} flux through pumps and channels, but they are expressed in only some organisms or cell types (Schaub and Heizmann, 2008; Brini and Carafoli, 2009; Nakamura et al., 2011; Schwaller, 2012).

CaM is highly conserved and is present in all cell types in all eukaryotic organisms (Schaub and Heizmann, 2008; Yáñez et al., 2012). CaM contains four Ca^{2+}-binding EF hand domains in two cooperative pairs with different Ca^{2+} binding properties. Each of these domains binds one Ca^{2+} ion, for a total of four bound ions. The cooperativity of the Ca^{2+} binding sites ensures that CaM will be either fully bound to Ca^{2+} or completely empty the majority of the time (Schaub and Heizmann, 2008). At basal $[Ca^{2+}]_{cyt}$, CaM is in its Ca^{2+}-free apo form and regulates a plethora of Ca^{2+}-independent targets including the centrosome, myosins involved in vesicle trafficking, and cytoskeletal components necessary for endocytosis and metaphase spindle formation (Flory et al., 2000; Cyert, 2001; Schaub and Heizmann, 2008). When $[Ca^{2+}]_{cyt}$ rises during a Ca^{2+} signaling event, CaM binds Ca^{2+} very quickly and undergoes a drastic conformational change

that exposes hydrophobic surfaces and allows interaction with a different set of targets than the apo form (Clapham, 2007; Faas et al., 2011). There are over one hundred known Ca^{2+}-dependent CaM target proteins, including PM ATPases, NAD kinases, and myosin light chain kinase, regulating critical cellular processes such as Ca^{2+} transport, cyclic nucleotide metabolism, muscle contraction, cell cycle progression, changes in gene expression, and many others (Berridge et al., 2000; Schaub and Heizmann, 2008). Because apo CaM is often prebound to its targets in the absence of cytosolic Ca^{2+}, it can modulate the activity of those proteins on a millisecond time scale when $[Ca^{2+}]_{cyt}$ rises (Schaub and Heizmann, 2008). CaM is enriched in cellular microdomains where Ca^{2+} influx leads to very high local $[Ca^{2+}]$, contributing to the speed of the CaM response (Saucerman and Bers, 2008).

Interestingly, Ca^{2+}/CaM is involved in numerous negative feedback loops on $[Ca^{2+}]_{cyt}$. Ca^{2+}/CaM inhibits VGCC, IP_3R, and Orai in a Ca^{2+}-dependent manner, stopping Ca^{2+} flow into the cytosol once $[Ca^{2+}]_{cyt}$ has increased a certain amount (Bers, 2008; Berna-Erro et al., 2012; Parys and De Smedt, 2012). In addition, Ca^{2+}/CaM increases the activity of PMCA, SERCA, and NCX, by either direct or indirect means, speeding the return to basal $[Ca^{2+}]_{cyt}$ (Carafoli and Brini, 2000; Clapham, 2007).

Ca^{2+}/CaM regulates Ca^{2+}-dependent transcription mainly through the activation of a protein phosphatase and a family of protein kinases called Ca^{2+}/CaM-dependent kinases (CaMKs) (Schwaller, 2012). CaMKs have been shown to regulate various TFs, including CREB, serum response factor (SRF), activating transcription factor-1 (ATF-1), and myocyte enhancer factor 2 (MEF2).

CaMKs also affect transcription by regulating nuclear localization of the Ca^{2+}-sensitive transcriptional repressor DREAM (Bers, 2008; Ronkainen et al., 2011). In addition to regulating cellular processes by modulating transcription, CaMKs also directly regulate ion fluxes through Ca^{2+}, Na^{+}, and K^{+} channels; axon outgrowth; cell cycle progression; neurotransmitter release; memory consolidation; fertilization; cell proliferation; and the immune response, all by direct phosphorylation of targets involved in these processes (Maier, 2012; Skelding and Rostas, 2012). Of particular interest is the CaMK feedback on $[Ca^{2+}]_{cyt}$: positive feedback by activation of VGCC and RyR and negative feedback by deactivation of the SERCA inhibitor phospholamban (Bers, 2008).

CALCINEURIN AND NFAT

The sole protein phosphatase regulated by Ca^{2+}/CaM is calcineurin (Cn), which is also a Ca^{2+} sensor itself. Ca^{2+}/CaM binds Cn with higher affinity than it binds CaMKs, allowing selective regulation and timing of Ca^{2+}-responsive signaling pathways (Saucerman and Bers, 2008). Like CaM, Cn is ubiquitously expressed and highly conserved in all organisms, with over 50% identity in one of its subunits between mammals and yeast (Rusnak and Mertz, 2000). Cn comprises a tightly associated heterodimer of the catalytic CnA subunit and the smaller regulatory CnB subunit. CnA contains the catalytic domain, a CnB-binding domain, and a Ca^{2+}/CaM-binding autoinhibitory domain that binds to and blocks the substrate-binding site of the catalytic domain in the absence of Ca^{2+}/CaM. Binding of Ca^{2+}/CaM, but not apo CaM, displaces the autoinhibitory domain and increases V_{max} of CnA. CnB contains four EF hand domains that

bind Ca^{2+}, similarly to CaM. Unlike CaM, however, CnB can weakly bind and activate CnA in the absence of Ca^{2+}. Ca^{2+} binding to CnB increases its ability to bind and activate CnA, lowering the K_m of the enzyme. In order to be fully functional, CnA requires the binding of both Ca^{2+}/CaM and free Ca^{2+} to CnB; the phosphatase is inactive at basal $[Ca^{2+}]_{cyt}$ but activated during Ca^{2+} signaling events (Wang et al., 2008; Li et al., 2009; 2011).

Cn is one of the crucial factors in the flow of information from the initiators of Ca^{2+} signals to the effectors of cellular responses and has many direct targets (Li et al., 2011). In neurons, Cn dephosphorylates and activates neuronal nitric oxide synthase, increasing the production of nitric oxide, which regulates synaptic plasticity and excitotoxicity (Groth et al., 2003). Synaptic vesicle endocytosis in multiple types of neurons is triggered by Cn dephosphorylating a required group of proteins known as dephosphins (Cousin and Robinson, 2001). Endocytosis of synaptic vesicles is important both for recycling of membranes, to reset the nerve terminal for further signaling, and for internalization of neurotransmitter receptors, which allows for processes of neuronal plasticity such as long term depression (Groth et al., 2003; Yamashita, 2012). Exocytosis of synaptic vesicles under high-frequency stimulation also requires Cn (Kumashiro et al., 2005). Cn dephosphorylates tubulin and microtubule-associated proteins to promote microtubule growth and stabilization (Groth et al., 2003). Cn also regulates Ca^{2+}-mediated MAPK signaling by dephosphorylation of a scaffold protein required for kinase activation (Li et al., 2011).

Cn has been shown to directly regulate the activity of Ca^{2+} transporters, creating feedback loops. Cn physically interacts with at least one form of NCX

and inhibits its activity *in vivo* (Katanosaka et al., 2005; Shigekawa et al., 2007). This creates a positive feedback loop, preventing the ending of Ca^{2+} signals before they have the required effect. Cn inhibits the L-type VGCC and some ligand-gated channels, possibly through an intermediate, setting up a fast negative feedback loop (Li et al., 2011; Reese and Taglialatela, 2011). Cn also regulates the activity of other ion transporters, contributing to the general control of ion homeostasis (Reese and Taglialatela, 2011). Some of this feedback will be examined in later chapters.

In addition to its direct dephosphorylation targets, Cn regulates the activity of another phosphatase, protein phosphatase 1 (PP1), through dephosphorylation and inhibition of homologous PP1 inhibitors DARPP-32 and inhibitor-1. PP1 then regulates ion transport, gene transcription, synaptic transmission, cell cycle, and neuronal survival in a Ca^{2+}-dependent way even though it does not bind Ca^{2+}. PP1 may regulate some of the same targets as Cn, either in the same or opposite way, leading to complex regulation that is not fully understood (Connor et al., 2000; Groth et al., 2003; Hurley et al., 2007).

Another major role of Cn is regulation of transcription. While Cn can affect the activity of some Ca^{2+}-regulated TFs such as CREB, its major direct effector is the nuclear factor of activated T-cells (NFAT) family of TFs (Clapham, 2007). Though different NFAT genes are expressed in different cell types, they are largely redundant (Padhan and Varma, 2010). Dephosphorylation of NFAT by Cn leads to translocation of the Cn-NFAT complex to the nucleus and activation of transcription (Rusnak and Mertz, 2000). Nuclear kinases GSK-3,

CK1, and DYRK1a phosphorylate NFAT, leading to its export and reduction of transcription of its targets (Müller et al., 2009).

Although first discovered in the immune system, Cn-NFAT signaling is ubiquitous, controlling such processes as T-cell activation, differentiation of muscle cells, memory formation, myelination, and development of the nervous and cardiovascular systems (Crabtree and Graef, 2008; Kao et al., 2009; Padhan and Varma, 2010; Shin et al., 2011). Due to the high affinity of Ca^{2+}/CaM for Cn, the Cn-NFAT pathway is sensitive to small changes in $[Ca^{2+}]_{cyt}$ and is very responsive to activating signals (Saucerman and Bers, 2008). Since NFAT is regulated by phosphorylation, an extremely rapid reaction, its activation state accurately reflects Cn activation and $[Ca^{2+}]_{cyt}$. Cn-NFAT signaling can be quickly turned on and just as quickly turned off when stimulating conditions change (Cyert, 2003; Dolmetsch, 2003). Complex feedback on $[Ca^{2+}]_{cyt}$ is evident at the transcriptional level: Cn-NFAT signaling upregulates the transcription of IP_3R, one member of the TRPC family, DYRK1a, some PMCA genes, and one NCX gene while downregulating the transcription of one PMCA gene and another NCX gene (Genazzani et al., 1999; Li et al., 2000; Shigekawa et al., 2007; Schwaller, 2010; Berridge, 2012). The physiological relevance of these contradictory feedback loops is not fully understood, but will be probed experimentally in later chapters.

REGULATION OF CALCINEURIN

While proper response to environmental conditions is vital to cell and organism survival, inappropriate response is detrimental. Therefore, tight

regulation of signaling cascades is critical. As already mentioned, Cn is subject to multiple types of feedback regulation to fine-tune its activity.

Cn activity is dependent on, and therefore regulated by, $[Ca^{2+}]_{cyt}$ through Ca^{2+} activation of both CaM and CnB. Due to this dependence, Ca^{2+} channels and pumps that control $[Ca^{2+}]_{cyt}$ can be seen as regulators of Cn themselves. As already discussed, Cn modulates the activity of multiple Ca^{2+} transporters, affecting both influx and efflux, and thereby regulates its own activation. This regulation is either fast, by dephosphorylation of the transporter or an interacting protein, or slow, by regulation of transcription through NFAT.

Other transcriptional feedback loops exist through the Cn-NFAT pathway. NFAT stimulates its own transcription, enhancing the effect of prolonged Cn activation (Crabtree and Graef, 2008). NFAT also upregulates the transcription of the regulators of Cn (RCAN) family of proteins, which binds the catalytic domain of activated CnA and has complex effects on Cn activity (Davies et al., 2007). In different experimental systems, RCANs were shown to have either a stimulatory or inhibitory effect on Cn. It has been suggested that the conflicting results can be partially explained by dose-dependent effect of RCAN on Cn; the result of changing the level of RCAN depended on the starting level in each experimental system (Shin et al., 2011). However, it has been shown that phosphorylation state of RCAN also determines its effect on Cn (Mehta et al., 2009). RCAN contains many phosphorylatable residues, and may serve to integrate signaling inputs from multiple signaling pathways. Binding of RCAN to Cn is regulated by phosphorylation at some of these sites (Jung et al., 2011). High levels of partially-phosphorylated RCAN competitively inhibit Cn activity

by preventing binding of other substrates, creating negative feedback through the Cn-NFAT pathway (Mehta et al., 2009).

RCAN stimulation of Cn requires priming phosphorylation by MAPK pathway kinases or DYRK1a, full phosphorylation by GSK-3, ubiquitination by the SCF^{Cdc4} ubiquitin ligase complex, and degradation by the proteasome. Blocking any of these steps locks RCAN into an inhibitory interaction with Cn, indicating that RCAN may normally effect positive feedback on Cn function as a suicide chaperone for Cn maturation and reactivation (Hilioti et al., 2004; Kishi et al., 2007; Mehta et al., 2009). In Chapter 5, I will present additional experiments to support and modify this view. Interestingly, Cn dephosphorylates the residue phosphorylated by GSK-3, reinforcing the negative feedback in the Cn-NFAT-RCAN pathway (Shin et al., 2011).

Cn opposes GSK-3 activity by dephosphorylation of its substrates, many of which are cell-type specific. Cn also activates GSK-3 by direct dephosphorylation. This would seem to set up a futile feedback cycle in which Cn activates GSK-3 but prevents it having any effect. This may be resolved by further cell-type specificity, with Cn activating GSK-3 only in cell types in which they do not have overlapping targets (Kim et al., 2009).

MISREGULATION OF CALCINEURIN

Since Cn signaling is so conserved and so critical, it is unsurprising that many pathological consequences have been linked to misregulation of this pathway. Both increasing and decreasing Cn-NFAT signaling in the mouse embryo caused pre-natal lethality, indicating the importance of precise

regulation Cn activity (Müller et al., 2009; Uchida et al., 2010). In adult tissues, defects of Cn signaling have been seen in, and implicated in the development of, a range of diseases.

Alzheimer's Disease (AD) has been described as resulting from a chronic increase in basal $[Ca^{2+}]_{cyt}$, which is especially detrimental in the aging brain where the balance of Ca^{2+}-dependent pathways is already perturbed (Berridge, 2011; Reese and Taglialatela, 2011). This increase in neuronal $[Ca^{2+}]_{cyt}$ leads to the symptoms of AD in multiple ways, many of which require Cn. Memory formation and storage is controlled by the balance of long-term potentiation (LTP), which promotes short-term memory formation, and long-term depression (LTD), which promotes short-term memory erasure after transfer to long-term memory storage. LTP requires transcription activation by CREB, which is inhibited by Cn (Reese and Taglialatela, 2011). In contrast, Cn facilitates LTD by activation of PP1 (Berridge, 2011). Increased $[Ca^{2+}]_{cyt}$ leads to increased Cn activity, which favors LTD over LTP. This leads to premature erasure of short-term memories before they can be transferred to long-term memory storage and thereby to the cognitive symptoms of AD. Cn also stimulates hyperphosphorylation of tau, an important microtubule-associated protein, so that it no longer performs its necessary cellular functions and forms cytotoxic aggregates (Yu et al., 2008). Although Cn can dephosphorylate tau under normal conditions, upregulated Cn cannot, and tau becomes hyperphosphorylated, possibly through the hyperactivation of GSK-3 by Cn (Yu et al., 2008; Reese and Taglialatela, 2011). Hyperactive Cn further promotes neurodegeneration by activation of the apoptotic protein BAD and through NFAT-dependent

excitotoxic cell death (Reese and Taglialatela, 2011). Many of the morphological changes that precede neuronal atrophy and degeneration can be blocked by Cn inhibitors (Bezprozvanny, 2010).

Precise Cn regulation is critical in cardiac function. Congestive heart failure, caused by the inability of the heart to meet increased pumping demands, is caused by hypertrophy of the cardiac muscle (Berridge, 2012). Cn-NFAT signaling is both necessary and sufficient for hypertrophy in the adult heart; expression of constitutively active Cn induces hypertrophy in the absence of pathologic stimulation and inhibition of Cn prevents hypertrophy under stimulating conditions (Molkentin et al., 1998; Nakamura et al., 2011). In contrast, in a mouse model of adult-onset dilated cardiomyopathy (DCM), the third most-common cause of heart failure, deletion of Cn caused greater than 50% mortality in the first three weeks of life (Heineke et al., 2010). Further investigation revealed elevated levels of cardiomyocyte death in Cn-deficient DCM mice, indicating a protective effect of Cn. The symptoms of DCM were reduced by mild overexpression of active Cn (Heineke et al., 2010).

Increased Cn-NFAT activity has been seen in kidney tissues of mouse models of both types 1 and 2 diabetes, leading to renal hypertrophy and misregulation of the extra-cellular matrix. Upregulation of RCAN1.4 has also been seen in these tissues, and this upregulation is dependent on increased Cn activity (Jang et al., 2011).

The genes for both RCAN1 and DYRK1a, which phosphorylates both NFAT and RCAN, are located in the Down Syndrome (DS) critical region of human chromosome 21. Trisomy of chromosome 21 causes DS, the symptoms of

which include cardiac defects and early-onset AD features (Jung et al., 2011). These symptoms can be attributed to a misregulation in Cn-NFAT signaling, caused by overexpression of DYRK1a and RCAN1 from the extra copy of the genes present on the trisomic chromosome (Hilioti et al., 2004; Jung et al., 2011).

Given the many severe effects of changes in Cn activity, it is important to be able to directly measure the effects and activation state of Cn. Cn-dependent processes have been probed by modulating Cn protein levels with genetic overexpression and knockdown and modulating Cn activity with pharmacological inhibition (Molkentin et al., 1998; Heineke et al., 2010; Jang et al., 2011; Reese and Taglialatela, 2011). Activation state of Cn has been measured by observation of the phosphorylation state of purified endogenous substrates, phosphatase activity of purified enzyme on synthetic or purified endogenous substrates, and transcript level of Cn-NFAT-regulated genes (Yu et al., 2008; Kim et al., 2009; Nakamura et al., 2011). All of these methods are at least somewhat indirect and do not look at Cn straightforwardly in living cells. In order to directly study this important Ca^{2+} signaling factor, I have employed the model organism *Saccharomyces cerevisiae*, baker's yeast.

CALCINEURIN AND ITS UPSTREAM REGULATORS IN YEAST

The yeast *Saccharomyces cerevisiae* is a good model system for studying Ca^{2+} signaling for many reasons. In higher eukaryotes, study of Cn is complicated by gene redundancy, difficulty of genetic manipulation, complex cultivation requirements, and expense. Yeast have much less redundancy in cellular pathways, making determination of the role of a single factor much less

complicated than in mammalian cells (Rodríguez et al., 2012). This comparative simplicity also allows for relatively easy computational approximation of the Ca^{2+} homeostasis and signaling systems (Cui et al., 2009b; Demaegd et al., 2013). Many tools exist to facilitate genetic manipulation of yeast, including a completely sequenced and well annotated genome with few introns, reliable methods for genetic transformation and protein expression, and simple and cheap cultivation (Goffeau et al., 1996; Ton and Rao, 2004; Müller and Grossniklaus, 2010).

The basic components of the Ca^{2+} homeostasis and signaling systems are highly conserved in yeast and mammalian cells and the systems operate similarly. Most of the mammalian proteins involved have counterparts in yeast (Cui et al., 2009b). This high level of conservation allows methods and hypotheses developed in yeast to be applied to mammalian systems (Müller and Grossniklaus, 2010). Study of the key factors of these systems, especially Cn, can be expected to provide valuable insights into the operation of these systems in higher eukaryotes (Miyakawa and Mizunuma, 2007).

Like mammalian cells, yeast maintain low $[Ca^{2+}]_{cyt}$, in the range of 100 nM (Iida et al., 1990; Miseta et al., 1999). Yeast use an assortment of pumps and exchangers similar to those in mammalian cells to maintain the Ca^{2+} gradient, but the distribution of these Ca^{2+} transporters is somewhat different. Yeast do not have any Ca^{2+}-ATPases in the PM but have a pump of the PMCA family in the vacuole membrane, called Pmc1 (Cunningham and Fink, 1994). The yeast vacuole is an acidic storage and degradation oraganelle similar to the lysosome of animal cells (Cunningham, 2011). The vacuole is the primary Ca^{2+} storage

organelle of yeast, containing millimolar concentration of Ca^{2+}, but only approximately 10 μM is free ions. The rest is buffered by inorganic polyphosphate and cannot be released (Dunn et al., 1994). Yeast also have a Ca^{2+}-ATPase of the SPCA family called Pmr1 in the membrane of the Golgi complex. Ca^{2+} in the Golgi is essential, as depletion leads to activation of stress response pathways (Cunningham, 2011). Pmc1 and Pmr1 are redundant for an essential function, clearing Ca^{2+} from the cytosol, and a strain lacking both pumps is inviable in standard growth conditions (Cunningham and Fink, 1994). The relative contribution of the two pumps seems to vary by assay conditions, but they are necessary for long-term growth in high extracellular $[Ca^{2+}]$ ($[Ca^{2+}]_{ex}$) (Cunningham and Fink, 1994; Tang and Liu, 2010).

In contrast to mammalian cells, yeast do not have a SERCA pump and do not use the ER as a significant store or source of Ca^{2+} (Cronin et al., 2002). $[Ca^{2+}]_{ER}$ is 10 μM, which is more than ten times lower than mammalian cells (Bonilla et al., 2002; Cyert and Philpott, 2013). However, Ca^{2+} in the ER is still 100 times higher than $[Ca^{2+}]_{cyt}$ and is necessary for essential functions (Cunningham, 2011). Spf1, a P-type ATPase of the broadly conserved but uncharacterized subtype V, has been identified in the ER membrane of yeast (Cronin et al., 2002). While studies of Spf1 have been unable to identify its substrate, it has been shown to be necessary for cell wall integrity, protein trafficking, ER enzyme function, proper protein stability and folding, transmembrane protein insertion fidelity, and ER membrane composition (Suzuki and Shimma, 1999; Cronin et al., 2000; Tipper and Harley, 2002; Vashist et al., 2002; Ando and Suzuki, 2005; Krumpe et al., 2012). Although Spf1 does not show Ca^{2+} transport activity, Spf1

function partially overlaps that of Pmr1 and some *SPF1* knockout phenotypes can be suppressed by raising $[Ca^{2+}]_{ex}$, indicating a role for Spf1 and the ER in Ca^{2+} homeostasis (Cronin et al., 2000; 2002; Vashist et al., 2002; Sørensen et al., 2012). Mitochondria do not play a role in Ca^{2+} homeostasis in yeast (Cyert and Philpott, 2013).

Although the yeast genome does not contain homologs of the NCX or NCLX families of Na^{+}/Ca^{2+} exchangers, yeast do have uncharacterized homologs of the CCX family of cation/Ca2+ exchangers that have been termed Ccx1 and Ccx2 (Cai and Lytton, 2004; Lytton, 2007). In Chapter 2, I will show that knockout of *CCX1* and *CCX2* does not affect activation of Cn-Crz1 in the conditions tested. More active in yeast is the CAX family proton $(H^{+})/Ca^{2+}$ exchanger Vcx1, which is localized to the vacuole membrane (Cunningham and Fink, 1996; Pozos et al., 1996). Vcx1 is responsible for maintaining low basal $[Ca^{2+}]_{cyt}$ and removing Ca^{2+} from the cytoplasm immediately after a shock with high $[Ca^{2+}]_{ex}$, though the vacuolar Ca^{2+} store is maintained mainly by Pmc1 (Miseta et al., 1999; Cui et al., 2009a). Lastly, a member of a novel family of putative H+/Ca2+ exchangers in the Golgi membrane, termed Gdt1, is essential for maintaining Ca^{2+} in the Golgi in absence of Pmr1 (Demaegd et al., 2013).

In yeast, $[Ca^{2+}]_{cyt}$ rises in response to a variety of physiological stimuli including mating pheromones, high environmental pH, ER stress, depletion of Ca^{2+} in the secretory pathway, and a variety of anti-fungal drugs as well as changes in $[Ca^{2+}]_{ex}$ (Locke et al., 2000; Bonilla et al., 2002; Bonilla and Cunningham, 2003; Roberts et al., 2012). Yeast do not have homologues of IP_3Rs or RyRs and the ER does not have a role in Ca^{2+} release. The most reliable pool of

Ca^{2+} for signaling is the vacuole, which releases Ca^{2+} through Yvc1, a homologue of mammalian TRPC channels (Bonilla and Cunningham, 2002; Zhou et al., 2003). Yvc1 is activated by mechanical force and high $[Ca^{2+}]_{cyt}$, releasing Ca^{2+} by a CICR mechanism in response to osmotic upshock and hydrogen peroxide (Zhou et al., 2003; Su et al., 2009; Popa et al., 2010).

Ca^{2+} also enters from outside the cell in response to the majority of the physiological stimuli mentioned above. Influx is primarily through two PM channels with different Ca^{2+} affinities known as the high-affinity Ca^{2+} influx system (HACS) and the low-affinity Ca^{2+} influx system (LACS) (Muller et al., 2001; 2003). HACS comprises Cch1, Mid1, and Ecm7, which are homologous to the VGCC subunits of mammals (Martin et al., 2011). HACS is activated in response to mating pheromone by the transcription factor Ste12 (Muller et al., 2001). HACS is also activated by MAPK in response to depletion of Ca^{2+} in the secretory pathway in a process analogous to store-operated Ca^{2+} entry in mammalian cells (Locke et al., 2000; Cunningham, 2011). HACS is not needed for a response to elevated $[Ca^{2+}]_{ex}$ and is unaffected by the concentration of magnesium (Mg^{2+}) (Locke et al., 2000; Cui et al., 2009a). Like HACS, LACS is stimulated in the response to mating pheromone, and may be physiologically more important in this condition. The components of LACS have not yet been fully identified, but Fig1 has been shown to be required for LACS activity along with a group of genes involved in polarized growth and cell fusion during mating (Muller et al., 2003). There is evidence for other Ca^{2+} influx pathways, both inhibited and unaffected by Mg^{2+}, including a glucose-induced Ca^{2+} influx pathway (Bonilla et al., 2002; Cui et al., 2009a; Bouillet et al., 2012).

As in mammals, CaM is the primary sensor for Ca^{2+}, though yeast CaM only binds three Ca^{2+} ions due to a deletion in one EF hand domain. CaM is localized to the spindle pole body throughout the cell cycle and has roles in polarized growth, mitosis, vesicle fusion, and endocytosis. Ca^{2+}/CaM activates the CaMKs Cmk1 and Cmk2, which are involved in stress responses, and Cn (Cyert, 2001).

Yeast Cn has many targets and regulates Ca^{2+} homeostasis, stress responses and signaling, and the G2/M transition of the cell cycle (Cyert, 2001). Cn controls $[Ca^{2+}]_{cyt}$ through regulation of both influx and efflux. Cn inhibits HACS after stimulation by direct dephosphorylation and inhibits Vcx1 through an unknown mechanism (Cunningham and Fink, 1996; Locke et al., 2000; Muller et al., 2001). This sets up two different types of feedback loops. Cn inhibition of HACS is a simple negative feedback loop whereby a Ca^{2+} signal is quickly ended once the downstream pathway has been turned on in response (Muller et al., 2001; Bonilla and Cunningham, 2003). Cn inhibition of Vcx1 is delayed relative to the initiation of a Ca^{2+} stimulus and Vcx1 activity keeps $[Ca^{2+}]_{cyt}$ low. This generates a double negative feedback loop which allows for bistability in the system, thereby preventing small perturbations in $[Ca^{2+}]_{cyt}$ from activating Cn spuriously as well as preventing dissipation of large signals before the proper response has been initiated (Cui et al., 2009a; Cunningham, 2011). Ccx2 may be inhibited by Cn; the nature of the feedback loop thus created would depend on the physiological role of Ccx2. The unidentified Ca^{2+} influx pathways in the PM are also predicted to be feedback inhibited by Cn, similarly to the regulation of

HACS (Cui et al., 2009b). Cn regulation of and by Pmc1 and Vcx1 will be addressed further in Chapter 4.

Cn affects multiple signaling pathways and stress responses through dephosphorylation of its targets. The direct targets of Cn include Slm1 and Slm2, an essential gene pair that regulates the actin cytoskeleton, mediates the response to heat stress, and is involved in sphingolipid signaling and metabolism; Frt1 (also called Hph1), an integral ER membrane protein which is activated by Cn in response to high pH; and its own regulators Rcn1 and Rcn2, which will be discussed below (Heath et al., 2004; Bultynck et al., 2006). Cn is required to prevent cell death by the inhibition of reactive oxygen species accumulation in stressed cells; to mediate tolerance to high pH, cell wall damaging agents, and excess cations in the environment; for viability during prolonged exposure to mating pheromone; and in response to a variety of other stresses (Cunningham and Fink, 1994; Cyert, 2001; 2003; Zhang et al., 2006; Cyert and Philpott, 2013). In response to these stresses, Cn can inhibit the G2/M cell cycle transition by upregulating the activity of the checkpoint kinase Swe1 (Miyakawa and Mizunuma, 2007).

As in mammals, Cn also affects cellular processes in yeast through transcriptional regulation. The *S. cerevisiae* genome does not contain a homolog of the NFAT TFs, but it does have an analogous Cn-dependent TF known as Crz1 (Cyert, 2003). A region of Crz1 has weak similarity to the NFAT proteins, indicative of its very similar mechanism of regulation by Cn (Cyert, 2003; Miyakawa and Mizunuma, 2007). When Crz1 is dephosphorylated by Cn, a nuclear localization signal is unmasked that directs Crz1 to the nucleus. Once

there, Crz1 binds a DNA sequence known as the Cn-dependent response element (CDRE) in the promoters of target genes (Matheos et al., 1997; Stathopoulos and Cyert, 1997; Stathopoulos-Gerontides et al., 1999). Crz1 has approximately one hundred transcriptional targets involved in ion transport, cell wall maintenance, lipid metabolism, vesicle trafficking, and signaling (Yoshimoto et al., 2002; Hilioti et al., 2004). Notable among these are the *PMC1* and *PMR1* genes encoding the Ca^{2+} pumps (Matheos et al., 1997). Their transcriptional upregulation by Cn creates slow negative feedback loops that keep Ca^{2+} signals from continuing indefinitely. Crz1 also upregulates its own transcription in a slow positive feedback loop that favors the persistence of signals that reach the threshold for prolonged Crz1 activation (Matheos et al., 1997).

Yeast have one canonical member of the RCAN family and one divergent member, called Rcn1 and Rcn2 respectively (Mehta et al., 2009). The genes for both yeast RCANs are upregulated by Crz1 (Mehta et al., 2009). As in mammals, Rcn1 stimulates Cn activity when phosphorylated by the GSK-3 family kinase Mck1, ubiquinated, and degraded by the proteasome (Hilioti et al., 2004; Kishi et al., 2007; Mehta et al., 2009). Inhibition of any of these steps prevents Cn activation, as does overexpression of Rcn1 (Mehta et al., 2009). Rcn2 lacks the motifs that have been shown to be required for Cn stimulation and probably acts solely as a feedback inhibitor (Mehta et al., 2009). Chapter 5 will include experiments that address the nature of Cn-Rcn1 feedback.

MEASUREMENT OF CALCINEURIN

Considering the importance of proper function of the Cn pathway and the clinical possibilities offered by selective manipulation of Cn activity, understanding the endogenous regulation of Cn is crucial. In order to determine how its activity is regulated, Cn activity must be measured *in vivo*.

To date, Cn activity has usually been measured indirectly. Growth or death assays can be done in conditions that require Cn for growth or survival, such as high $[Ca^{2+}]_{ex}$ and treatment with anti-fungal drugs. By testing single- and multiple-gene knockouts in these conditions, genes can be identified that modify Cn activity. While a lot can be learned from these assays, one major drawback is that cell growth and survival are susceptible to the confounding effects of strain background, culture media, and non-specific consequences of genetic manipulation and drug treatment (Dudgeon et al., 2008).

Another commonly used assay for Cn activity uses the *lacZ* gene, which produces the enzyme β-galactosidase, under control of the Cn-dependent transcription factor Crz1. By transforming yeast cells with a plasmid carrying the *lacZ* gene behind a CDRE sequence, β-galactosidase will be produced in proportion to Cn activation and then its enzymatic activity can be measured (Stathopoulos and Cyert, 1997). The amount of β-galactosidase activity, as determined by the conversion of a clear substrate to a colored product, is assumed to correlate to Cn activity. While this assay is useful for measuring Cn-dependent transcription, it does not directly measure Cn activity and the readout depends on mRNA translation and enzymatic activity. Another method to look at Cn-dependent gene transcription that does not depend on translation and

enzymatic activity is gene microarrays (Laviña et al., 2012). These have been used to test for effects of the disruption of other pathways on the activation of Cn.

Aside from the specific drawbacks for each of these assays, they all lack resolution in observing both individual cell variability and change over short time scales. These assays measure large populations of cells. This is a problem if certain subpopulations of cells, such as older cells or newly budded cells, respond differently to given conditions. The measurements obtained from these assays are averages, which can be skewed by even a few outliers. These assays also measure only a specific time point or points and cannot be used for observing immediate responses. A probe is needed that allows for observation of single cells in real time.

Live imaging of Cn-dependent signaling in yeast has been done using multiple independently constructed fluorescent Crz1 fusion probes (Stathopoulos-Gerontides et al., 1999; Wiesenberger et al., 2007; Cai et al., 2008; Laviña et al., 2012; Bodvard et al., 2013). In standard culture conditions, the fluorescence is primarily cytoplasmic. Addition of $CaCl_2$ to the growth medium causes the majority of the visible probe in nearly all of the cells to synchronously translocate to the nucleus within 15 minutes at high concentrations of extracellular Ca^{2+}, with a slightly longer delay at low concentrations. After a characteristic dwell time, the signal returns to the cytoplasm.

Despite the obvious utility of these probes for study of Cn, only one group has used fluorescently tagged Crz1 to examine the dynamics of the Cn-Crz1 transcriptional system in response to Ca^{2+} stimulation. Cai *et al.* observed Crz1-

GFP in cells responding to high $[Ca^{2+}]_{ex}$ for extended time courses. Under prolonged stimulation, the cells exhibited unsynchronized all-or-none "bursts" of Crz1-GFP nuclear localization that had not previously been observed. This prolonged response to stimulation indicates that the regulation of Cn activity is more complicated than a simple on/off switch. Coexpression of a cell-cycle phase marker with Crz1-GFP showed no evidence of cell-cycle regulation and no correlation between bursts in mother and daughter cells. These bursts were eliminated by the Cn inhibitor FK-506, indicating that they are dependent on Cn signaling. However, coexpression of a probe for $[Ca^{2+}]_{cyt}$ revealed that while some of the bursts coincided with transient spikes in $[Ca^{2+}]_{cyt}$, most did not. Surprisingly, only the frequency of the bursts was increased by increasing $[Ca^{2+}]_{ex}$, while the amplitude and duration of these bursts were unaffected by Ca^{2+} concentration.

Based on these observations, Cai *et al.* proposed a model of Cn signal encoding that utilizes frequency modulated (FM)-coordination of Crz1 nuclear localization. This would allow scaled transcriptional responses from different promoters at all levels of stimulation. Measurement of Crz1-driven fluorescent protein expression from a variety of both synthetic and natural promoters demonstrated that all of the gene products exhibited identical Ca^{2+} dependence curves when normalized, providing experimental support to this model. This coordination of gene expression allows for maintenance of constant ratios of upregulated proteins at all levels of expression. In this manner, cells could ensure that all subunits of a multimer protein complex are present at the correct stoichiometry at all levels of expression. Msn2, another stress-response

transcription factor, showed similar behavior, suggesting that this model of how external signals are interpreted by the regulators that control transcription factors may apply to many pathways in the cell. Broader application of this principle is further implied by frequency encoding seen in cytoplasmic Ca^{2+} waves in mammalian systems (Berridge et al., 2000).

While they thoroughly discussed the impact of FM-coordinated Crz1 localization bursts, the investigators paid little attention to the origin and regulation of these bursts. Fluorescently tagged Crz1 is an ideal system for studying the complex regulation of Cn in live cells in real time, as begun by Cai *et al.* In Chapter 2, I will explore some of the factors that affect the shape of the transcriptional response curve to stimulation. I will then, in Chapter 3, introduce a newly developed feedback-inert fluorescent probe of Cn activity. Based on observations made using this probe, I will describe a new phenomenon I have termed "flickers" in unstimulated cells. In Chapters 4 and 5, I will use this new probe to address other aspects of Crz1 nuclear localization and Cn signaling. The experiments described in later chapters greatly increase understanding of Cn regulation and signaling at the single cell level.

CHAPTER TWO: EXPLORING THE ROLE OF CYTOSOLIC CALCIUM REGULATION IN CALCINEURIN-DEPENDENT GENE EXPRESSION

INTRODUCTION

The calcium (Ca^{2+})-regulated phosphatase calcineurin (Cn) is a crucial factor in the flow of information from the initiators of Ca^{2+} signals to the effectors of cellular responses and has many direct targets that effect the response to Ca^{2+} (Li et al., 2011). In addition to acting through these immediate effectors, Cn also regulates gene expression by controlling the nuclear localization of the nuclear factor of activated T-cells (NFAT) family of transcription factors (TF) in mammals and the analogous Crz1 TF in yeast (Matheos et al., 1997; Clapham, 2007). These TFs regulate many genes over a wide range of stimulation intensities (Cyert, 2003; Shin et al., 2011).

Previous studies have investigated how expression from individual Crz1-responsive promoters varies in response to changes in stimulation intensity or Crz1 expression (Matheos et al., 1997). Some of the promoters studied showed linear increases in transcription in response to increasing external calcium chloride ($CaCl_2$) concentration ($[CaCl_2]_{ex}$) while others showed exponential increases. Total transcription, as measured by β-galactosidase activity assays, also varied widely between promoters.

In order to determine what contributes to the variation in responses to identical stimuli, two artificial promoters comprising one or four tandem repeats of the Cn-dependent response element (CDRE) were directly compared. In this chapter, I show that repeats of the Crz1-binding region increase the probability of binding and activation but do not change the shape of the response curve.

I then investigated the role of maintenance of cytosolic Ca^{2+} equilibrium in the shape of the transcriptional response curves. Yeast cells use vacuolar Ca^{2+}

transport to regulate cytosolic Ca^{2+} equilibrium. The Ca^{2+} ATPase Pmc1 and the proton (H^+)/Ca^{2+} exchanger Vcx1 have distinct roles in regulating cytosolic Ca^{2+} concentration ($[Ca^{2+}]_{cyt}$) (Cunningham and Fink, 1994; 1996). *PMC1* transcription is upregulated by Cn-Crz1 signaling, closing a negative feedback loop in which Cn-Crz1 activates Pmc1 and Pmc1 inhibits Cn-Crz1 (Matheos et al., 1997). *VCX1* is not transcriptionally regulated by Cn-Crz1, but Vcx1p is inhibited by Cn through an unknown mechanism, which creates a double negative feedback loop; Cn and Vcx1 inhibit each other, potentially leading to bistability in the system (Cunningham, 2011). Vcx1 suppresses noise in Cn-Crz1 signaling by maintaining $[Ca^{2+}]_{cyt}$ below the threshold of Cn activation in the face of small perturbations. Only large changes in $[Ca^{2+}]_{cyt}$ can activate Cn, which then inhibits Vcx1 to allow $[Ca^{2+}]_{cyt}$ to remain high. This is effectively a positive feedback loop because Cn promotes its own continued activation. Simultaneously deleting both vacuolar Ca^{2+} transporters leads to higher $[Ca^{2+}]_{cyt}$ in response to addition of $CaCl_2$ to the medium and therefore increases the baseline noise in the system (Miseta et al., 1999). It would also cause more activation of Cn by turning the positive feedback to a constitutive "on" state and by eliminating negative feedback through Pmc1p. This would lead to more activation of the Cn-Crz1 pathway, due to increased noise and greater activation of Cn.

The experiments with the 1X and 4X-CDRE promoters were repeated in *pmc1Δ vcx1Δ* deletion strains. These experiments suggested that misregulation of $[Ca^{2+}]_{cyt}$ led to changes in the gene expression response and that the differently sensitive promoters responded differently.

MATERIALS AND METHODS

Yeast strains, plasmids, and media

All yeast strains were derived from parental strain W303-1A by standard transformations and mating crosses. Cells were grown in rich YPD or synthetic complete (SC) media, prepared as described (Sherman et al., 1986).

CCX1 (YJR106W) was knocked out by Longtine PCR of the pFA6a-kanMx6 plasmid using primers CCX1 - F11 and CCX1 - R11 to replace the coding region with the gene for G418 resistance (Longtine et al., 1998). *CCX2 (YDL206W)* was knocked out by Longtine PCR of the pFA6-natR plasmid using primers CCX2 - F11 and CCX2 - R11 to replace the coding region with the gene for nourseothricin (nat) resistance. The PCR products were transformed into yeast strains K665 and K632 using standard transformation techniques and selected on appropriate drugs. Proper knockout was confirmed by PCR of genomic DNA using primers flanking the coding regions. Candidates with appropriately sized bands were mated to create strains TAY001-016.

Strains TAY001, 004, 013, and 016 were transformed with plasmids pAMS342 and pAMS366 using standard transformation techniques and selected on SC-URA. These plasmids carry the *lacZ* gene, which codes for the β-galactosidase enzyme, under control of a promoter containing one or four tandem copies of the CDRE (Stathopoulos and Cyert, 1997).

Table 2-1. *Yeast strains used in Chapter 2.*

Strain Name	Genotype	Source
K665	*pmc1::TRP1 vcx1Δ*	Kyle Cunningham
K634	*pmr2::HIS3 MAT***α**	Kyle Cunningham
TAY001	*WT*	this study
TAY004	*ccx1::G418 ccx2::NAT*	this study
TAY013	*pmc1::TRP1 vcx1Δ*	this study
TAY016	*pmc1::TRP1 vcx1Δ ccx1::G418 ccx2::NAT*	this study

All strains are isogenic derivatives of strain K601/W303-1A (*MAT***a** *ade2-1 can1-100 his3-11,14 leu2-3,112 trp1-1 ura3-1*).

Table 2-2. *Primers used in Chapter 2.*

Primer Name	Sequence
CCX1 - F11	TACTCGTTCATCCTCTCCACATACGGCCGTACACAA GCAACAATAACACAATAATacatggaggcccagaataccc
CCX1 - R11	CGGCGCCAGATAAATGTCACAAAAACAAATTTTTC GGGAGGCACTCTTGCAAGCTcagtatagcgaccagcattcac
CCX2 - F11	CTCCTTACCTTTATTTGTAAATGCTACTCTTCATTTA TCAAATTTTTTAAAGCAGacatggaggcccagaataccc
CCX2 - R11	TGTTAATATATTTATTATAGCTTGTATATAAAAAAT GAAATCTTGATTTATTAAAcagtatagcgaccagcattcac

Capitalized regions are sequences immediately up- and down-stream of the gene. Lowercase regions match the plasmid template for PCR.

***Table 2-3**. Plasmids used in Chapter 2.*

Plasmid Name	Description	Source
pAMS342	*1X-CDRE-lacZ*	Stathopolous and Cyert (1997)
pAMS366	*4X-CDRE-lacZ*	Stathopolous and Cyert (1997)

β-galactosidase activity assays

The transformed strains were grown overnight at 30°C in 2 mL SC-URA in a 24-well dish with aeration. OD_{600} of a 1:10 dilution was measured in a Genesys 5 spectrophotometer (Spectronic Insruments). All cultures were diluted back to an OD_{600} of 0.3 in 5 mL SC-URA. Cultures were grown at 30°C with aeration for 90-150 minutes. Equal densities of cells were harvested and resuspended in 5/3X YPD supplemented with 8.33 mM succinic acid (YPDS). 200 μL of cells were added to 1 mL of 5/3X YPDS and 800 μL of $CaCl_2$ dilution to a final volume of 2 mL in a 24-well dish. The range of final concentrations for $CaCl_2$ was 0 and 0.4 to 400 mM in 11 dilutions. Final concentration of succinic acid was 5 mM. Cells were grown in $CaCl_2$ at 30°C with aeration for 4 hours. Cells were harvested, permeabilized, substrate was added, and reactions were stopped as described, with volumes scaled down to a final volume of 1.5 mL (Guarente, 1983). Reaction times were shorter for the 4X promoter than the 1X. Cell density of untreated cultures was measured by optical density at 650 nm and of the final supernatants at 405 nm using a Thermomax microplate reader spectrophotometer (Molecular Devices). The SOFTmax Pro software was used. Miller units (MU) were calculated using the following formula:

$MU = (OD_{405} - blank)/((OD_{650} - blank) * reaction\ time\ [min]) * 1000$

Statistical analysis

Experiments were conducted in triplicate starting with three randomly selected overnight cultures. Each replicate was normalized to its maximum expression value. Normalized expression curves were linearly interpolated to calculate the $CaCl_2$ concentrations for 50% of maximum expression (EC_{50}) and 10% of maximum expression (EC_{10}).

Expression and EC means were compared with an unpaired, two-sample t-test with equal variance using the Matlab (Mathworks) ttest2 function. Differences in expression or concentration were called significant for p-values below 0.05.

RESULTS

Promoter repeats increase gene expression at low calcium concentrations

Gene expression was measured using the *1X-CDRE-lacZ* and *4X-CDRE-lacZ* reporter gene constructs in WT. The *lacZ* gene codes for the β-galactosidase enzyme, which converts a clear substrate into a yellow product whose concentration can be measured optically. Concentration of the enzymatic product correlates to concentration of the enzyme which is dependent on Crz1-driven gene expression. The range of $[CaCl_2]_{ex}$ tested was chosen to cover from close to baseline to extreme stimulation. This range allowed for accurate measurement of both basal and maximal gene expression and determination of the concentration that caused half maximal (50%) expression (EC_{50}). Although the *4X-CDRE-lacZ* reporter had 21 times higher maximum expression than the *1X-CDRE-lacZ* reporter, after normalization to the maximum at 200 mM $CaCl_2$ it can be seen that both reporters have similar levels of basal expression, ~0.6-0.8% of maximum (Fig. 2-1). The EC_{50} and EC_{10} for the 4X reporter were both lower than for the 1X, the EC_{10} by two-fold, indicating that the curve is shifted to the left. This means that the 4X reporter is more sensitive to raising $[CaCl_2]_{ex}$. This shift is significant at $[CaCl_2]_{ex}$ from 1.5 to 25 mM. At higher $[CaCl_2]_{ex}$, where the values are above the EC_{50}, the curves converge on maximal expression. Thus, when the probability of Crz1 binding to the promoter is low, in low stimulation, CDRE repeats measurably increase binding probability. When that probability is already high, in high stimulation, the repeats do not have an effect.

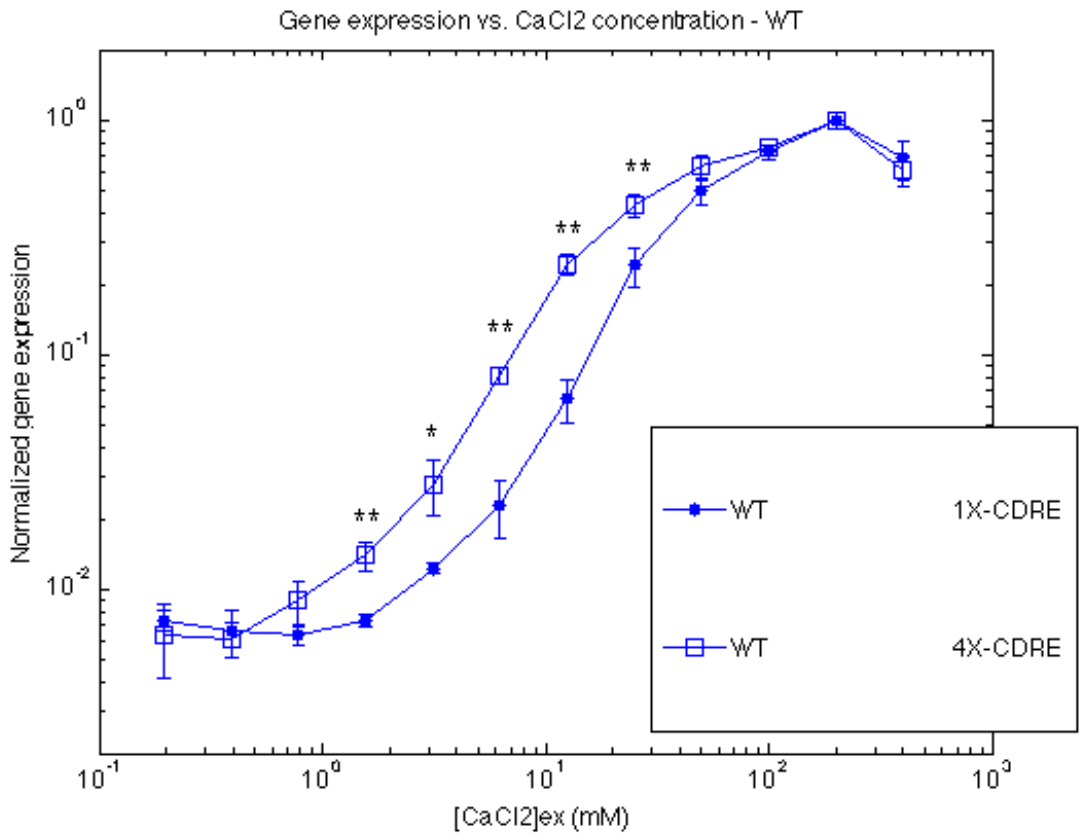

Figure 2-1. *Promoter repeats increase gene expression at low calcium concentrations.*

WT strains carrying *1X-CDRE-lacZ* or *4X-CDRE-lacZ* plasmids were treated with varying concentrations of $CaCl_2$ and then β-galactosidase activity was measured. Expression was normalized to the maximum of each replicate and then averaged. 0 mM $CaCl_2$ was plotted at 0.20 mM because of the log scale. Symbols are means of 3 replicates and error bars represent standard deviation. * = $p<0.05$ ** = $p<0.01$

The Ccx1 and Ccx2 proteins do not affect gene expression coordination

The *CCX1* and *CCX2* genes encode putative Ca^{2+} exchangers that are homologous to the CCX family of exchangers present in mammals, but they have not yet been characterized in yeast. Because they may facilitate transport of Ca^{2+} into or out of the cytoplasm, or both, they were hypothesized to have an effect on *CDRE-lacZ* reporter gene expression. To test this, *ccx1Δ ccx2Δ* double knockout mutants were created and transformed with the reporter plasmids. The normalized values for gene expression of the *ccx1Δ ccx2Δ* strains are almost identical to those for the WT strains (Fig. 2-2). This confirmed the effect of the different promoters while ruling out a role for Ccx1p and Ccx2p in regulating the noise, sensitivity, or gene expression coordination in these conditions.

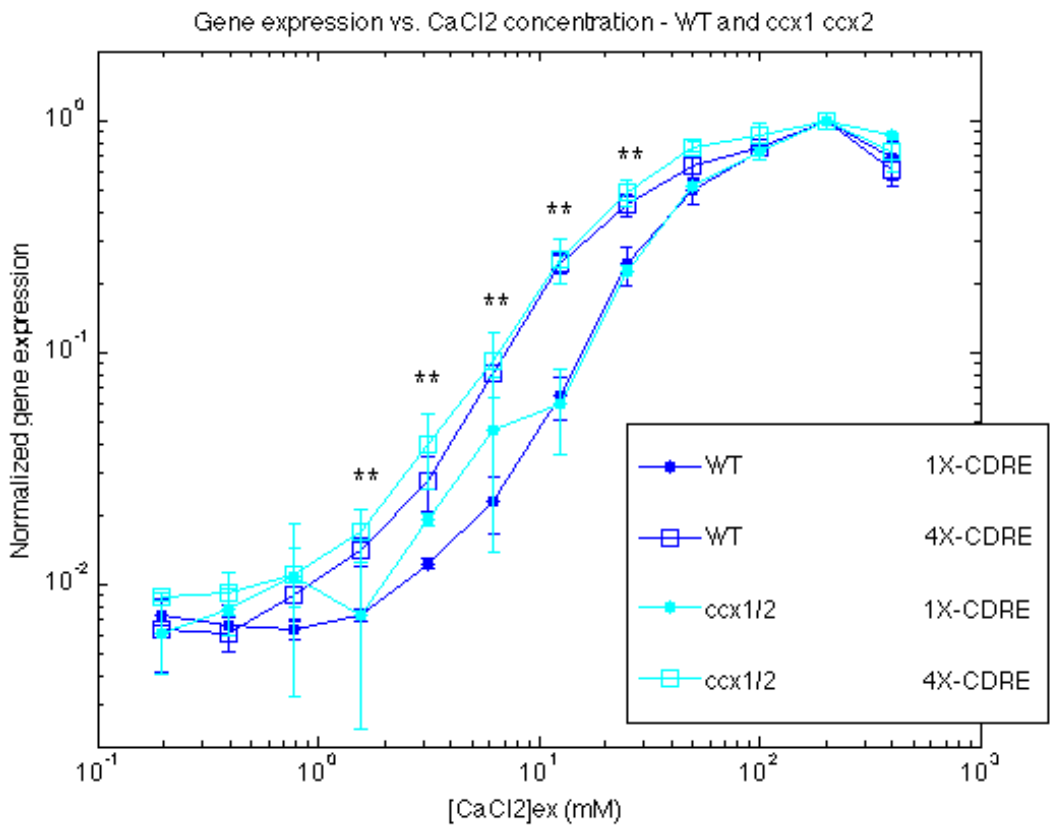

Figure 2-2. *The Ccx1 and Ccx2 proteins do not affect gene expression coordination.*

ccx1Δ ccx2Δ strains carrying *1X-CDRE-lacZ* or *4X-CDRE-lacZ* plasmids were treated with varying concentrations of $CaCl_2$ and then β-galactosidase activity was measured. Expression was normalized to the maximum of each replicate and then averaged. 0 mM $CaCl_2$ was plotted at 0.20 mM because of the log scale. Symbols are means of 3 replicates and error bars represent standard deviation. ** = $p<0.01$ between 1X and 4X with WT and *ccx1Δ ccx2Δ* combined for each promoter. No significant differences were seen between WT and *ccx1Δ ccx2Δ* strains.

Knocking out vacuolar calcium transport increases gene expression

To test whether vacuolar Ca^{2+} transporters Pmc1p and Vcx1p have a role in regulating Crz1-dependent gene expression, *pmc1Δ vcx1Δ* double mutants and *ccx1Δ ccx2Δ pmc1Δ vcx1Δ* quadruple mutants were created and transformed with the reporter plasmids. Treatment of the *1X-CDRE-lacZ* strains with the broad range of $[CaCl_2]_{ex}$ used above showed that the mutant strains were shifted to the left relative to the WT and *ccx1Δ ccx2Δ* strains, similar to the difference between the *1X-* and *4X-CDRE-lacZ* in WT (Fig. 2-3 A). This indicates that Pmc1p and Vcx1p do have a role in regulating Crz1-dependent expression: they reduce sensitivity by maintaining cytosolic Ca^{2+} equilibrium. This is in agreement with results seen in other studies.

The *4X-CDRE-lacZ pmc1Δ vcx1Δ* double and quadruple mutants were also shifted to the left relative to controls and relative to the *1X-CDRE-lacZ* strains, but to a larger degree than the *1X* strains (Fig. 2-3 B). As with the WT strains, no significant differences were seen between *pmc1Δ vcx1Δ* and *ccx1Δ ccx2Δ pmc1Δ vcx1Δ* strains with either promoter. The change in EC_{10} between the promoters was approximately four-fold and normalized basal expression was almost twice as high in *4X-CDRE-lacZ pmc1Δ vcx1Δ*. This indicates that in addition to causing a gain in sensitivity to $CaCl_2$, knockout of Pmc1p and Vcx1p causes increased basal Cn-Crz1 activity.

Figure 2-3. *Knocking out vacuolar calcium transport increases gene expression.*

WT and *pmc1Δ vcx1Δ* strains carrying (A) *1X-CDRE-lacZ* or (B) *4X-CDRE-lacZ* plasmids were treated with varying concentrations of $CaCl_2$ and then β-galactosidase activity was measured. Expression was normalized to the maximum of each replicate and then averaged. 0 mM $CaCl_2$ was plotted at 0.20 mM because of the log scale. Symbols are means of 3 replicates and error bars represent standard deviation. * = $p<0.05$ ** = $p<0.01$

A

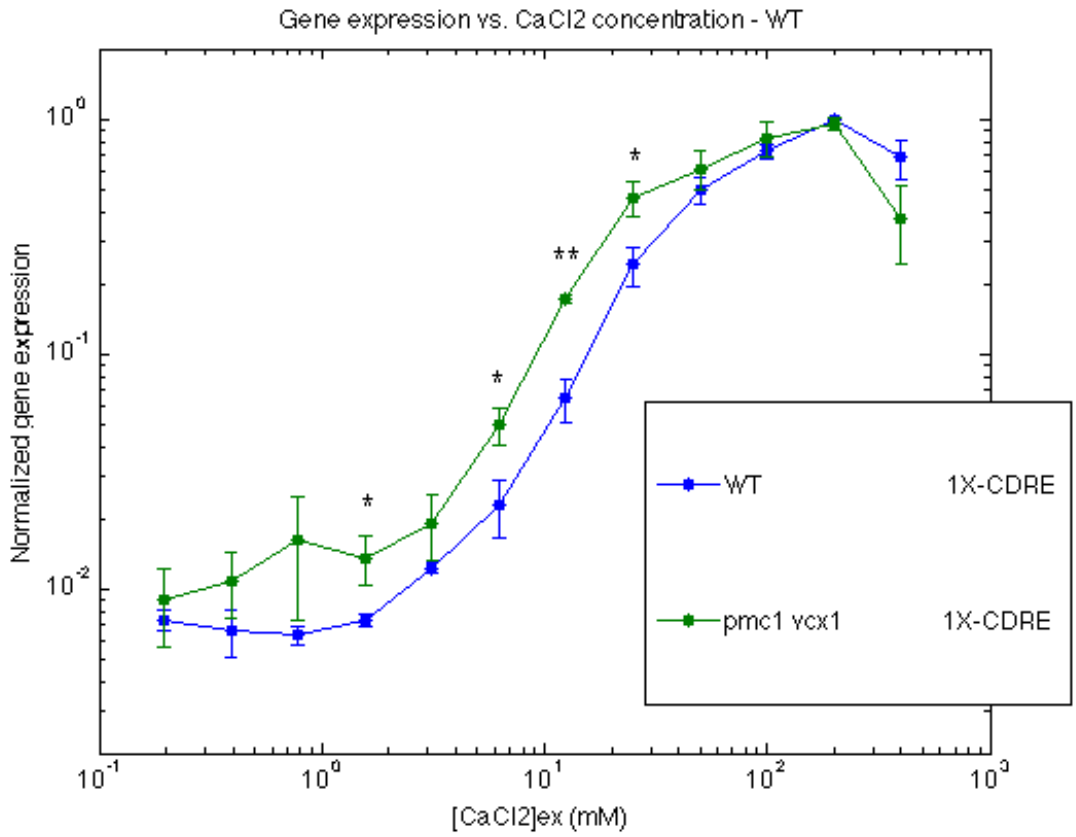

B

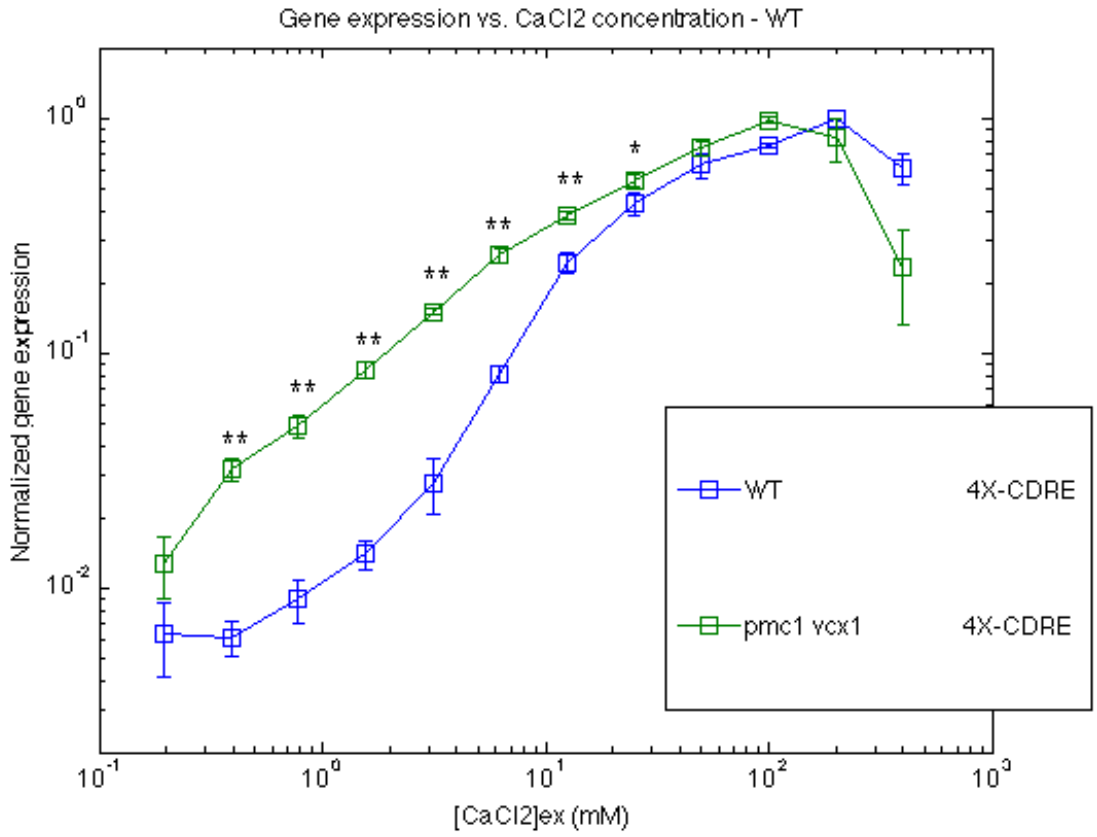
Gene expression vs. CaCl2 concentration - WT
Normalized gene expression
[CaCl2]ex (mM)
WT 4X-CDRE
pmc1 vcx1 4X-CDRE
**
**
**
**
**
*

DISCUSSION

Activation of Cn by stimulation with high $[CaCl_2]_{ex}$ causes different promoters to be transcribed at different levels in response to varying intensities of stimulation. In order to investigate what aspect of promoter architecture might contribute to these differences, I compared gene expression from two different artificial promoters, *1X-CDRE* and *4X-CDRE*, comprising one and four repeats of the minimal Crz1-binding region. I found that the 4X promoter had much higher expression at all levels of stimulation. When normalized, the curves were very similar in shape with the 4X curve shifted to the left, indicating that the larger changes in curve shape seen in other experiments are due to more than simple changes in binding probability.

Another group recently looked at normalized gene expression from a variety of Crz1-responsive promoters (Cai et al., 2008). They saw identical response curves for all synthetic and most natural promoters tested without any significant shift in sensitivity. From this, they constructed a model of frequency-modulated gene expression coordination. Based on this model, they postulated that expression from all Crz1-activated genes would be proportional at all levels of stimulation. While this would seem to contradict my results and previous work, the normalization used by Cai *et al.* may have led to misleading results. They did not see expression level out at maximum so they may have been normalizing to the middle of the true curve. Additionally, they normalized to their observed maximum and minimum instead of just the maximum. Further, they only tested higher concentrations of $CaCl_2$, where I saw overlapping curves, and not the lower range where I saw a shift. Though their model is interesting

and potentially useful if accurate, these differences in experimental methods lead me to doubt that their model is complete.

One drawback of both the *CDRE-lacZ* reporter that I used and the *CDRE-YPF* fluorescent reporter used by Cai *et al.* is that both of these systems measure folded protein, which is multiple steps removed from gene transcription. RNA microarrays or other more direct means of measuring gene expression would be better suited to accurately determining the shape of the Crz1-expression response curve in yeast.

Using the *CDRE-lacZ* reporter genes in the *ccx1Δ ccx2Δ* double knockout mutants showed no effect of knocking out these genes, indicating that Ccx1p and Ccx2p do not have a significant role in regulating Crz1p activation through control of Cn, calmodulin, or $[Ca^{2+}]_{cyt}$. These unstudied putative proteins are homologous to the CCX family of Ca^{2+} exchangers in mammals (Lytton, 2007). My findings suggest that Ccx1p and Ccx2 do not participate in Ca^{2+} influx or efflux, even in the absence of vacuolar Ca^{2+} transporters Pmc1p and Vcx1p. Further characterization of these proteins is needed to determine what role they do play in the cell.

In contrast to Ccx1p and Ccx2p, I found that Pmc1p and/or Vcx1p has a large effect on Crz1p activation. Knocking them both out increased sensitivity of the cells to $CaCl_2$ and changed the shape of the response of the 4X-CDRE promoter. The increased sensitivity is expected from the effect of these mutants on $[Ca^{2+}]_{cyt}$ (Miseta et al., 1999). The change in shape of the 4X response curve could be caused by elimination of feedback on Cn-Crz1 through either Pmc1p or Vcx1p. Pmc1p is part of a negative feedback loop through Cn-Crz1, the

elimination of which could increase the long-term level of Crz1 in the nucleus. On the other hand, Vcx1 is part of a double negative feedback loop with Cn, which could be understood as a positive feedback loop of Cn on itself in the presence of elevated $[Ca^{2+}]_{cyt}$ (Cunningham, 2011). Deleting *VCX1* could lower the $[Ca^{2+}]_{cyt}$ threshold for Cn activation, thereby activating the positive feedback at lower $[CaCl_2]_{ex}$ and increasing expression from the more sensitive promoter. Experiments with *pmc1Δ* and *vcx1Δ* single mutant strains are needed to differentiate the effects of Vcx1p and Pmc1p.

In order to more fully examine the Cn-dependent transcriptional response, and how it differs in varying conditions, more-direct examination of Crz1 is needed. In the next chapter, I will attempt to directly observe Crz1 activation using a newly developed GFP-Crz1(ΔZF) that fails to bind DNA and activate transcription.

CHAPTER THREE: DEVELOPMENT OF AN INERT PROBE FOR CALCINEURIN ACTIVITY

INTRODUCTION

In the previous chapter, I examined Cn-Crz1-dependent gene expression in response to a variety of conditions. I found that repeats of the core Crz1-binding promoter sequence increased sensitivity to external calcium chloride ($CaCl_2$) without changing the shape of the response curve, while eliminating vacuolar calcium (Ca^{2+}) transport dramatically increased expression at low stimulation. In order to more closely study these differences, I sought to observe Cn activation of Crz1 directly.

In order to do this, I developed an imaging protocol that uses a probe constructed from a fluorescent protein and modified Crz1. Crz1p induces transcription of both positive regulators of Cn activity, such as Rcn1, and negative regulators, such as the Ca^{2+} transporters Pmr1 and Pmc1, and even induces its own expression. As a result, the presence of full-length Crz1 within the probe could affect its own readout and complicate determining the effect of any one input on the system.

To study Cn localization without all of the above feedback, I deleted the C-terminus of the protein, which contains the three zinc finger (ZF) domains that bind DNA. The probe was expressed from a strong constitutive promoter to ensure that the signal in all cells was above autofluorescence background. I imaged this probe in a microfluidic flow chamber that constrains the cells to the plane of focus and I tracked individual nuclei by tagging a histone with a red fluorescent protein, mCherry. The microfluidic flow chamber provided for constant replenishment of the media over time and rapid switching between low- and high-Ca^{2+} media during imaging.

Using this inert probe and imaging system, I saw immediate, synchronized translocation of the probe to the nucleus in most cells in a field in response to the addition of $CaCl_2$-supplemented medium. The probe returned to the cytoplasm asynchronously after a dwell time that correlated to external $CaCl_2$ concentration ($[CaCl_2]_{ex}$). I also saw brief flashes of partial nuclear localization of the probe, which I have termed "flickering," in unstimulated cells growing in constant conditions. In wild-type (WT) cells in unsupplemented medium, I saw occasional flickers, generally lasting for five to twenty minutes. In strains lacking the vacuolar transporters Pmc1 and Vcx1, flickers were higher and more frequent. In strains lacking endogenous Crz1 and the Cn regulator Rcn1, flickers were lower and less frequent. This indicates that Cn is active in resting conditions and its activation is regulated by some of the same factors that regulate the response to calcium stress, as will be seen in later chapters. In this chapter, I characterize the new probe and imaging system and I analyze noisy basal signaling for the first time.

MATERIALS AND METHODS

Yeast strains, plasmids, and media

All yeast strains were derived from parental strain W303-1A by standard transformations and mating crosses. Cells were grown in rich YPD or synthetic complete (SC) media, prepared as described (Sherman et al., 1986).

Plasmid pEG760 containing full-length N-terminal-tagged *GFP-CRZ1* and *URA3* selection was obtained from the Grote lab (Johns Hopkins University). The DNA-binding domain was removed by cutting with XhoI and SalI and recircularizing the plasmid, now called pSM_232. This created a C-terminal truncation at residue 420. When cut with BclI, the plasmid integrated into the genome at the *SSO2* locus, inserting *URA3* and *GFP-CRZ1(ΔZF)*. The cut plasmid was transformed into yeast strain K1357 using standard transformation techniques and selected on SC-URA to create strain SM099. Proper integration was confirmed by microscopy.

Strains SM099 and TKY276 were mated according to standard techniques to create the full panel of mutants with all combinations of *pmc1Δ*, *vcx1Δ*, *crz1Δ*, and *rcn1Δ*, and *GFP-CRZ1(ΔZF)*, strains TAY061-124.

The cut plasmid was transformed again into yeast strain K1421 using standard transformation techniques and selected on SC-URA to create strain SM101. Proper integration was confirmed by microscopy. This new strain was needed because the previous strains had *RCN1* knocked out with the *HIS3* marker, but this marker was needed for the histone tagging. Strains with the *ADE2* marker were used instead.

Histone H2B was C-terminally tagged with mCherry by Longtine PCR of the pFA6a-mCherry-codon-optimized plasmid, carrying the *HIS3* gene for selection, obtained from the Wendland lab, using primers HTB2 - F-mCherry and HTB2 - R11 (Longtine et al., 1998). The PCR product was transformed into yeast strains SM101 and TAY070 using standard transformation techniques and selected on SC-HIS to create strains TAY125 and TAY126. Proper tagging was confirmed by microscopy.

Strains TAY125 and TAY126 were mated according to standard techniques to create the full panel of mutants with all combinations of *pmc1Δ*, *vcx1Δ*, *crz1Δ*, and *rcn1Δ* containing *GFP-CRZ1(ΔZF)* and *HTB2-mCherry*, strains TAY127-158.

Table 3-1. *Yeast strains used in Chapter 3.*

Strain	Genotype	Source
K1357	*pmc1::LEU2 vcx1Δ crz1::G418 MAT***a**	Sohum Mehta
K1421	*pmc1::LEU2 vcx1Δ crz1::G418 rcn1::ADE2 MAT***a**	Sohum Mehta
TKY276	*rcn1::HIS3 MAT*$\boldsymbol{\alpha}$	Kingsbury and Cunningham (2000)
SM099	*pmc1::LEU2 vcx1Δ crz1::G418 GFP-CRZ1(ΔZF)::URA3 MAT***a**	Sohum Mehta
SM101	*pmc1::LEU2 vcx1Δ crz1::G418 rcn1::ADE2 GFP-CRZ1(ΔZF)::URA3 MAT***a**	Sohum Mehta
TAY061	WT *MAT***a**	this study
TAY063	*pmc1::LEU2 MAT***a**	this study
TAY069	*GFP-CRZ1(ΔZF)::URA3 MAT***a**	this study
TAY070	*GFP-CRZ1(ΔZF)::URA3 MAT*$\boldsymbol{\alpha}$	this study
TAY071	*pmc1::LEU2 GFP-CRZ1(ΔZF)::URA3 MAT***a**	this study
TAY077	*crz1::G418 MAT***a**	this study
TAY085	*crz1::G418 GFP-CRZ1(ΔZF)::URA3 MAT***a**	this study
TAY125	*pmc1::LEU2 vcx1Δ crz1::G418 rcn1::ADE2 GFP-CRZ1(ΔZF)::URA3 HTB2-mCherry::HIS3 MAT***a**	this study
TAY126	*GFP-CRZ1(ΔZF)::URA3 HTB2-mCherry::HIS3 MAT*$\boldsymbol{\alpha}$	this study

TAY127	*GFP-CRZ1(ΔZF)::URA3 HTB2-mCherry::HIS3 MAT***a**	this study
TAY129	*pmc1::LEU2 GFP-CRZ1(ΔZF)::URA3 HTB2-mCherry::HIS MAT***a**	this study
TAY131	*vcx1Δ GFP-CRZ1(ΔZF)::URA3 HTB2-mCherry::HIS3 MAT***a**	this study
TAY133	*pmc1::LEU2 vcx1Δ GFP-CRZ1(ΔZF)::URA3 HTB2-mCherry::HIS3 MAT***a**	this study
TAY135	*crz1::G418 GFP-CRZ1(ΔZF)::URA3 HTB2-mCherry::HIS3 MAT***a**	this study
TAY137	*pmc1::LEU2 crz1::G418 GFP-CRZ1(ΔZF)::URA3 HTB2-mCherry::HIS3 MAT***a**	this study
TAY141	*pmc1::LEU2 vcx1Δ crz1::G418 GFP-CRZ1(ΔZF)::URA3 HTB2-mCherry::HIS3 MAT***a**	this study
TAY149	*pmc1::LEU2 vcx1Δ rcn1::ADE2 GFP-CRZ1(ΔZF)::URA3 HTB2-mCherry::HIS3 MAT***a**	this study
TAY157	*pmc1::LEU2 vcx1Δ crz1::G418 rcn1::ADE2 GFP-CRZ1(ΔZF)::URA3 HTB2-mCherry::HIS3 MAT***a**	this study

All strains are isogenic derivatives of strain K601/W303-1A (*ade2-1 can1-100 his3-11,14 leu2-3,112 trp1-1 ura3-1*).

***Table 3-2**. Primers used in Chapter 3.*

Primer Name	Sequence
HTB2 – F-mCherry	TGCCGTCTCCGAAGGTACTAGGGCTGTTACCAAAT ACTCCTCCTCTACTCAAGCCcagctgaagcttcgtacgc
HTB2 - R11	AAAATGCCACTAATAAAAAGAAAACATGACTAAA TCACAATACCTAGTGAGTGACcagtatagcgaccagcattcac

Capitalized regions are sequences immediately up- and down-stream of the STOP codon of *HTB2*. Lowercase regions match the plasmid template for PCR.

Growth assays

Strains were grown overnight in 200μL YPD at 30°C in a 96-well dish. Overnight culture was diluted back 300 times in 5/3X YPD supplemented with 8.33 mM succinic acid (YPDS). DMSO or 200 μM FK-506 in DMSO was added to a 1:150 final dilution. 120μL of cell dilution was added to 80μL calcium chloride ($CaCl_2$) or lithium chloride (LiCl) stock solutions in 96-well dishes to reach the final concentrations of ions. The range of final concentrations for $CaCl_2$ was 0 and 0.5 to 750 mM in 11 dilutions and for LiCl was 0 and 4 to 300 mM in 11 dilutions. Final concentration of FK-506 was 0.8 μM. Final concentration of succinic acid was 5 mM. Plates were incubated 24 hours at 30°C then OD_{650} was read on a Thermomax microplate reader spectrophotometer (Molecular Devices). The SOFTmax Pro software was used. 50% inhibitory concentration (IC_{50}) was calculated by interpolation to find $[CaCl_2]_{ex}$ or $[LiCl]_{ex}$ that allowed half maximal growth.

Microscopy

Three 1 mL serial dilutions of four strains were grown overnight at 30°C in SC-His-Ura. The entire 1 mL of the log-phase dilution was concentrated and suspended in ½X SC-His-Ura for microscopy. Volume of re-suspension was varied to result in approximately the same density for each strain. Cells were imaged at room temperature in CellASIC ONIX microfluidic plates using the perfusion control system to regulate media flow.

All microscopy was done at the Johns Hopkins University Integrated Imaging Center. Cells were imaged on a LSM 510 META confocal (Carl Zeiss) using a 100x/1.4 NA Plan-Apochromat (oil) DIC objective with a motorized stage. Excitation of the GFP was done using the 488nm laser and of mCherry using the 543 nm laser. The filters used were the green band pass filter from 505 to 530 nm and the red band pass filter from 560 to 615 nm. The optical slice thickness was 1 Airy Unit, 0.8 μm. The image size was 512x512 pixels for a 12-bit image. The image dimensions were 89.82x89.82 μm and the pixel size was 0.176 μm. The max scan speed was 1.60 μs/pixel and each line was averaged 4 times. Time-lapse images were obtained using the Multi-time plug-in of the AIM 4.2 software. When imaging four strains in a single experiment, images were obtained at each location approximately every 70 seconds, the minimum time for the microscope to image and move between all four locations. Due to drift in the z plane, the imaging had to be paused for occasional refocusing. This usually took less than one minute and was not done within ten minutes after switching media.

Graphing and image quantification

Individual time point images were combined into a single file by the microscope software. Further image manipulation was done in ImageJ 1.44o (http://rsbweb.nih.gov/ij/). Drift in the x-y plane was corrected using the StackReg plugin (http://bigwww.epfl.ch/thevenaz/stackreg/). Nuclei were identified by running "Analyze Particles" on the mCherry channel and a mask was generated. This mask was then applied to the GFP channel and intensity of the fluorescence was measured in the areas identified as nuclei. These measurements were then imported into Matlab (Mathworks), which graphed the intensity for each nucleus over time as single cell traces. Scripts for these analyses were obtained from Megan McClean (Hersen et al., 2008) and further modified to account for the longer time scale and cell division.

Coefficient of variation (CV) was calculated for each cell across a given time region with at least twenty fluorescence values in that time region. Standard error of the median CV of all cells was used to estimate 95% confidence intervals for the value of the median. If the bars representing the intervals do not overlap, the observations said to have statistically significant differences in their medians.

RESULTS

Experimental set-up

Cells were imaged while growing in CellASIC's ONIX microfluidic plates in continuously flowing media. This allowed for optimal cell growth conditions while keeping all cells in a single layer. These plates also allowed for fast and complete switching of media between up to six conditions, including complete washout of $CaCl_2$ or other signaling activator.

In order to accurately measure nuclear localization of Crz1, the nucleus was labeled by fluorescently tagging *HTB2*, one of the two histone H2B genes, with mCherry (Hersen et al., 2008). This allowed the red fluorescent nuclei to be identified independently of the probe and cells whose nuclei were not visible were eliminated from the analysis. A similar system, combining a truncated fluorescent NFAT and a fluorescent histone, has been used in mammalian cells (Lodygin et al., 2013).

Creation of inert probe of Cn activity

In order to ensure constant, high expression of the new probe, it was expressed from the strong, constitutive, feedback-free promoter GPD1. Some studies have shown that Crz1 overexpression induces Cn-independent gene transcription or affects the responsiveness of gene transcription (Matheos et al., 1997; Stathopoulos and Cyert, 1997). To prevent these effects, the C-terminus, containing the DNA-binding zinc-finger (ZF) domain, was removed. This also further reduced feedback of Crz1 and of factors that regulate $[Ca^{2+}]_{cyt}$ and Cn. GFP was fused to the N-terminus of Crz1. This created a protein, GFP-

Crz1(ΔZF), that is shuttled in and out of the nucleus in response to Cn that cannot bind DNA and therefore should be inactive with regards to transcription. Previous work has shown that GFP-Crz1(ΔZF) is translocated into and out of the nucleus in the same manner as full-length GFP-Crz1, which is fully functional and replaces Crz1p in deletion strain (Stathopoulos-Gerontides et al., 1999).

GFP-CRZ1(ΔZF) does not affect cell growth in standard medium

Before using the GFP-Crz1(ΔZF) probe, the probe's effects on cell growth have to be tested in standard conditions. The probe was expressed in the W303 WT background and growth was compared to growth of an isogenic strain without the probe. When grown in standard medium for 24 hours, the *GFP-CRZ1(ΔZF)* strain grew to the same cell density as the WT control strain, indicating that the probe has no effect in this condition (Fig. 3-1). In medium supplemented with high concentrations of $CaCl_2$, the *GFP-CRZ1(ΔZF)* strain grew more slowly than the control (Fig. 3-2). A smaller effect of the probe was seen in LiCl. This shows that the probe is not completely inert and interferes with the cellular response to toxic levels of these ions over long periods of time. However, when observed over only 6 hours in continuously flowing medium with 200 mM $CaCl_2$ added, most of the cells appeared normal in morphology, growth, and division.

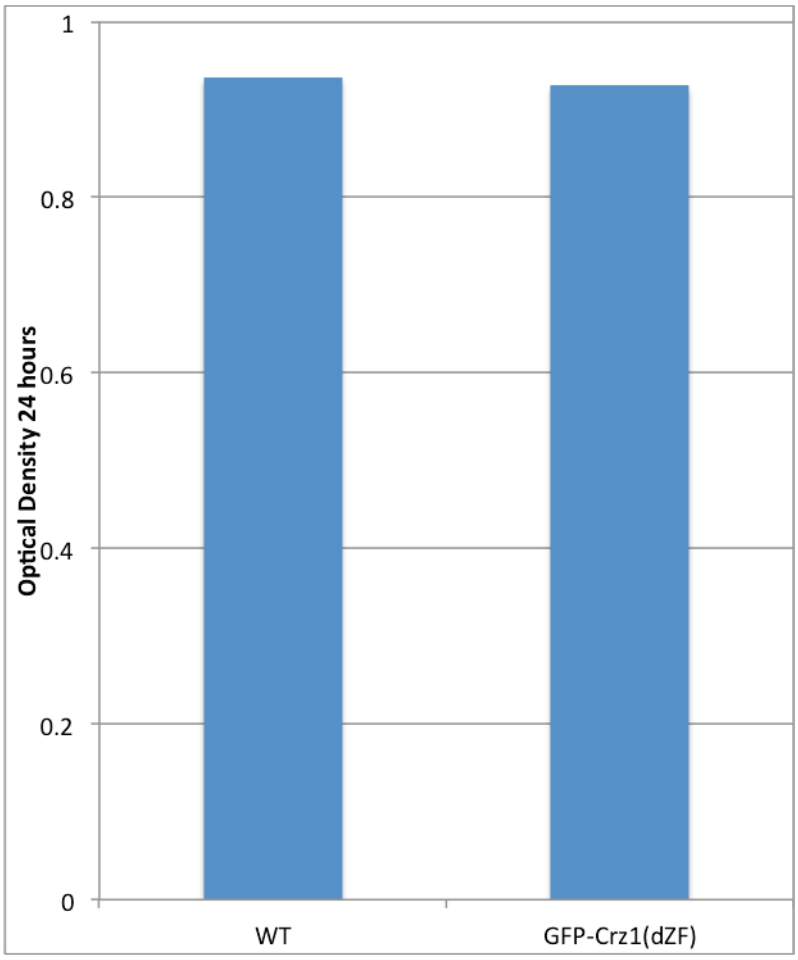

Figure 3-1. *GFP-CRZ1(ΔZF) does not affect cell growth in standard medium.*

WT strains with and without *GFP-CRZ1(ΔZF)* were grown in YPDS for 24 hours at 30°C.

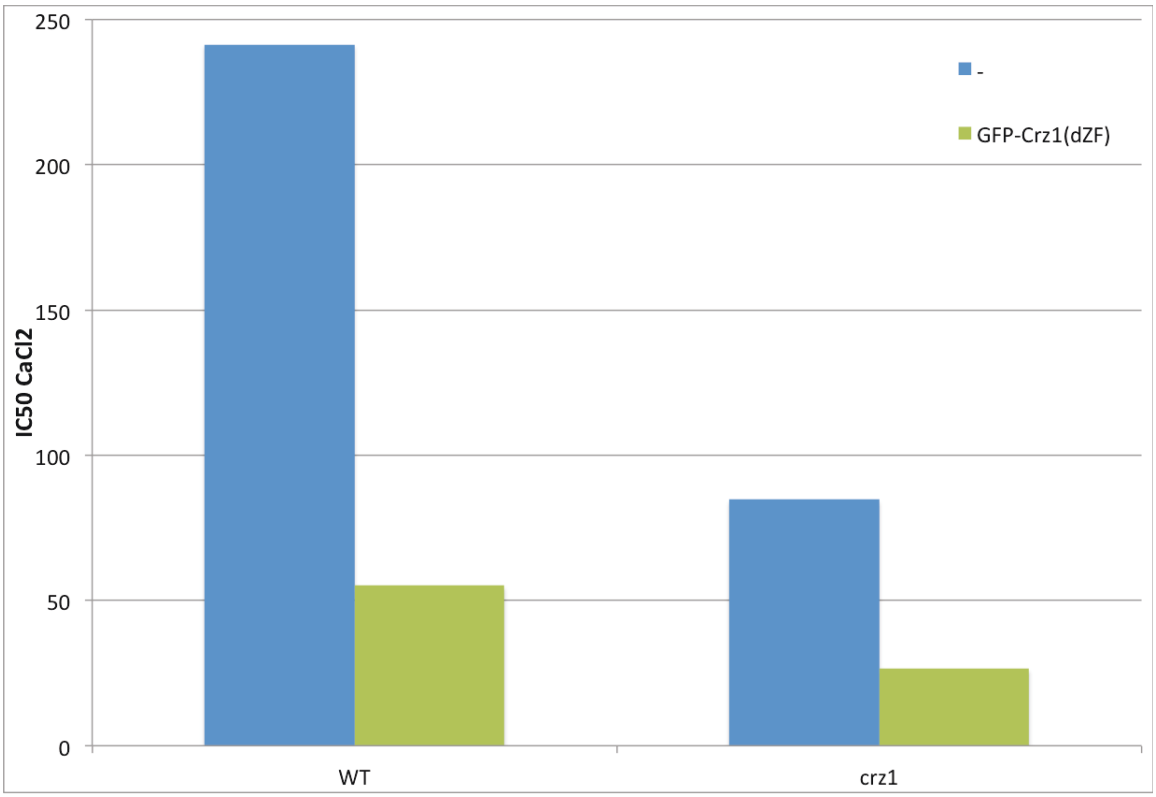

Figure 3-2. *GFP-CRZ1(ΔZF) slows growth in high concentrations of* $CaCl_2$.

WT and *crz1Δ* strains with and without *GFP-CRZ1(ΔZF)* were grown in YPDS with varying concentrations of $CaCl_2$ for 24 hours at 30°C.

GFP-CRZ1(ΔZF) does not activate or interfere with endogenous targets of Crz1

If the truncated probe is nonfunctional for gene expression, it would not replace the function of endogenous Crz1. To test this, the GFP-Crz1(ΔZF) probe was expressed in a *crz1Δ* strain. Crz1 is required for expression of Ena1p, a pump that transports Li^+ out of the cell and allows growth in medium containing elevated LiCl. If the probe induced gene expression, the *crz1Δ* strain expressing the probe would be more resistant to LiCl than the strain without it. The *crz1Δ GFP-CRZ1(ΔZF)* strain was slightly more sensitive to LiCl than *crz1Δ*, not resistant (Fig. 3-3). This indicates that the probe does not replace Crz1 function.

To be called inert, the probe must also not interfere with the cellular process it is being used to measure. Since it is overexpressed, it could titrate Cn and interfere with its other functions. To test this, Cn was examined for its ability to interact with two specific targets: the vacuolar Ca^{2+}/H^+ exchanger Vcx1p and the Cn-inhibitory complex comprising immunophilins and the drug FK-506. In *pmc1Δ* cells, which lack the vacuolar Ca^{2+} ATPase, Vcx1p is the only vacuolar Ca^{2+} transporter and its function is strongly inhibited by Cn. Therefore, *pmc1Δ* cells are hypersensitive to $CaCl_2$ and are rescued by deletion of Cn or inhibition with FK-506. If the probe interferes with Cn inhibition of Vcx1p, the probe will rescue growth of *pmc1Δ* cells. If the probe interferes with the ability of the immunophilin/FK-506 complex to bind and inhibit Cn, *pmc1Δ* cells would be hypersensitive even in the presence of FK-506. If the probe is truly inert, it will neither increase Ca^{2+} resistance of a *pmc1Δ* strain nor decrease resistance of the same strain in the presence of FK-506. The *pmc1Δ GFP-CRZ1(ΔZF)* strains showed slightly decreased Ca^{2+} resistance, rather than increased, indicating that

Cn inhibition of Vcx1p was unaffected by the presence of the probe (Fig. 3-4). Furthermore, FK-506 restored growth in high $CaCl_2$ in the *pmc1Δ GFP-CRZ1(ΔZF)* strains. Therefore it can be concluded that the probe does not interfere with Cn binding to the FK-506/FK binding protein complex either.

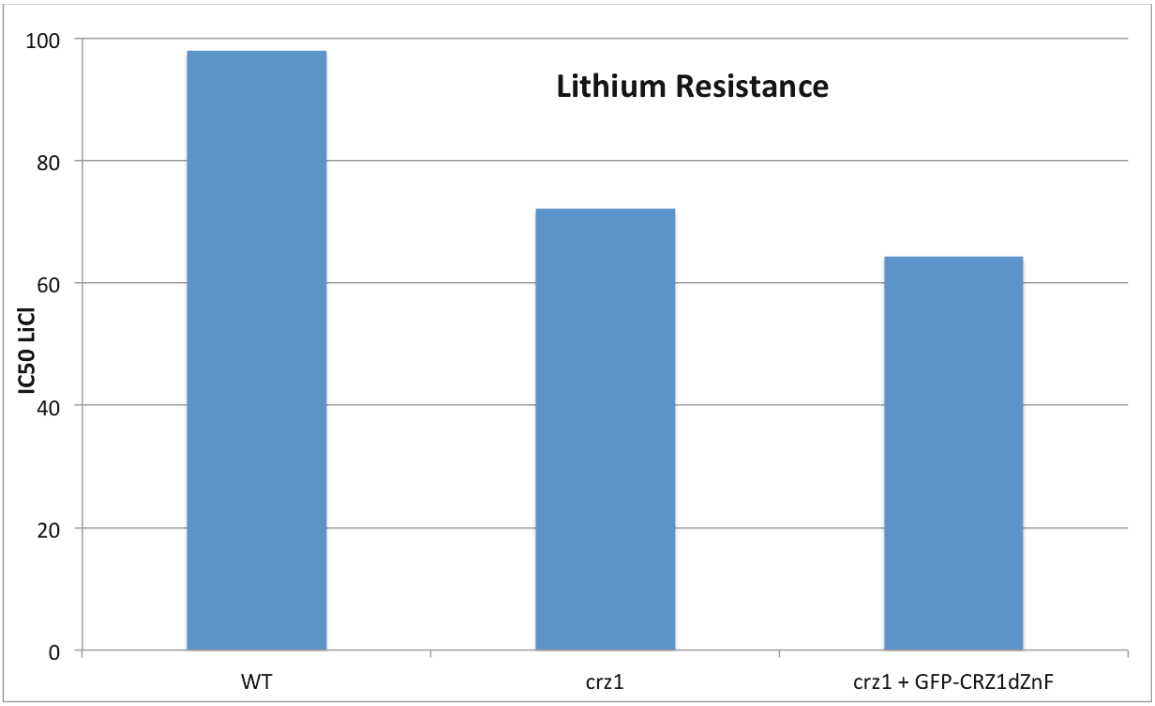

Figure 3-3. *GFP-Crz1(ΔZF) does not complement lack of Crz1p.*

WT, *crz1Δ*, and *crz1Δ GFP-CRZ1(ΔZF)* strains were grown in YPDS with varying concentrations of LiCl for 24 hours at 30°C.

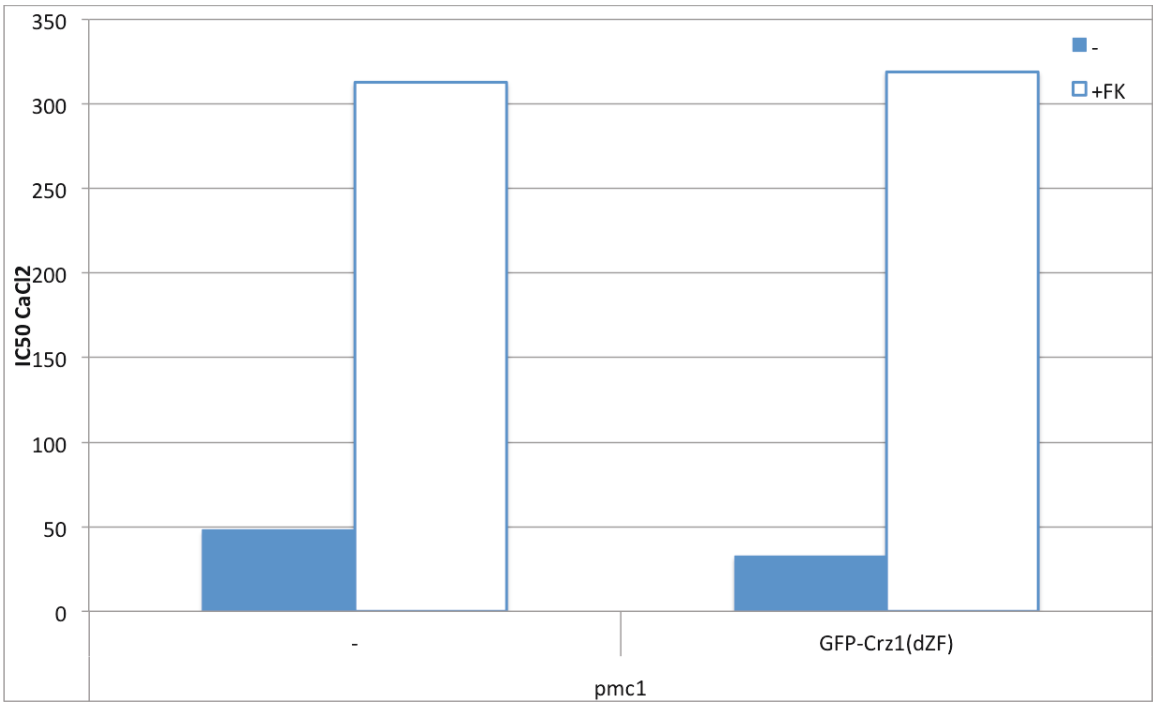

Figure 3-4. *GFP-CRZ1(ΔZF) does not interfere with Cn binding to targets.*

pmc1Δ and *pmc1Δ GFP-CRZ1(ΔZF)* strains were grown in YPDS with varying concentrations of $CaCl_2$ with or without 0.8 μM FK-506 for 24 hours at 30°C.

High frame rate causes some bleaching of GFP but not mCherry after 500 frames

In order to image the probe over the time scale observed in the β-galactosidase assays, the fluorescence needs to be stable enough to be imaged at least once per minute over at least five hours. To test for bleaching, cells were imaged at 20-second intervals over five hours in continuously flowing ½x medium. If the GFP and mCherry are stable, the signal would be constant over time; if bleaching occurs, fluorescence would decrease. The mCherry signal was steady over the entire movie, showing that there is no significant effect of mCherry bleaching (Fig. 3-5 A). In order to measure bleaching of the GFP, fluorescence intensity for the whole image was used because of the difficulty in identifying individual cells in close proximity. Downward peaks in intensity were caused by focal drift. There was a small decrease in the total GFP intensity by the end of the movie, but intensity is fairly steady through 500 frames (167 minutes), which constitutes more than the 360 frames of a 6-hour movie at the usual frame rate (Fig. 3-5 B). Cells also grew and divided normally for over 500 frames (167 minutes), showing that there is no negative effect of such intense light exposure. This means that phototoxicity and bleaching are not of concern during the course of a movie imaged less than once per minute.

Figure 3-5. *High frame rate causes some bleaching of GFP but not mCherry after 500 frames.*

pmc1Δ vcx1Δ crz1Δ cells were imaged at approximately 20-second intervals for over 300 minutes. 500 frames were captured in 160 minutes. (A) Nuclear mCherry fluorescence. Traces represent individual nuclei. (B) Mean GFP intensity of the whole field of cells over time. Downward peaks in intensity were caused by focal drift.

A

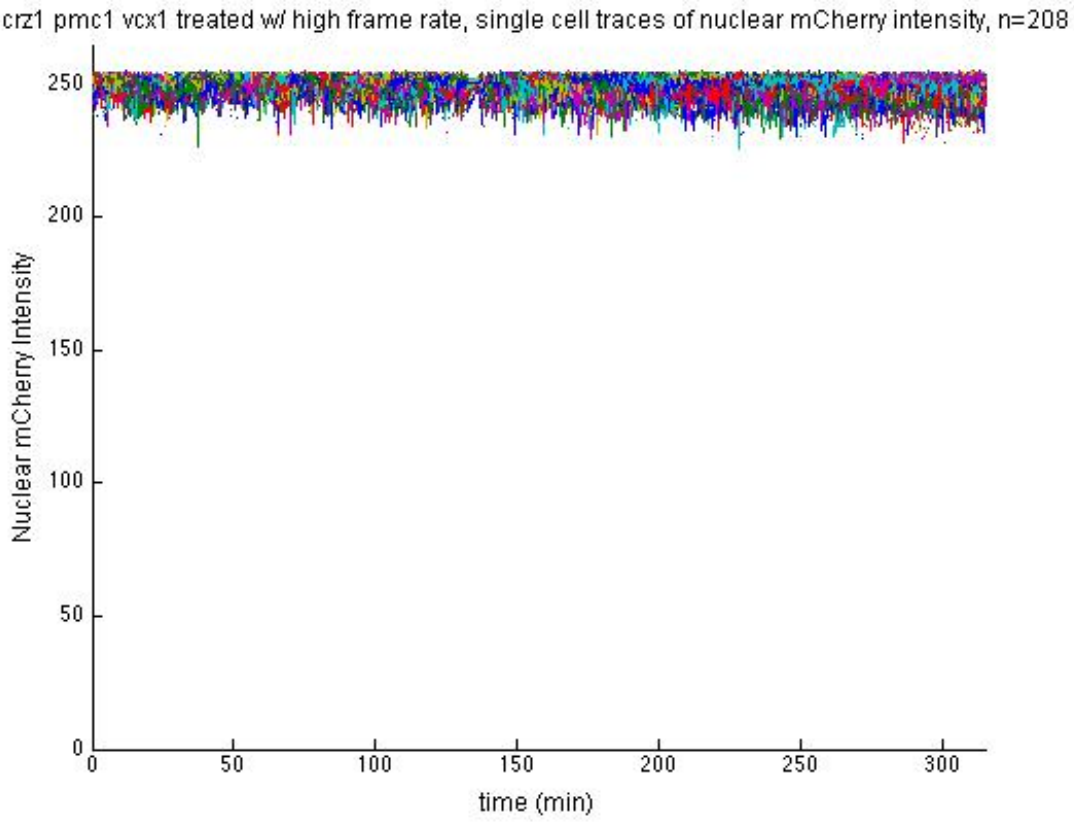

B

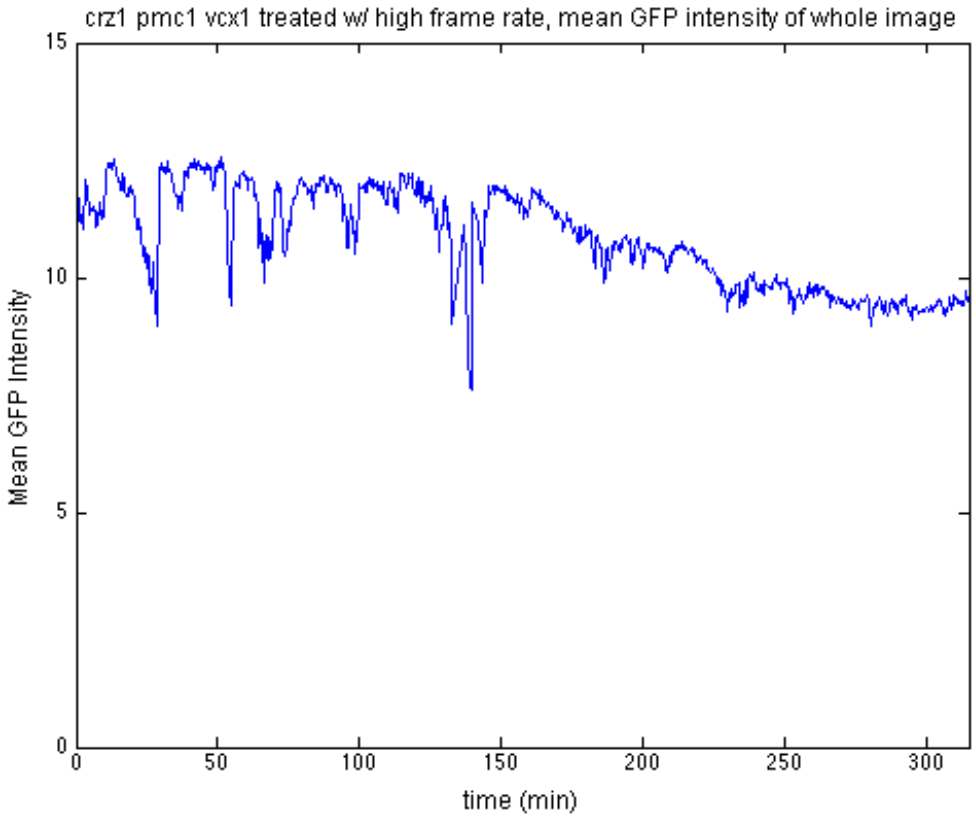
crz1 pmc1 vcx1 treated w/ high frame rate, mean GFP intensity of whole image
Mean GFP Intensity
time (min)
0
5
10
15
0
50
100
150
200
250
300

Microscopy

Wild-type cells expressing GFP-Crz1(ΔZF) and Htb2-mCherry were imaged in continuously flowing ½X selective media. Images were taken at 70-to-80-second intervals. Fields typically contained 10 to 400 cells. The red signal strongly marked the nucleus. The green signal was diffuse throughout the cytoplasm and was clearly excluded from the nucleus and vacuole, though occasional partial nuclear localization was seen in individual cells, lasting two to ten minutes (Fig. 3-6, A-J). Upon switching the flow to ½X media with 200 mM $CaCl_2$ added, the green signal became highly colocalized with the red (Fig. 3-6, K-O). This happened nearly synchronously in the majority of the cells. Some faint green signal was still visible in the cytoplasm of most cells, even when the nuclear signal was at its maximum. After a dwell time in the range of ten minutes, the green signal returned to being entirely cytoplasmic (Fig. 3-6, P-T). The timing and extent of the return of the probe to the cytoplasm was not uniform in the population. Some unsynchronized partial nuclear localization was seen during the prolonged $CaCl_2$ exposure, typically lasting between two and twenty minutes, similar to what was seen before addition of $CaCl_2$.

By using a mask generated from the locations of the red fluorescence to identify the nuclei, the green fluorescence in each nucleus could be quantified at each time point. From this, a graph could be generated to represent the entire movie in one image. Each line on the graph represents the mean GFP fluorescence in a single nucleus (Fig. 3-6 U).

Figure 3-6. *WT cells responding to addition of $CaCl_2$.*

WT cells in continuously flowing ½X SC. Medium switched to continuously flowing ½X SC + 200 mM $CaCl_2$ at 1:29:20 (89 min.). (A-T) Scale bar 10 μm. (U) Single cell traces of nuclear GFP intensity over time. Black bar on time axis indicates medium supplemented with 200 mM Ca^{2+}.

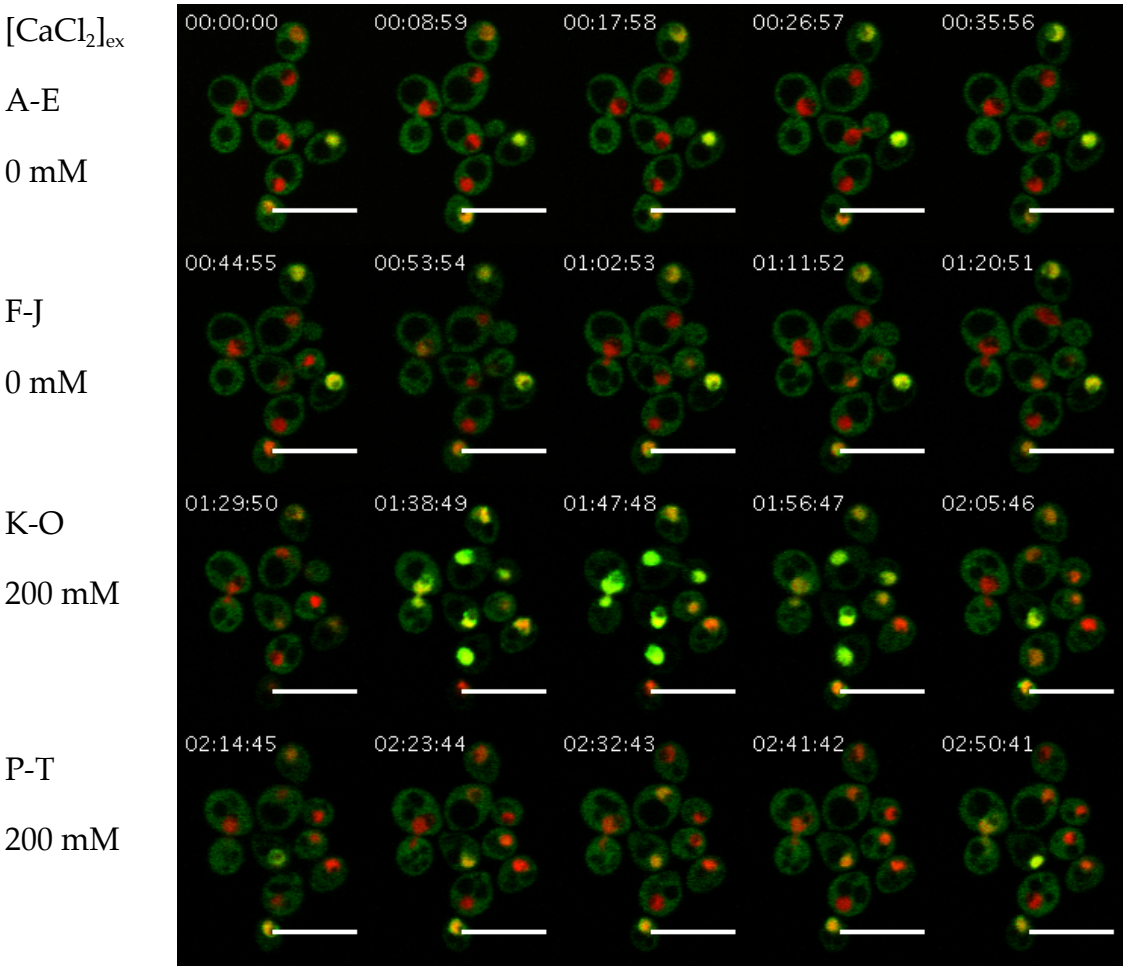

U

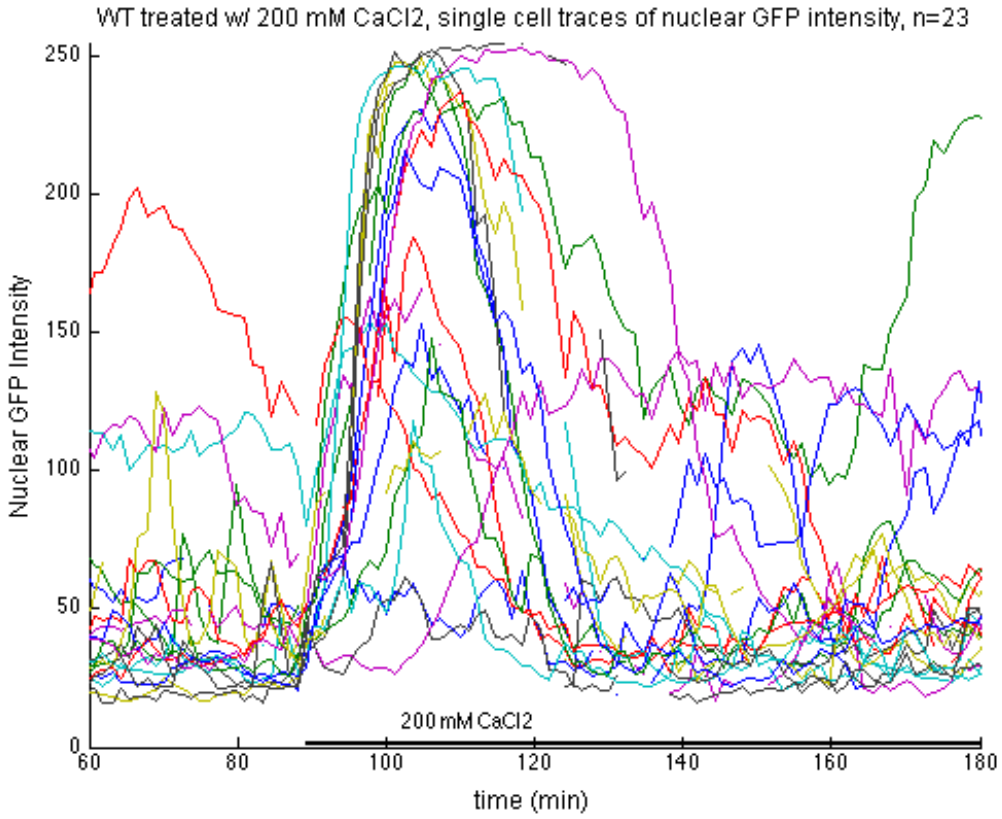
WT treated w/ 200 mM CaCl2, single cell traces of nuclear GFP intensity, n=23
Nuclear GFP Intensity
250
200
150
100
50
0
200 mM CaCl2
60
80
100
120
140
160
180
time (min)

The addition of $CaCl_2$ was used here to induce Cn signaling because it has been shown to raise $[Ca^{2+}]_{cyt}$ quickly (Miyakawa and Mizunuma, 2007). Although not physiological, this stimulus allows study of the Cn response to Ca^{2+} without turning on other response pathways that might cause feedback onto Cn.

Probe translocation is dependent on Ca^{2+} and Cn

In order to use the probe to study the response to Ca^{2+} stimulation, it is necessary to confirm that it is responsive to Ca^{2+}. It is possible that the peak in nuclear fluorescence is caused the change in pressure used to rapidly switch the medium in the flow chamber, or by some other artifact of the experimental system, and that the probe does not represent Ca^{2+}-dependent activation of Crz1. To test this, cells were switched from ½X SC to the same medium from a different inlet using the same increase in pressure (Fig. 3-7, A and C). In these strains, no peak was seen that corresponds to the peak seen in cells switched to ½X SC supplemented with 200 mM $CaCl_2$ (Fig. 3-7, B and D). Similar scaled responses were seen in higher and lower concentrations of $CaCl_2$ (Fig. 3-7 E-H). Additionally, when the medium was switched back to unsupplemented ½X SC during the nuclear localization peak, the nuclear fluorescence signal ended abruptly (Fig. 3-7 I). These results confirm that the probe is responding to the increase in $[CaCl_2]_{ex}$.

Since the GFP-Crz1(ΔZF) probe retains the SRR domain required for interaction with Cn, its nuclear localization should also depend on Cn (Stathopoulos-Gerontides et al., 1999). To test this, the Cn inhibitor FK-506 was added to the medium. When switched from unsupplemented ½X SC to ½X SC

with 0.8 μM FK-506, the partial nuclear localization seen in some cells disappeared (Fig. 3-8, compare left to center portion). Additionally, when $CaCl_2$ was added in the presence of FK-506, no peak of nuclear localization was seen (Fig. 3-8, right portion). This confirms that nuclear localization of the GFP-Crz1(ΔZF) probe is dependent on Cn activity.

Figure 3-7. *Peak in nuclear fluorescence is caused by $CaCl_2$.*

(A-D) WT cells in continuously flowing ½X SC. Black bar on time axis indicates the switch to the same medium from a different well (A, C) or to medium supplemented with 200 mM $CaCl_2$ (B, D). A and B were run in parallel; C and D were run in parallel. (E-H) Single experiment with range of $CaCl_2$ concentrations added: (E) 0, (F) 100, (G) 200, and (H) 300 mM $CaCl_2$. (I) *pmc1Δ vcx1Δ crz1Δ* cells in continuously flowing ½X SC. Black bars on time axis indicates medium supplemented with 200 mM $CaCl_2$, (I) then back to unsupplemented medium.

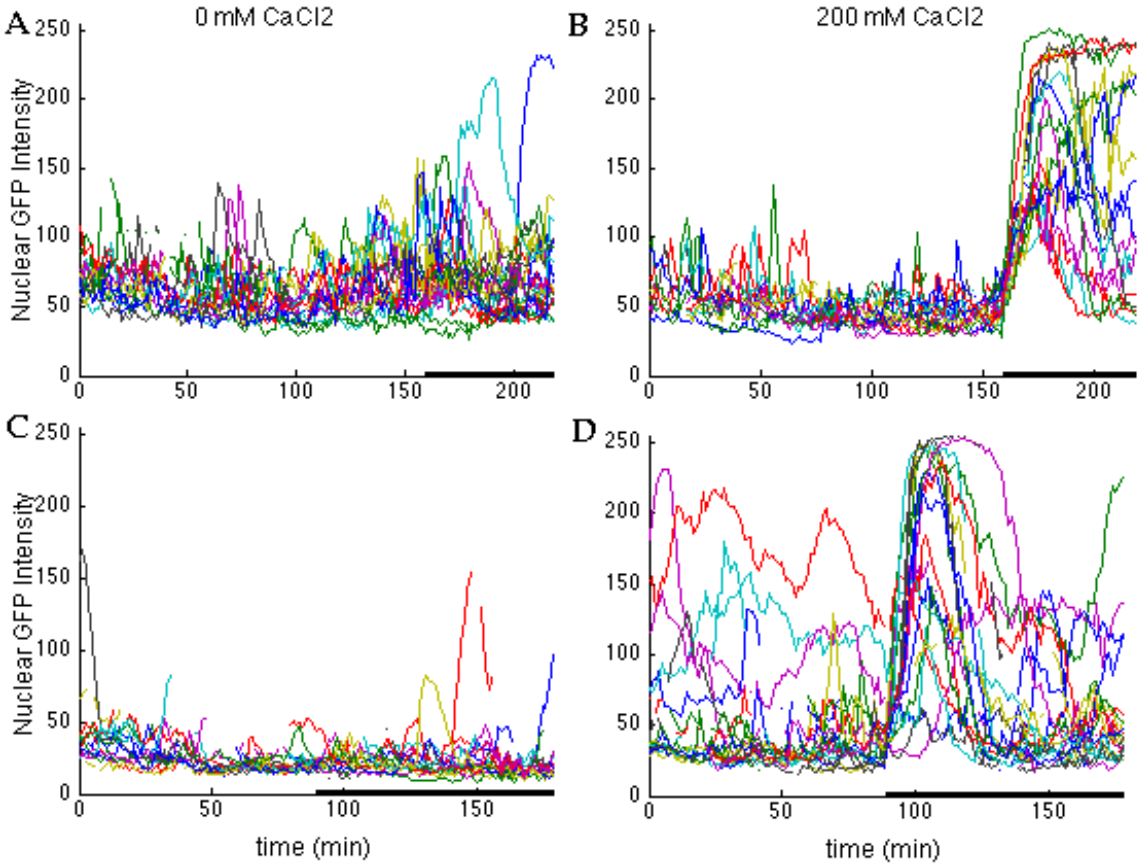

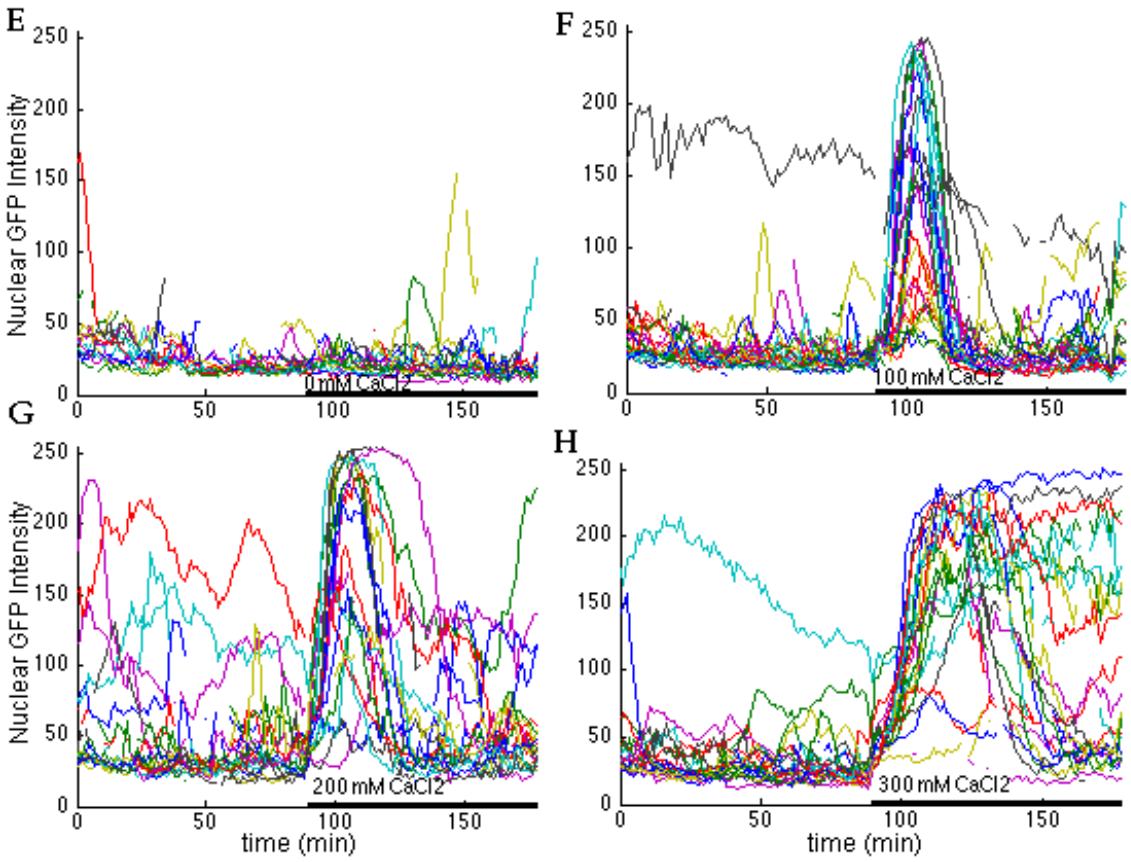
E
F
G
H
Nuclear GFP Intensity
time (min)
0 mM CaCl2
100 mM CaCl2
200 mM CaCl2
300 mM CaCl2
0
50
100
150
200
250

I

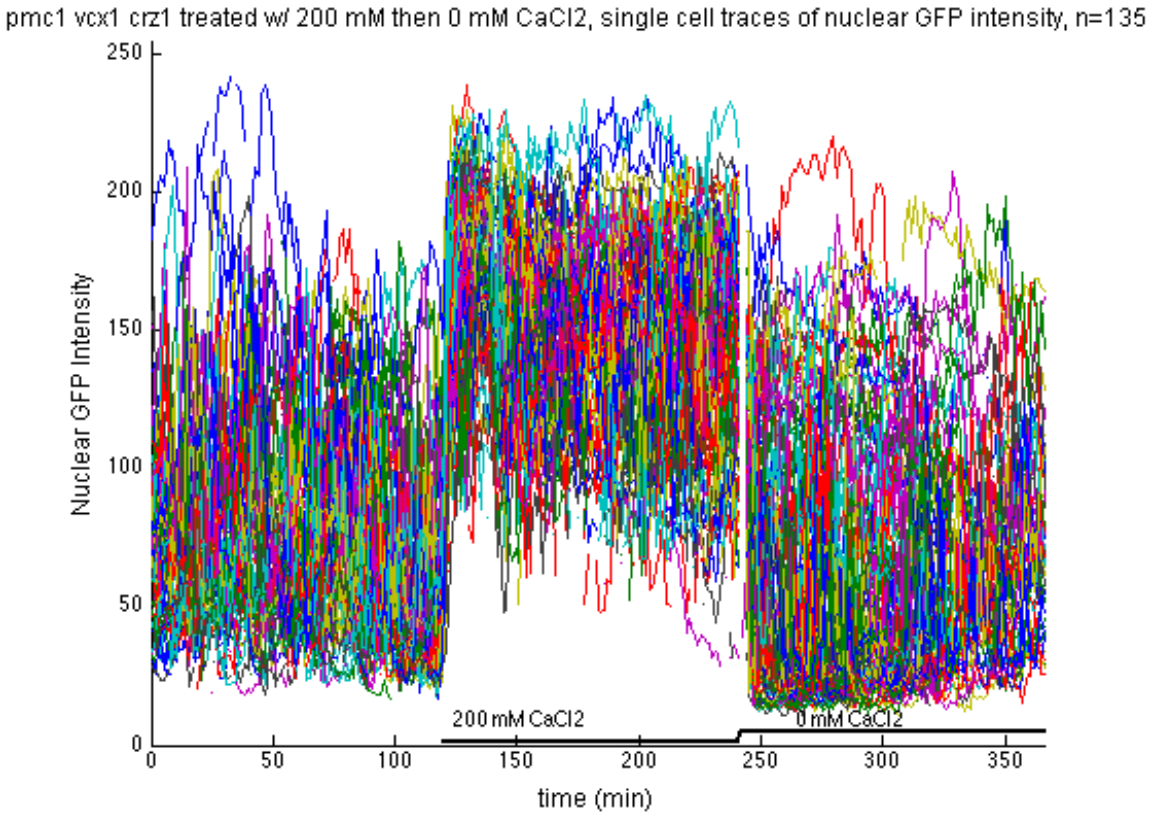
pmc1 vcx1 crz1 treated w/ 200 mM then 0 mM CaCl2, single cell traces of nuclear GFP intensity, n=135
Nuclear GFP Intensity
250
200
150
100
50
0
0
50
100
150
200
250
300
350
time (min)
200 mM CaCl2
0 mM CaCl2

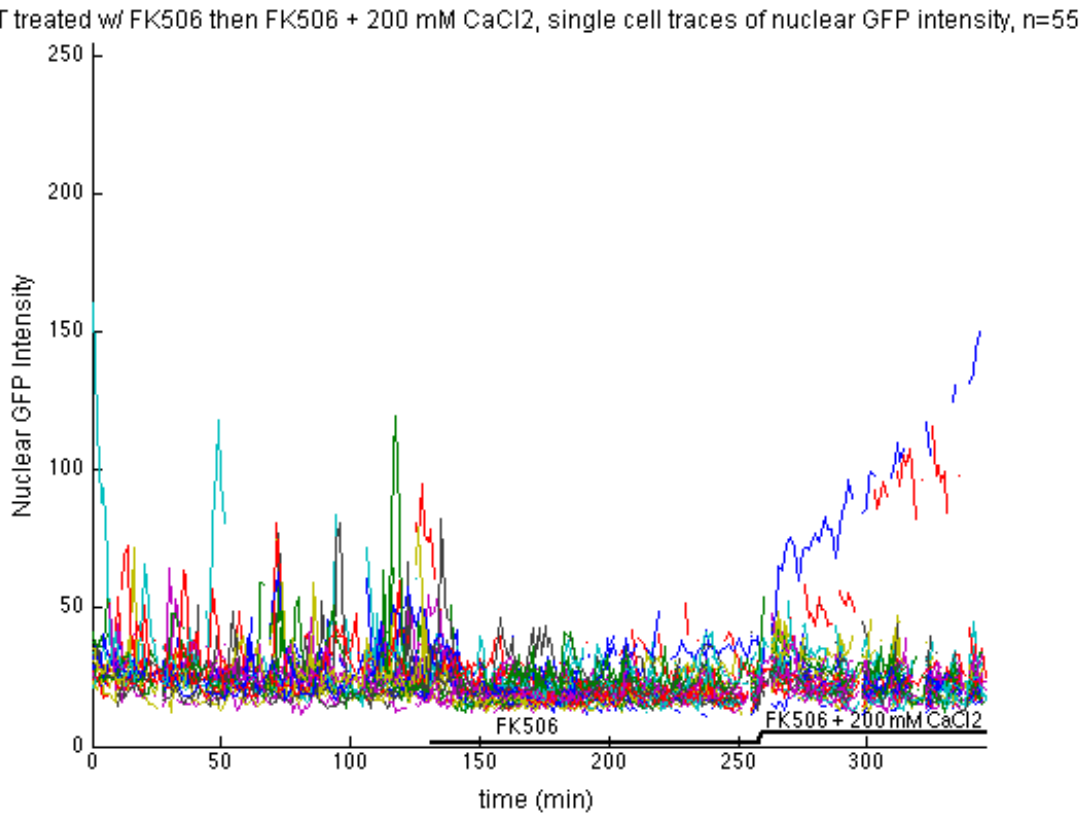

***Figure 3-8**. Inhibition of Cn reduces nuclear signal.*

WT cells in continuously flowing ½X SC. Blacks bar on time axis indicates the switch to ½X SC with 0.8 μM FK-506 then with 0.8 μM FK-506 and 200 mM $CaCl_2$.

Probe shows "flickering" in constant conditions

Examination of the region of adaptation, after the initial response peak has dissipated, of the above graphs (Fig. 3-7) reveals a region of noisy nuclear fluorescence that is not synchronized between cells. Some cells show brief partial nuclear localization of the probe and then return to baseline while others remain at higher signal, fluctuating between low and high nuclear localization. These fluctuations have been named "flickers" and they are evident before treatment, in low-Ca^{2+} medium, as well as in cells that have adapted to high-Ca^{2+} medium. Flickering may represent Cn activity in cells at equilibrium. It occurs to differing degrees in a variety of conditions such as unsupplemented medium and the presence of FK-506, and varies by strain. Flickering can be quantified by calculating coefficient of variation (CV) of the nuclear fluorescence of each cell, as described above, because CV measures how much the values deviate from the mean. CV is independent of the mean, so higher background fluorescence in a particular strain or replicate does not affect CV. Higher CV indicates more change in nuclear fluorescence. This implies that Cn is activating the probe more often in cells with higher CVs. Measurement of CV allows direct comparison of Cn activation between strains or between conditions.

Pmc1 and Vcx1 suppress flickering

WT cells growing in unsupplemented ½X SC medium showed some flickering. Deletion of either *PMC1* or *VCX1* caused more flickering, as measured by the increase in CV (Fig. 3-9). This indicates that disruption of vacuolar Ca^{2+} transport causes increased Cn activity even in the absence of

stimulation or excess external Ca^{2+}. This effect on $[Ca^{2+}]_{cyt}$, and thereby on Cn activity, is expected in the case of Vcx1. The exchanger is active when Cn activity is low and keeps Cn activity low when it is active. It is somewhat surprising, however, that knockout of Pmc1p has a measurable effect, since its expression is low in the absence of stimulation. Despite this, it appears either that there is enough Cn-independent expression of Pmc1p or that flickering causes enough Cn-dependent gene expression for Pmc1p to regulate cytosolic Ca^{2+} equilibrium in resting conditions.

It is difficult to determine the relative contributions of Pmc1p and Vcx1p to flickering since there is some variation between experiments in the increase of CV from WT to single mutants. It is clear that there is a small additive effect, indicating that both transporters contribute to $[Ca^{2+}]_{cyt}$ homeostasis in resting conditions.

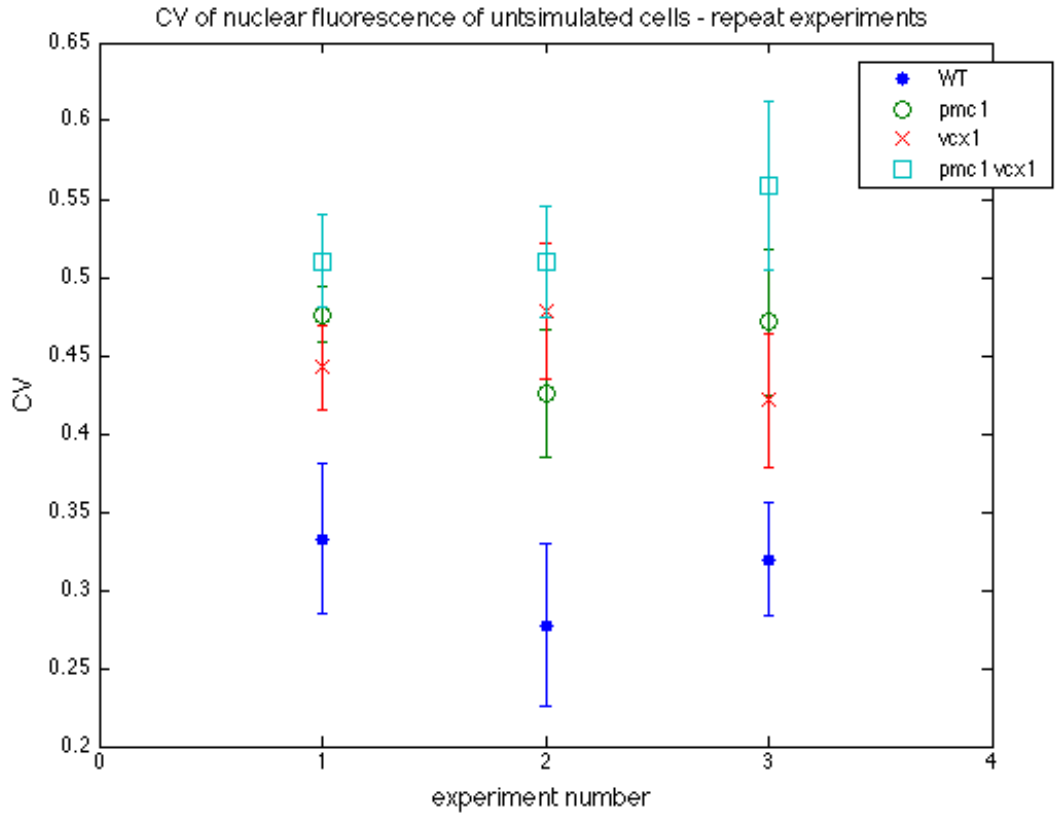

Figure 3-9. *Pmc1 and Vcx1 suppress flickering.*

CVs of WT, *pmc1Δ*, *vcx1Δ*, and *pmc1Δ vcx1Δ* cells in continuously flowing ½X SC for (experiments 1, 2) 200 or (experiment 3) 100 minutes. Symbols are median values of CVs and bars represent standard error of the median.

Flickering is dependent on Cn

As shown in Fig. 3-8, flickering in WT is suppressed by the addition of FK-506. Flickering in the strains lacking the vacuolar transporters is suppressed as well (Fig. 3-10). CVs in all strains plus FK-506 are similarly low, indicating that the increase in CVs in the deletion mutants is caused by increased Cn activity. This extra activity is fully suppressed by FK-506.

Crz1 increases flickering

If the Pmc1p activity seen in unstimulated WT cells is dependent on transcriptional upregulation by Crz1p, knocking out *CRZ1* should have the same effect as knocking out *PMC1*. Instead of an increase in flickering, however, the *crz1Δ* strain showed a small decrease in flickering. There was still an increase in flickering in the *pmc1Δ crz1Δ* strain relative to the *crz1Δ* strain, but flickering in the *pmc1Δ crz1Δ* strain was lower than in the *pmc1Δ* strain (Fig. 3-11). These differences indicate that the Pmc1p activity that suppresses flickering in WT is not dependent on Crz1p. Additionally, the increase in flickering caused by deleting either *PMC1* or *VCX1* is partially dependent on Crz1p. This suggests that there is a Crz1p-dependent factor that contributes to flickering. This is opposed by vacuolar Ca^{2+} transport through Pmc1 and Vcx1.

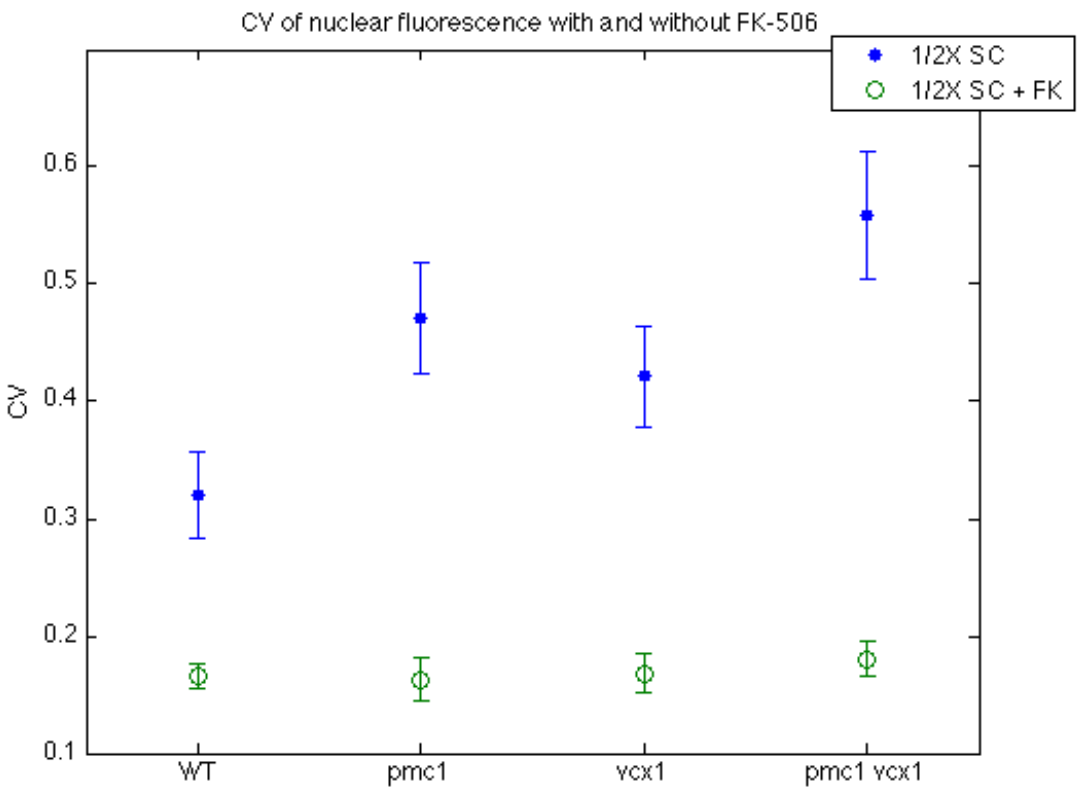

Figure 3-10. *Flickering is dependent on Cn.*

CVs of WT, *pmc1Δ*, *vcx1Δ*, and *pmc1Δ vcx1Δ* cells in continuously flowing ½X SC or ½X SC with 0.8 μM FK-506 for 100 minutes in each condition. Symbols are median values of CV and bars represent standard error of the median.

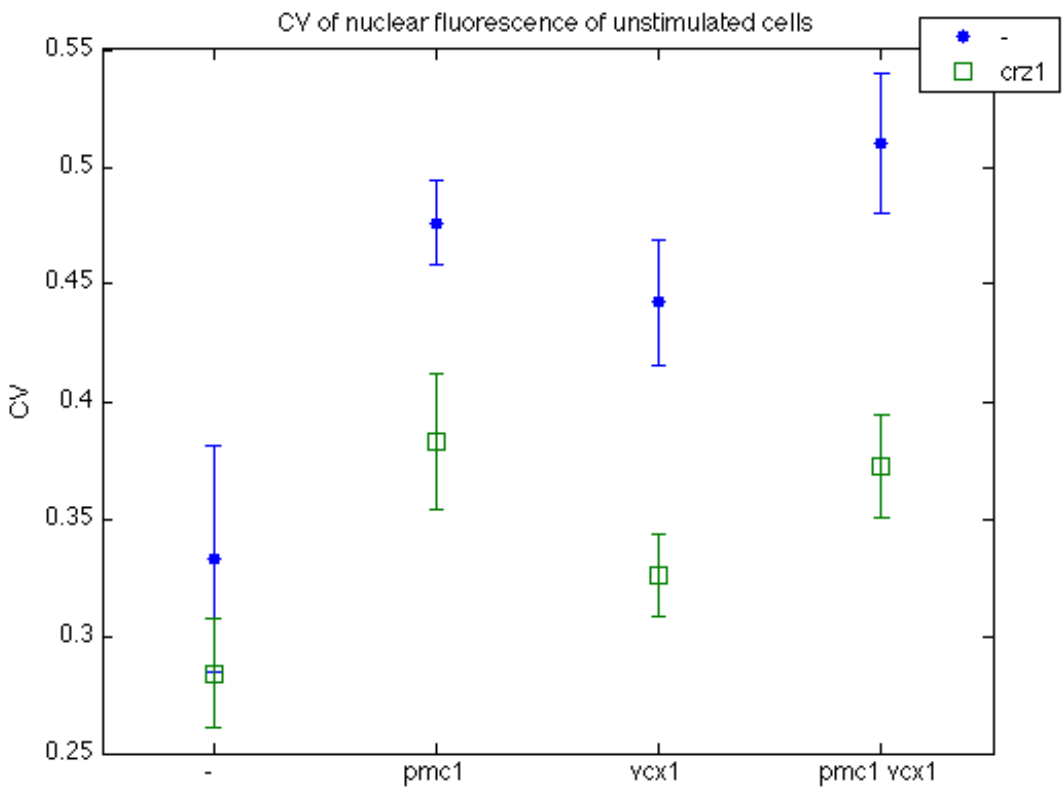

Figure 3-11. *Crz1 increases flickering.*

CVs of WT, *pmc1Δ*, *vcx1Δ*, *pmc1Δ vcx1Δ*, *crz1Δ*, *pmc1Δ crz1Δ*, *vcx1Δ crz1Δ*, and *pmc1Δ vcx1Δ crz1Δ* cells in continuously flowing ½X SC for 100 minutes. Symbols are median values of CVs and bars represent standard error of the median. *CRZ1* strains were run separately from *crz1Δ* strains.

Rcn1 increases flickering independently of Crz1

One possible target of Crz1p that could be contributing to flickering is the Cn chaperone Rcn1p. If it is, knocking out *RCN1* in strains containing *CRZ1* should lower flickering in the same way that knocking out *CRZ1* does but have no effect in *crz1Δ* strains. *pmc1Δ vcx1Δ rcn1Δ* strains did have less flickering than the strains expressing *RCN1*, but this decrease was also seen in the strains lacking *CRZ1* (Fig. 3-12). This indicates that Rcn1p contributes to flickering in a Crz1-independent way. Further, this shows that the high flickering caused by disruption of vacuolar Ca^{2+} transport requires Rcn1p activity.

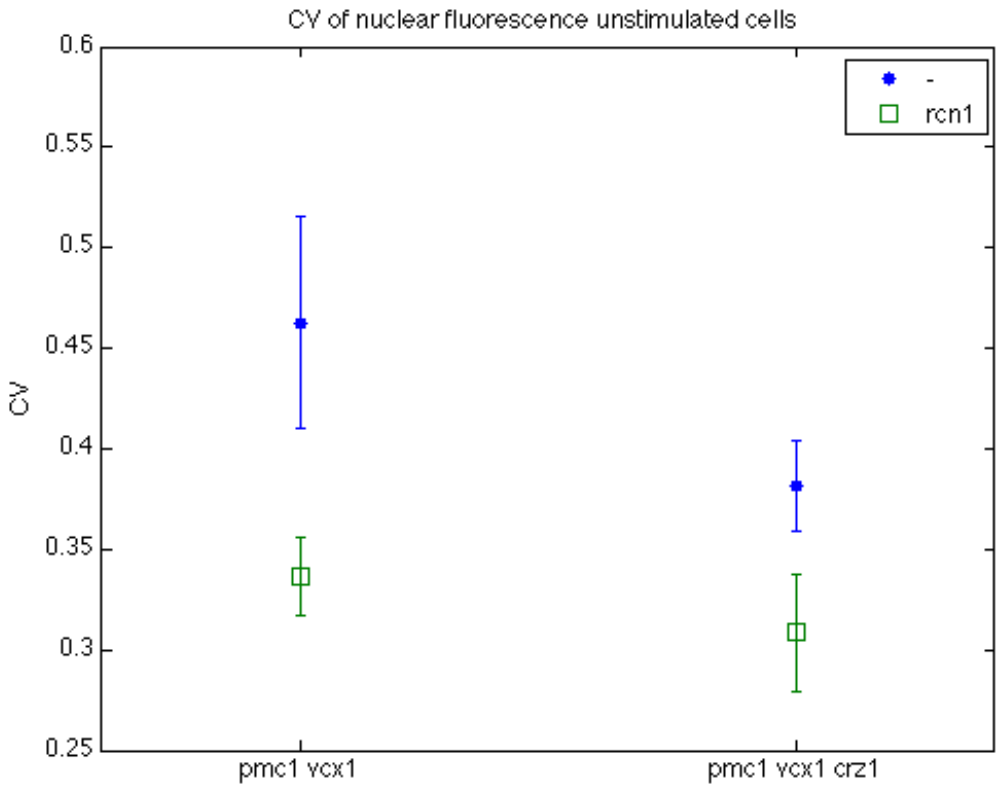

Figure 3-12. *Rcn1 increases flickering independently of Crz1.*

CVs of *pmc1Δ vcx1Δ*, *pmc1Δ vcx1Δ crz1Δ*, *pmc1Δ vcx1Δ rcn1Δ* and *pmc1Δ vcx1Δ crz1Δ rcn1Δ* cells in continuously flowing ½X SC. Symbols are median values of CVs and bars represent standard error of the median. Values are from multiple experiments pooled together.

DISCUSSION

Measurement of Cn activity will be crucial to clinical manipulation of Cn signaling. Nuclear localization of Crz1 is a close readout of Cn activation. By observing the movement of GFP-tagged Crz1 within the cell, changes in the activation state of Cn can be determined. Existing assays for measuring Cn activity are not precise and lack resolution. I have described the development of a novel inert probe for Cn activity using an inactive, truncated form of the transcription factor Crz1 fused to GFP. Although the probe does cause some toxicity in the presence of high concentrations of Ca^{2+} and Li^{+}, it can be considered inert because it does not affect growth in standard medium or low concentrations of $CaCl_2$, it does not replace Crz1 function in a *crz1Δ* strain, and it does not interfere with calcineurin's ability to inhibit its target Vcx1 or be inhibited by the drug FK-506.

Other experiments using a similar, full-length Crz1-GFP probe showed that blue light, such as is used to induce GFP fluorescence, caused the probe to permanently localize to the nucleus in the absence of other stresses (Bodvard et al., 2013). Therefore, the nuclear localization seen above could be simply due to the light used to see it. That experiment used continuous illumination, however, and the experiments described above used short, intermittent illumination. The low level of nuclear GFP-Crz1(ΔZF) localization seen in the absence of $CaCl_2$ (Figs. 6-7) indicates that light is not a significant stress in these conditions.

I confirmed that the GFP-Crz1(ΔZF) probe measures Cn activity by imaging the probe in the presence of the Cn inhibitor FK-506. When Cn is

inhibited, the probe remains entirely cytoplasmic except when the cells are stimulated by very high extracellular Ca^{2+}.

This new probe has allowed me to examine the effects of many cellular factors on Cn activation in both stimulating and non-stimulating conditions. I found that Cn is active in non-stimulating conditions and can be suppressed by FK-506. This activity causes flickering of the probe into and out of the nucleus which can be quantified to compare Cn activation in different conditions.

The Ca^{2+} transporters in the vacuole act as negative regulators of Cn by keeping cytosolic Ca^{2+} concentration low and thereby preventing Cn activation. They also remove Ca^{2+} after a signaling event to turn off Cn and end the signal. I found that fully functional vacuolar Ca^{2+} transport is needed to prevent hyperactivation of Cn in non-stimulating conditions. Flickering is increased by deleting either vacuolar transporter, Pmc1p or Vcx1p, and further increased by deleting both. This shows that disregulating cytosolic Ca^{2+} equilibrium by compromising vacuolar Ca^{2+} transport leads to increased Cn activity. Readouts of transcription would be needed to determine if this increased Cn activity is a productive attempt to upregulate *PMC1* and other genes that are needed to control cytosolic Ca^{2+} equilibrium or if it is unproductive shuttling of Crz1p without activating transcription.

I also see that Crz1p is necessary for basal Cn activity in non-stimulating conditions. Neither Pmc1p nor Rcn1p is necessary for Crz1p to promote flickering, indicating that another target or targets of Crz1p are needed for full Cn activity even in the absence of stimulation. Over 150 other targets of Crz1p have been described in the literature, including genes involved in ion transport,

cell signaling, and protein degradation (Yoshimoto et al., 2002). Analysis of mutants for selected targets of Cn in the presence and absence of *CRZ1* would allow identification of the factor or pathway that is increasing Cn activity in a Crz1-dependent manner. The positive effect of Crz1 on flickering also shows that the flickering in WT likely activates a positive feedback loop through Crz1-dependent gene transcription. Cn/Crz1-dependent transcription in the absence of stimulation is probably needed to maintain "housekeeping" levels of targets such as Pmc1, which would modulate the positive feedback on Crz1. The presence of these feedback loops indicates that the readouts of transcription described above would probably show that the increase in flickering in Ca^{2+} transporter deletion strains increases transcription.

Rcn1 is a member of a family of presumed Cn chaperones, known as regulators of Cn (RCANs), whose role in Cn regulation is still debated. Different studies have showed different roles of RCANs, both stimulatory of Cn and inhibitory (Sanna et al., 2006). In my experiments, I see that Rcn1p increases Cn activity independently of Crz1-dependent transcription. This suggests that Rcn1p acts as a chaperone to assemble, localize, or activate Cn. The precise role of Rcn1p will be studied further in Chapter 5.

The microscopy experiments described here were conducted in ½X SC medium, which has 0.1 mM $CaCl_2$. Therefore, it would be interesting to determine if the Ca^{2+} needed to activate Cn flickering is entering from outside the cell or being released from internal stores. Although most of the Ca^{2+} in the vacuole is bound to inorganic phosphate and unavailable, some of it can be released by the vacuolar Ca^{2+} channel Yvc1p (Palmer et al., 2001; Cunningham,

2011). In order to differentiate the possible sources of Ca^{2+} influx, flickering could be examined both in strains lacking *YVC1* and in medium containing BAPTA (1,2-bis(o-aminophenoxy)ethane-N,N,N',N'-tetraacetic acid) or another Ca^{2+} chelator. If these experiments show that Ca^{2+} is entering from outside the cell, the Ca^{2+} influx pathways HACS and LACS could be examined for their roles in this condition (Cyert and Philpott, 2013). Additionally, presence or absence of flickering could be used to screen for the additional Ca^{2+} influx pathways proposed by Cui *et al.* (2009a).

Another group using a similar probe saw a similar response to addition of $CaCl_2$, but they saw different patterns of nuclear localization both in the absence of stimulation and after adaptation (Cai et al., 2008). In the absence of stimulation, they saw very little nuclear localization of their probe. After adaptation, they saw short periods of nuclear localization with intensity similar to the initial response with baseline localization between these "bursts." Bursts were not synchronized between cells. They describe bursting as being "all-or-none," which is unlike flickering that was generally to a lower intensity than the initial response and did not always return to baseline. This discrepancy is likely due to the difference in expression levels between that probe and my new probe. Their probe was expressed from the endogenous *CRZ1* locus, under its own transcriptional regulation, while my probe is overexpressed. Whatever is causing these later bursts may be a weaker activator of translocation than the initial stimulation with Ca^{2+}, so it can activate all of the endogenously expressed probe but not all of the overexpressed probe.

Now that this new probe has been developed and characterized, it can be used to further examine the effects of various factors in the Cn/Crz1 pathway on Cn activation. In the following chapters, the GFP-Crz1(ΔZF) probe will be used to examine the activation of Cn in response to stimulation. The roles of Pmc1p, Vcx1p, Crz1p, and Rcn1p will be tested both at the initiation of Cn activation and in prolonged signaling conditions.

CHAPTER FOUR: THE ROLE OF VACUOLAR CALCIUM TRANSPORTERS PMC1 AND VCX1 IN CALCINEURIN/CRZ1 DYNAMICS

INTRODUCTION

Calcineurin (Cn) activity is dependent on, and therefore regulated by, cytosolic calcium (Ca^{2+}) concentration ($[Ca^{2+}]_{cyt}$) through the binding of both Ca^{2+}/calmodulin (CaM) and free Ca^{2+} (Rusnak and Mertz, 2000). Because of this dependence, Ca^{2+} transporters that control $[Ca^{2+}]_{cyt}$ can be seen as regulators of Cn. This is especially true of the pumps and exchangers that remove Ca^{2+} from the cytosol, because they are responsible for long-term maintenance of $[Ca^{2+}]_{cyt}$, which controls Cn activity (Cunningham, 2011). In yeast, the most important of these transporters is the Ca^{2+} ATPase Pmc1, which functions in the vacuole membrane to transport ~90% of the Ca^{2+} that is found in that organelle (Cunningham and Fink, 1994; Cunningham, 2011). Growth assays have shown that Pmc1 is required for long-term growth in high external $[Ca^{2+}]$ ($[Ca^{2+}]_{ex}$) (Matheos et al., 1997). Because *PMC1* transcription is upregulated by Cn-Crz1 signaling, Pmc1 is part of a negative feedback loop with Cn, in which Cn activates Pmc1 and Pmc1 inhibits Cn (Matheos et al., 1997).

Also in the vacuole is the proton (H^+)/Ca^{2+} exchanger Vcx1 (Cunningham and Fink, 1996; Rusnak and Mertz, 2000). While growth assays have shown that Vcx1 seems to have little role in the long-term response to high $[Ca^{2+}]_{ex}$ in wild-type cells, it is necessary for growth in high $[Ca^{2+}]_{ex}$ when Cn is inhibited or absent. Vcx1 is primarily active in unstimulated cells and in the immediate response to high $[Ca^{2+}]_{ex}$ (Cunningham and Fink, 1994; Cui et al., 2009a; Cunningham, 2011). Vcx1 is inhibited by Cn through an unknown mechanism, which creates a double negative feedback loop; Cn and Vcx1 inhibit each other, leading to bistability in the system (Cunningham, 2011). It has been

hypothesized that when Cn is on, Vcx1 is off and when Cn is off, Vcx1 is on, with little population of intermediate states.

The experiments summarized above have determined whether or not Pmc1 and Vcx1 have roles in specific conditions, such as growth in high $[Ca^{2+}]_{ex}$ or in the absence of Cn, but they cannot determine when the transporters have their effects. Especially of interest is how soon after Cn activation its inhibitory effect on Vcx1 can be seen.

Using the new GFP-CRZ1(ΔZF) probe described in the last chapter, I saw that fully functional vacuolar Ca^{2+} transport is necessary to maintain baseline Cn activity in non-stimulating conditions. The next step is to look at the response to stimulation. In this chapter, I directly observed the effects of Pmc1 and Vcx1 activity on calcineurin activation dynamics in the initial minutes of exposure to elevated $[Ca^{2+}]_{ex}$ and during prolonged growth in this condition. As expected, calcineurin is more active when the vacuolar transporters are removed because $[Ca^{2+}]_{cyt}$ rises more quickly and remains high longer (Miseta et al., 1999). I see that at high $[CaCl_2]_{ex}$, both Pmc1p and Vcx1p are necessary for controlling $[Ca^{2+}]_{cyt}$, since deletion of either transporter causes Cn to be activated more quickly and to stay active longer. Interestingly, at lower $[CaCl_2]_{ex}$, either transporter alone is sufficient to restore $[Ca^{2+}]_{cyt}$ equilibrium.

MATERIALS AND METHODS

Yeast strains, plasmids, and media

All yeast strains were derived from parental strain W303-1A by standard transformations and mating crosses. Cells were grown in synthetic complete (SC) media, prepared as described (Sherman et al., 1986).

Strains TAY127-158, the full panel of mutants with all combinations of *pmc1Δ*, *vcx1Δ*, *crz1Δ*, and *rcn1Δ* containing *GFP-CRZ1(ΔZF)* and *HTB2-mCherry*, were created as described in Chapter 3.

Table 4-1. *Yeast strains used in Chapter 4.*

Strain	Genotype	Source
TAY127	*GFP-CRZ1(ΔZF)::URA3 HTB2-mCherry::HIS3*	this study
TAY129	*pmc1::LEU2 GFP-CRZ1(ΔZF)::URA3 HTB2-mCherry::HIS*	this study
TAY131	*vcx1Δ GFP-CRZ1(ΔZF)::URA3 HTB2-mCherry::HIS3*	this study
TAY133	*pmc1::LEU2 vcx1Δ GFP-CRZ1(ΔZF)::URA3 HTB2-mCherry::HIS3*	this study
TAY135	*crz1::G418 GFP-CRZ1(ΔZF)::URA3 HTB2-mCherry::HIS3*	this study
TAY137	*pmc1::LEU2 crz1::G418 GFP-CRZ1(ΔZF)::URA3 HTB2-mCherry::HIS3*	this study
TAY139	*vcx1Δ crz1::G418 GFP-CRZ1(ΔZF)::URA3 HTB2-mCherry::HIS3*	this study
TAY141	*pmc1::LEU2 vcx1Δ crz1::G418 GFP-CRZ1(ΔZF)::URA3 HTB2-mCherry::HIS3*	this study

All strains are isogenic derivatives of strain K601/W303-1A (*MAT***a** *ade2-1 can1-100 his3-11,14 leu2-3,112 trp1-1 ura3-1*).

Microscopy

All samples were prepared and microscopy was done as described in Chapter 3.

Graphing and image quantification

Nuclear fluorescence of the probe over time was calculated as described in Chapter 3.

In order to determine the half-maximal points for each cell trace, traces were first smoothed using the Lowess smoothing function in Matlab Curve Fitting Toolbox (Mathworks), with parameters to fit a 1st degree polynomial mode. Gaps were eliminated before smoothing. The half-maximal value was then determined by measuring half the distance from the lowest value within two timepoints before the addition of $CaCl_2$ to the highest value within thirty timepoints after the addition of $CaCl_2$. The times for this value were determined by interpolation. Cells were excluded from calculation of half max if there were no fluorescence values within two timepoints before or thirty timepoints after the addition of $CaCl_2$ or if nuclear fluorescence decreased immediately after addition. Delay is the time of media switching subtracted from the time of the half max of the rise. Duration, also called peak width, is the time of the half max of the rise subtracted from the time of the half max of the recovery. Where the trace did not cross half max of the recovery during the imaging period, the value was projected using the slope from the highest value to the last value in the trace.

Standard error of the median (SEM) for delay and duration were calculated as described for CV in Chapter 3.

When SEM bars overlapped, medians for all four strains in the experiment were compared with a Kruskal-Wallis (KW) non-parametric ANOVA test using the Matlab kruskalwallis function. If the KW test returned a rejection of the null hypothesis of the same median for all strains with $p<0.05$, a multiple comparison test was used to determine which pairs of strains had significantly different medians using the Matlab multcompare function. These significant differences were indicated by stars on the plots.

RESULTS

GFP-CRZ1(ΔZF) nuclear dwell time is dependent on calcium concentration

The new GFP-CRZ1(ΔZF) probe and imaging system developed in the previous chapter were able to detect effects of $[CaCl_2]_{ex}$, Cn inhibitors, and Ca^{2+} transporters on the initial response to $[CaCl_2]_{ex}$ elevation. Measuring this response will allow determination of the contribution of Pmc1p and Vcx1p to Cn activation in response to sudden $[CaCl_2]_{ex}$ elevation.

The two measures of the initial response that are affected by $[CaCl_2]_{ex}$ and the Ca^{2+} transporters are the time required for maximal, and half-maximal, probe nuclear localization following a change in $[CaCl_2]_{ex}$ and the length of the initial peak of probe nuclear localization. ImageJ and Matlab were used to quantify the baseline probe fluorescence in each mCherry-positive nucleus and the maximal probe fluorescence in that nucleus after switching to $CaCl_2$-supplemented medium. The time required for the nuclear probe signal to rise and fall through the half-maximal point were calculated for each cell and used to determine "response delay" and "response duration." A decrease in response delay indicates that Cn is activated more quickly in a given condition. An increase in response duration indicates that Cn is staying active longer. Median and standard error of the median for each of these values were calculated for all cells in a field.

This method was applied to WT cells exposed to varying concentrations of $CaCl_2$. No effect was seen when $[CaCl_2]_{ex}$ was not raised (Fig. 4-1 A). Peaks of nuclear fluorescence were seen in most cells when $[CaCl_2]_{ex}$ was raised to 100,

200, or 300 mM $CaCl_2$ (Fig. 4-1 B-D). Quantification of the response duration shows that there was a small effect of increasing stimulation from 100 to 200 mM $CaCl_2$ and a big effect of increasing from 200 to 300 mM (Fig. 4-1 E).

Figure 4-1. *GFP-CRZ1(ΔZF) nuclear dwell time is dependent on calcium concentration.*

WT cells in continuously flowing ½X SC. (A-D) Single cell traces of nuclear GFP-CRZ1(ΔZF) fluorescence. Black bar on time axis indicates the switch to medium supplemented with (A) 0, (B) 100, (C) 200 or (D) 300 mM $CaCl_2$. (E) Values of the response duration after switching to medium supplemented with 100, 200, or 300 mM $CaCl_2$. Symbols are median values of response duration and bars represent standard error of the median. ** $p<0.01$

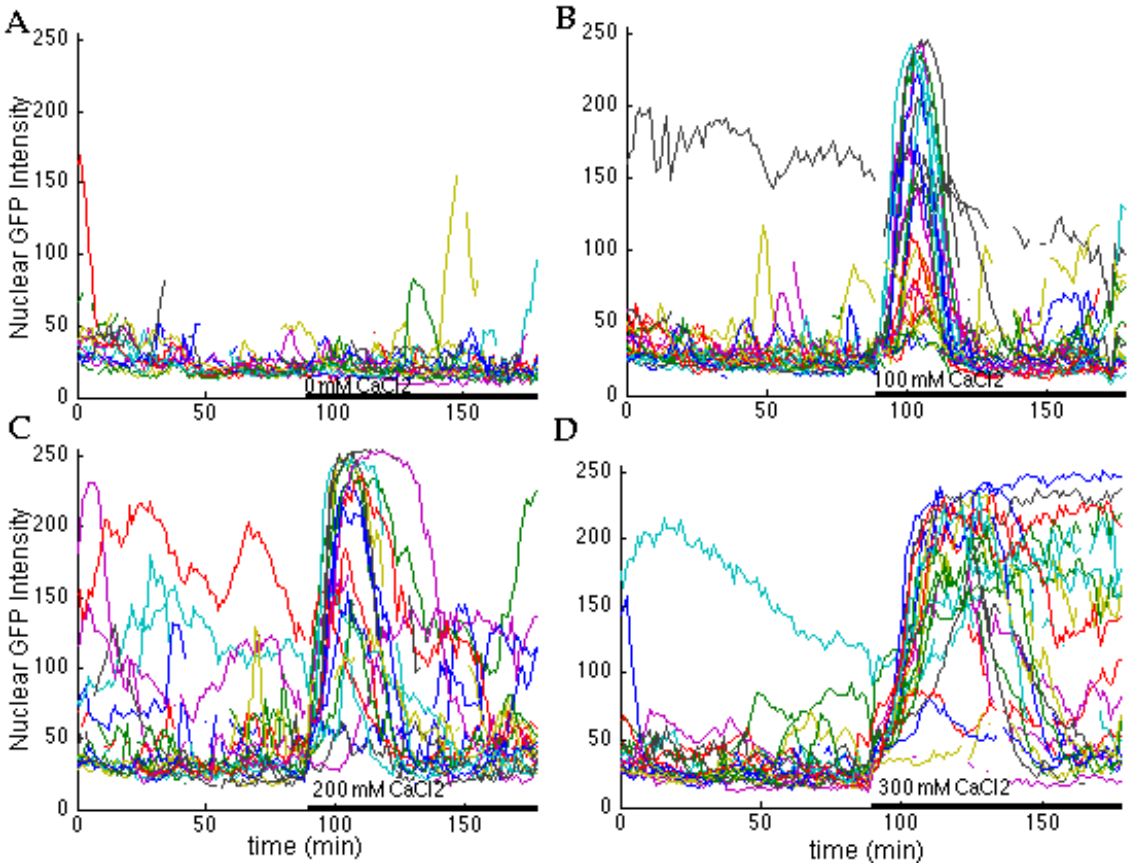

E

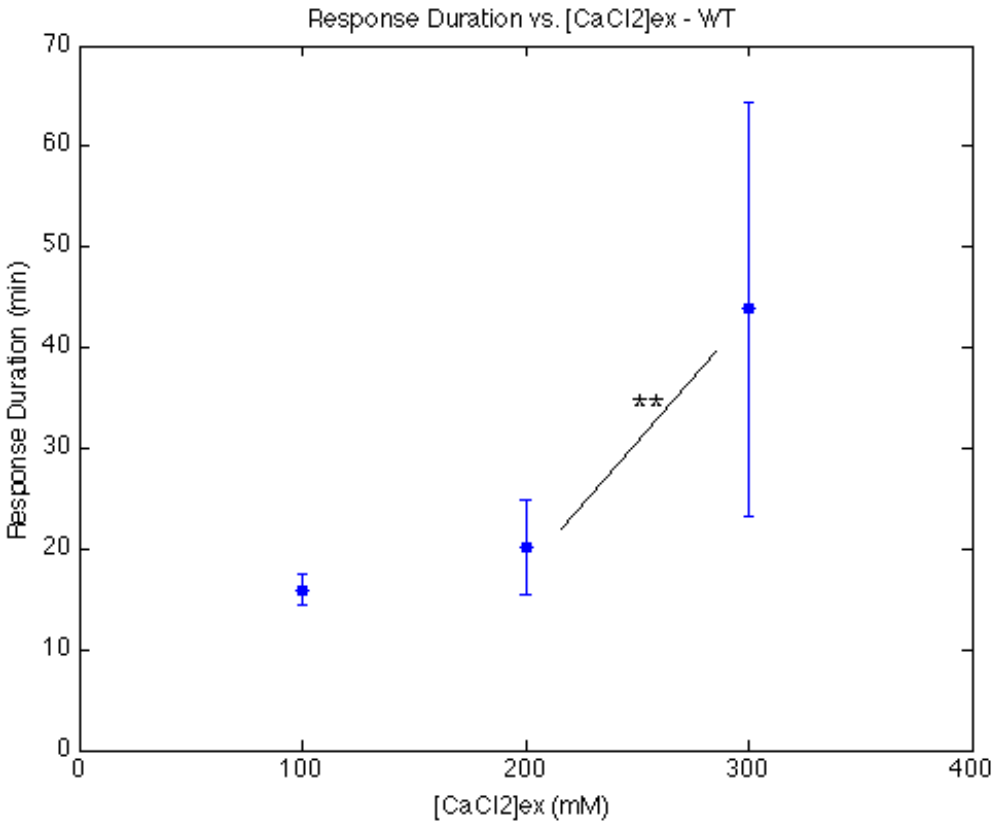
Response Duration vs. [CaCl2]ex - WT
Response Duration (min)
[CaCl2]ex (mM)
**
0
10
20
30
40
50
60
70
0
100
200
300
400

Vcx1 opposes Cn activation at early and late stages of the response to calcium

Vcx1p is active when Cn activity is low. In the previous chapter, examination of Cn activation flickers revealed that Cn is active in non-signaling conditions but that Vcx1 is not inhibited by that low activity. It was also shown that Ca^{2+} transport by either Pmc1p or Vcx1p kept Cn activity lower. Since Vcx1p reduced Cn activation in the absence of stimulation, it is hypothesized that Vcx1p will also oppose Cn activation in the immediate response to stimulation. Comparison of response delay in WT and *vcx1Δ* deletion strains showed a 5-fold decrease in Cn activation time (Fig. 4-2 A).

After it is activated by a stimulus, Cn inhibits Vcx1p. If this inhibition occurs during the peak of Cn activation, represented by the peak of nuclear probe fluorescence, deletion of Vcx1p would not have an effect on response duration. Comparing WT and *vcx1Δ* deletion strains showed a 2-fold increase in response duration (Fig. 4-2 B). This indicates that Cn was more active in the absence of Vcx1p, and therefore that Vcx1p was still active for at least an hour after stimulation. This is in accord with previous studies (Miseta et al., 1999).

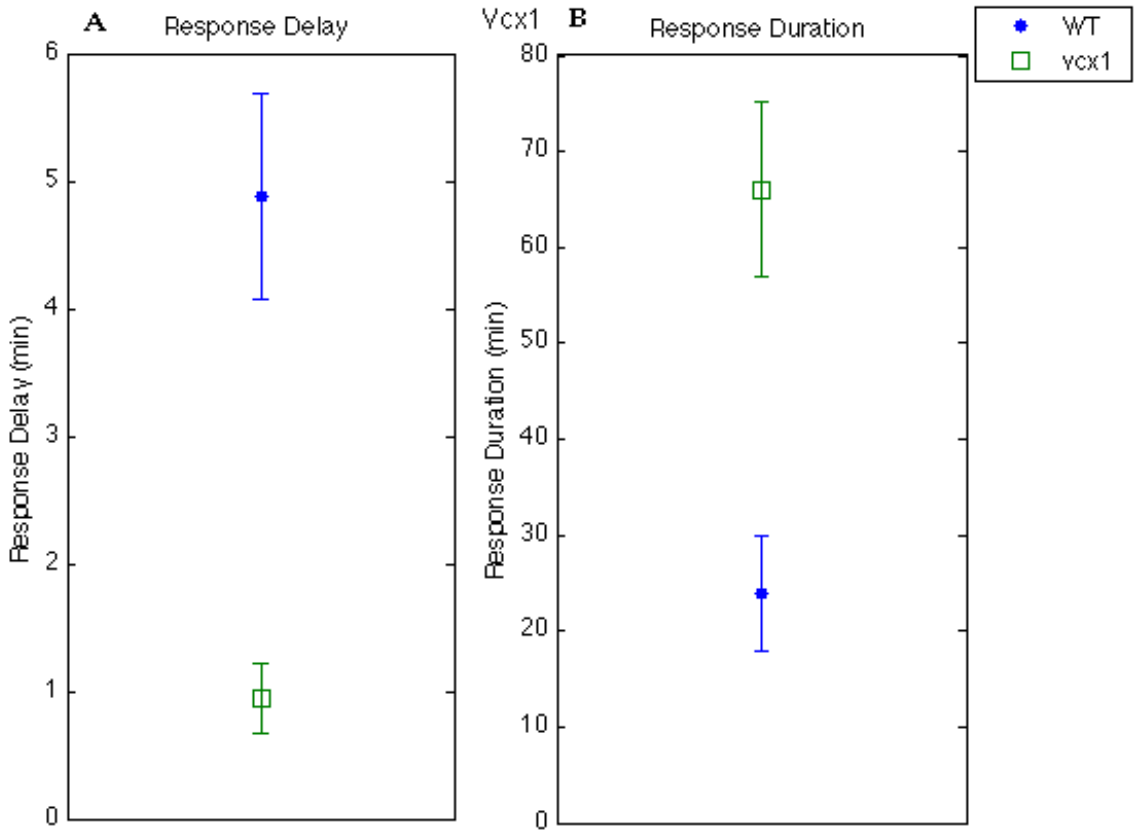

Figure 4-2. *Vcx1 opposes Cn activation at early and late stages of the response to calcium.*

WT and *vcx1Δ* cells in continuously flowing ½X SC. Values of the (A) response delay and (B) response duration after switching to medium supplemented with 200 mM $CaCl_2$. Symbols are median values of delay and duration and bars represent standard error of the median.

Pmc1 opposes Cn activation at early and late stages of the response to calcium

Similarly to Vcx1p, Pmc1p was shown to reduce Cn activity in the absence of stimulation. Therefore, Pmc1p would also be expected to delay Cn activation. Comparison of response delay in WT and *pmc1Δ* deletion strains showed a 5-fold decrease in Cn activation time (Fig. 4-3 A), as was seen for *vcx1Δ*.

Pmc1p has a lower capacity for Ca^{2+} transport than Vcx1p, so it is possible that it is overwhelmed in the immediate aftermath of Ca^{2+} influx and that its contribution to lowering $[Ca^{2+}]_{cyt}$ would be undetectable. If this is the case, response duration would not be lengthened in a *pmc1Δ* strain the way it is in a *vcx1Δ* strain. Comparing WT and *pmc1Δ* deletion strains showed a 2-fold increase in response duration (Fig. 4-3 B). This indicates that Pmc1p is necessary to restore basal $[Ca^{2+}]_{cyt}$ just as Vcx1p is.

There was no further effect on either response delay or response duration in the *pmc1Δ vcx1Δ* double mutant. This indicates that there is no additive effect of deleting both transporters. While this could mean that the transporters work together, it is more likely that deletion of a single transporter causes maximal activation of Cn. The vacuolar transporters constitute the major pathway for regulating $[Ca^{2+}]_{cyt}$, but yeast have other Ca^{2+} transporters that can partially compensate and set an upper limit on Cn activation when the vacuolar export pathway is compromised.

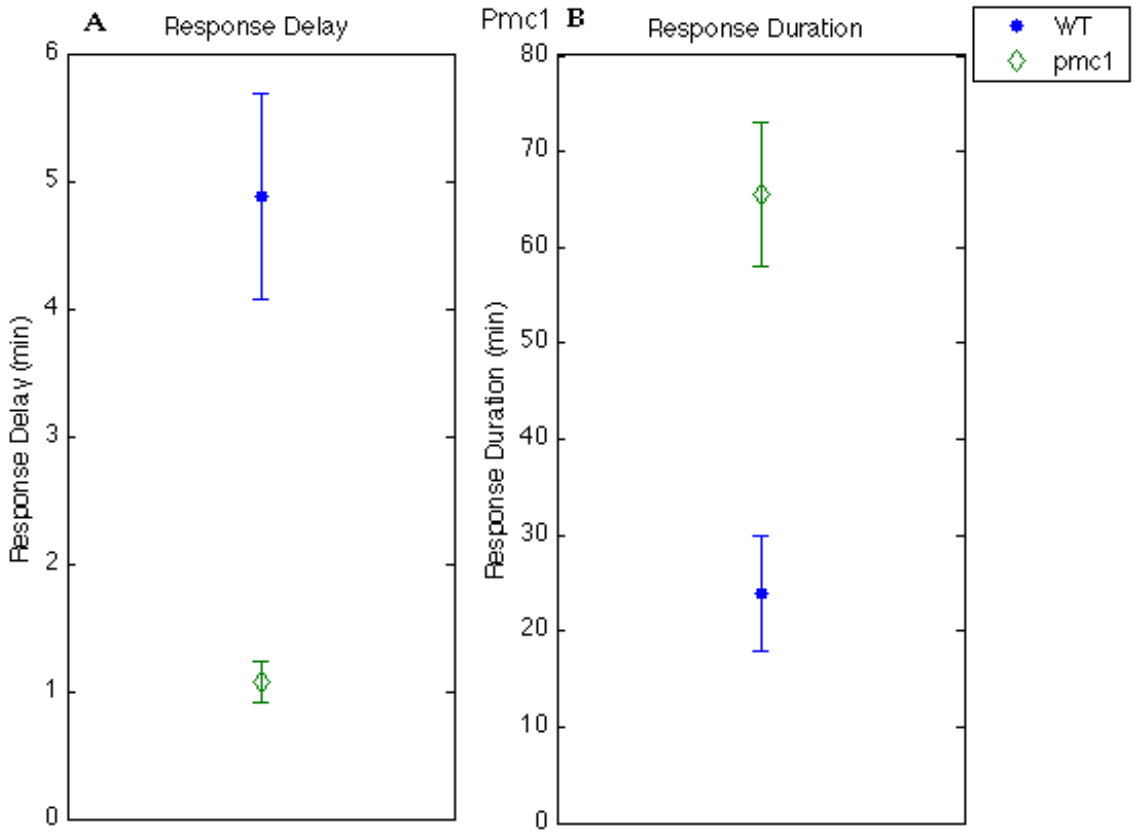

Figure 4-3. *Pmc1 opposes Cn activation at early and late stages of the response to calcium.*

WT and *pmc1Δ* cells in continuously flowing ½X SC. Values of the (A) response delay and (B) response duration after switching to medium supplemented with 200 mM $CaCl_2$. Symbols are median values of delay and duration and bars represent standard error of the median.

Crz1p is not needed for early Pmc1p activity

The Pmc1p function in the absence of stimulation seen in the previous chapter did not require upregulation by Crz1p. Since there is no time for a transcriptional effect in the immediate response to stimulation, it is hypothesized that the effect of Pmc1p on response delay will also be independent of Crz1p. Comparison of response delay between WT and *crz1Δ* strains shows no effect of the knockout (Fig. 4-4 A). If there had been an effect of Crz1p on Pmc1p, the *crz1Δ* strain would have had a shorter delay, similar to the *pmc1Δ* strain.

The *pmc1Δ crz1Δ* strain has a very slow response to stimulation. It is possible that this indicates that Crz1p is necessary for Cn activation in the absence of Pmc1p. However, other experiments with this strain showed shorter delays, approaching the values for the *pmc1Δ* strain, while values for the WT and the *crz1Δ* strains, as well as for the *pmc1Δ vcx1Δ* and the *pmc1Δ vcx1Δ crz1Δ* strains, were similar in all experiments. There may have been some problem with contamination of the *pmc1Δ crz1Δ* strain or unusually high day-to-day variation. Due to this, no conclusions can be drawn about the role of Crz1p in the initial Cn response to $CaCl_2$ in the absence of Pmc1p.

While Crz1p is not necessary for Pmc1p activity in the absence of or immediate response to stimulation, it may have a detectable effect on the ability of Pmc1p to shorten the response duration. If it does, a *crz1Δ* strain would have an extended response, similar to the *pmc1Δ* strain. The *crz1Δ* and *pmc1Δ crz1Δ* strains looked like WT and *pmc1Δ* respectively, however, indicating that transcriptional feedback does not have an effect within the first hour or two of the Cn response to stimulation (Fig. 4-4 B).

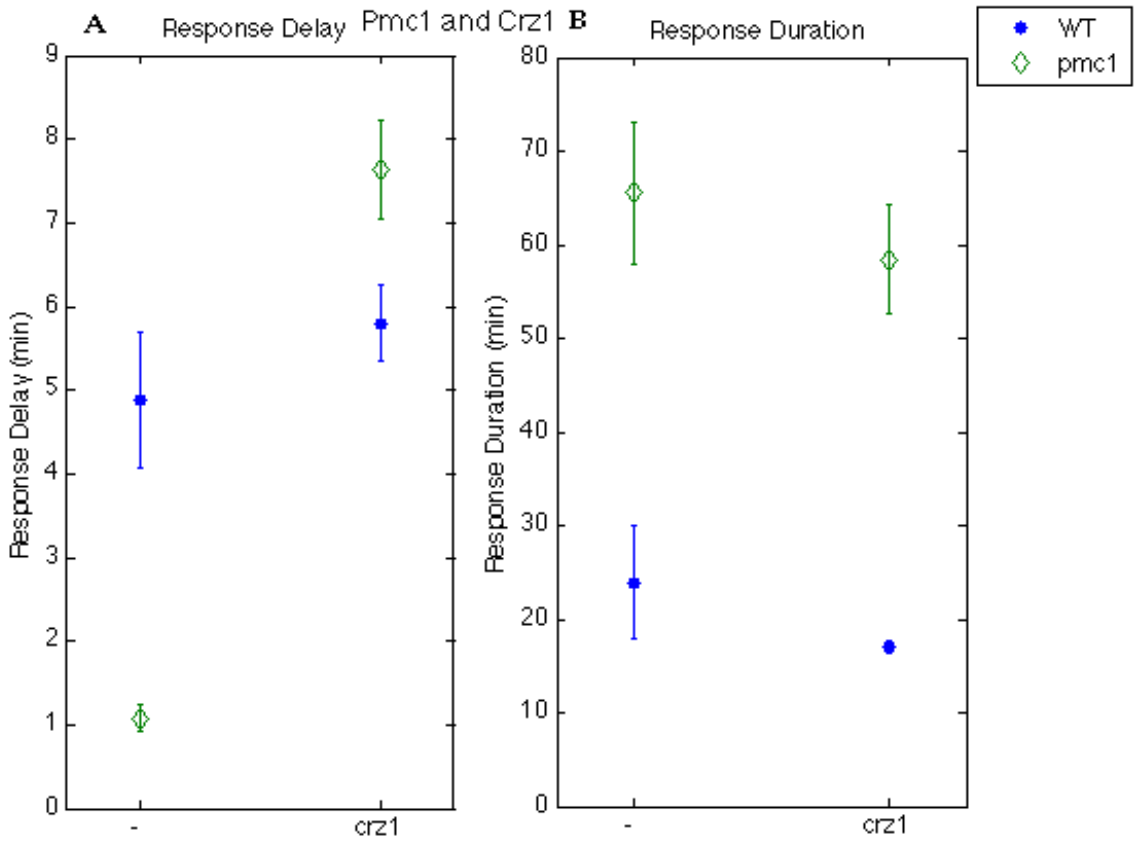

Figure 4-4. *Crz1p is not needed for early Pmc1p activity.*

WT, *pmc1Δ*, *crz1Δ*, and *pmc1Δ crz1Δ* cells in continuously flowing ½X SC. Values of the (A) response delay and (B) response duration after switching to medium supplemented with 200 mM $CaCl_2$. Symbols are median values of delay and duration and bars represent standard error of the median.

Effects of Pmc1 and Vcx1 are dependent on concentration

In the above experiments, there were no significant differences between *pmc1Δ* strains and *vcx1Δ* strains in either response delay or response duration, implying that they have overlapping roles. After the addition of lower concentrations of extracellular $CaCl_2$, the effects of Pmc1p and Vcx1p on response can be more clearly differentiated (Fig. 4-5). The amplitude and duration of the nuclear localization of the probe in the *crz1Δ pmc1Δ vcx1Δ* strains were similar after addition of 200, 100, or 50 mM $CaCl_2$. In 100 mM $CaCl_2$, only Vcx1p had an effect as the only vacuolar Ca^{2+} transporter. In 50 mM $CaCl_2$, deletion of either *PMC1* or *VCX1* alone had no effect on the response; only deleting both lengthened the response. Vcx1p had a bigger effect, but either transporter functioning alone prevented disregulation of $[Ca^{2+}]_{cyt}$. This indicates that either Pmc1p alone or Vcx1p alone can control $[Ca^{2+}]_{cyt}$ in the face of very small perturbations. Vcx1p alone, with its higher capacity for Ca^{2+} transport, can handle somewhat larger perturbations, but both transporters together are needed for the largest perturbations. The transporter deletion strains were not compared to *crz1Δ* with both transporters present in these conditions.

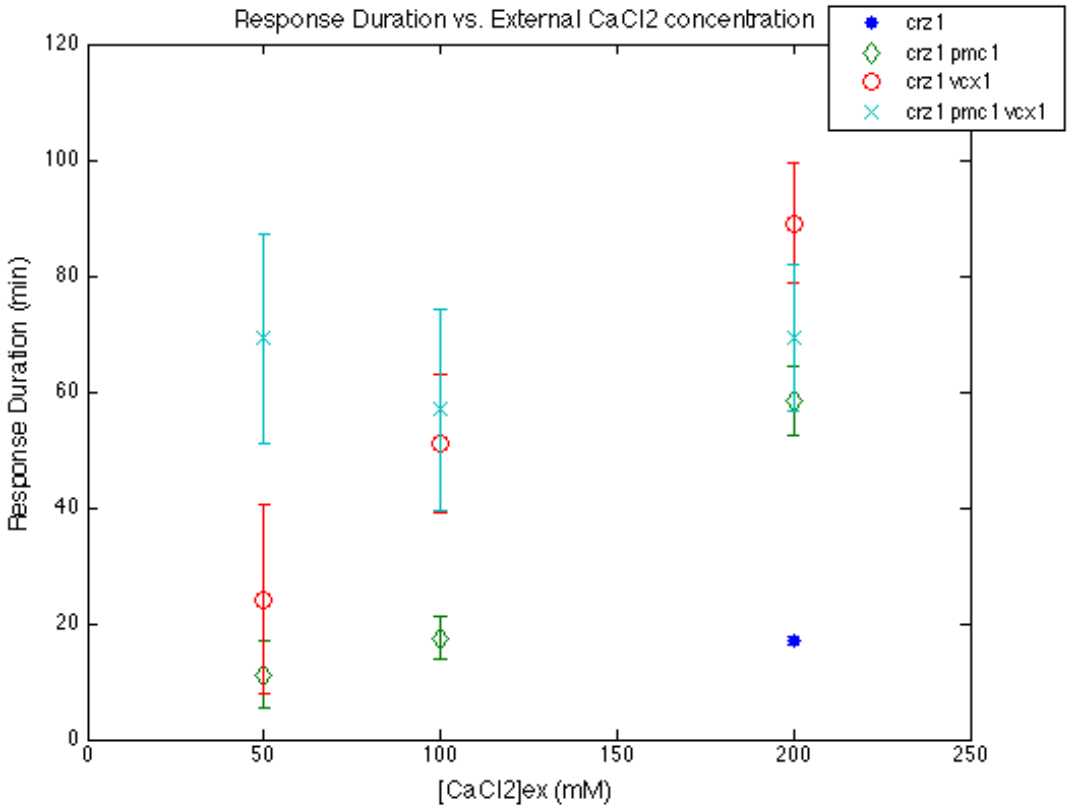

Figure 4-5. *Effects of Pmc1 and Vcx1 are dependent on concentration.*

crz1Δ, *crz1Δ pmc1Δ*, *crz1Δ vcx1Δ*, and *crz1Δ pmc1Δ vcx1Δ* cells in continuously flowing ½X SC. Values of the peak width after switching to medium supplemented with 50, 100, or 200 mM $CaCl_2$. Cells were imaged for at least 120 minutes after the addition of $CaCl_2$. Peak widths longer than the imaging time were determined by extrapolation. Symbols are median values of delay and duration and bars represent standard error of the median. Experiments with different concentrations were run separately.

DISCUSSION

I used the new GFP-CRZ1(ΔZF) probe described in the last chapter to investigate the roles of the vacuolar Ca^{2+} transporters Pmc1p and Vcx1p on Cn activation. Examination of the time for the probe to reach half-maximal nuclear localization shows that maintenance of $[Ca^{2+}]_{cyt}$ in the face of a rise in $[Ca^{2+}]_{ex}$ is dependent on the activity of both Pmc1p and Vcx1p. Transcriptional upregulation by Crz1p is not necessary for Pmc1p to have an effect. This is consistent with the findings in the previous chapter that both vacuolar Ca^{2+} transporters are needed to maintain cytosolic Ca^{2+} equilibrium.

I then examined the roles of Pmc1p and Vcx1p in adaptation to prolonged high $[CaCl_2]_{ex}$. Here I found that both Pmc1p and Vcx1p contribute to quickly restoring low $[Ca^{2+}]_{cyt}$ and ending the Cn signal in high $[CaCl_2]_{ex}$. In responding to smaller elevations of $[CaCl_2]_{ex}$, the individual transporters were sufficient. This effect is independent of the presence or absence of Crz1p. The Cn/Crz1p-independent effect of Pmc1p on $[Ca^{2+}]_{cyt}$ and Cn activation in this condition is consistent with the fact that there is low basal transcription of *PMC1* in the absence of Crz1p and that transcriptional upregulation takes on the order of one hour to have an effect (Stathopoulos and Cyert, 1997; Miseta et al., 1999). Imaging was continued for only about an hour in 200 mM $[CaCl_2]_{ex}$ after activation of Cn so no effects of transcriptional upregulation were seen. Longer imaging would allow determination of the role of Crz1p upregulation on Pmc1p activity. Additionally, longer imaging would capture the time of Vcx1p inhibition by activated Cn. I would expect to see differences in the duration of the Cn signal in single transporter deletion strains at long time scales in high

$[CaCl_2]_{ex}$. In the experiments with lower concentrations of external $CaCl_2$, imaging was continued longer, but no effects were seen. This is likely because the signal has been ended in strains that express the transporters by the time transcription of Pmc1p and inhibition of Vcx1p would be seen. Examination of flickering after adaptation in these conditions might reveal differences between strains.

Previous work has shown that the v-SNARE Nyv1p inhibits Pmc1p activity in the absence of stimulation (Takita et al., 2001). It would be interesting to conduct this experiment in the *nyv1Δ* strain or in the presence of *NYV1* overexpression to see if the probe can detect this regulation on this time scale.

CHAPTER FIVE: THE ROLE OF RCN1, PUTATIVE CALCINEURIN CHAPERONE, IN CALCINEURIN REGULATION

INTRODUCTION

The regulators of calcineurin (RCAN) family of proteins is a highly conserved family of calcineurin (Cn)-binding small proteins found in organisms from yeast to mammals (Kingsbury and Cunningham, 2000; Hilioti and Cunningham, 2003). This family of proteins is one of only two that have been found to be targets of Cn in both yeast and mammalian systems (Guiney et al., 2015). RCANs have a conserved PxIxIT-like motif that is similar to the Cn-interacting sequence of the Cn-regulated NFAT transcription factors and a highly conserved SP motif that is a substrate for dephosphorylation by Cn (Vega et al., 2002; Mehta et al., 2009). RCANs directly bind the catalytic CnA subunit without requiring or interfering with binding by the activator calmodulin (CaM) or the regulatory CnB subunit (Rothermel et al., 2000; Vega et al., 2002; Hilioti and Cunningham, 2003; Davies et al., 2007).

Paradoxically, RCANs have been seen to both stimulate and inhibit Cn *in vivo*. Overexpression studies in mammals, nematode, and fungi showed reduced Cn activity, reduced Cn-dependent transcription, and reduced nuclear localization of NFAT, indicating that RCANs inhibit Cn (Fuentes et al., 2000; Kingsbury and Cunningham, 2000; Rothermel et al., 2000; Cao et al., 2002; Ermak et al., 2002; Hill et al., 2002; Vega et al., 2002; Lee et al., 2003; Minami et al., 2004). It was later shown in yeast that the minimal inhibitory domain of the yeast RCAN, Rcn1, requires the PxIxIT-like motif, which simply competes with other substrates for access to a critical docking site on Cn (Mehta et al., 2009). In contrast to these overexpression studies, most knockout and knockdown studies in fungi and mouse also showed reduced Cn activity and reduced Cn-dependent

transcription, indicating that at endogenous levels, RCANs are needed for full Cn signaling (Görlach et al., 2000; Kingsbury and Cunningham, 2000; Vega et al., 2003; Fox and Heitman, 2005; Sanna et al., 2006). The regions of Rcn1 required for stimulation of Cn included a conserved C-terminal tail-motif, the Cn-docking motifs, and phosphorylation of the highly conserved SP-repeats but not the N-terminal RRM-domain (Mehta et al., 2009). Interestingly, the ability of Rcn1 to stimulate Cn in yeast cells also depended on ubiquitylation of the protein by the E3 ubiquitin ligase SCF-Cdc4 and degradation by the 26S proteasome (Kishi et al., 2007; Mehta et al., 2009). These findings together suggest that RCANs may function as competitive inhibitors of Cn when overexpressed or incompletely phosphorylated, ubiquitylated, and turned over, but more physiologically they function as activators of Cn and potentially as chaperones for either Cn biogenesis or recycling (Mehta et al., 2009).

Further complicating the understanding of the physiological roles of RCANs is the presence of feedback loops. Transcription of some RCAN genes can be upregulated by Cn through NFAT/Crz1 in both fungi and animals, including Rcn1 in yeast, creating a positive feedback loop if Rcn1 is stimulatory of Cn and a negative feedback loop if it is inhibitory (Kingsbury and Cunningham, 2000; Yang et al., 2000; Ermak et al., 2002; Wang et al., 2002; Lee et al., 2003). RCANs are dephosphorylated by Cn, which prevents ubiquitylation and thereby degradation, which could create a negative feedback loop (Hilioti et al., 2004).

RCANs have been proposed to stimulate Cn as a chaperone for assembly of its subunits, stability, localization, activation, or availability to other targets

(Hilioti et al., 2004; Fox and Heitman, 2005; Sanna et al., 2006; Kishi et al., 2007; Mehta et al., 2009). Binding to Cn and degradation of RCAN are both required for stimulatory activity, indicating a transient interaction (Mehta et al., 2009). RCAN knockout had no effect on Cn abundance, indicating that RCANs regulate Cn directly (Sanna et al., 2006), but it did result in the loss of catalytic iron ions from the active site of yeast Cn (K. W. Cunningham and R. Lill, unpublished results). The simplest hypothesis to explain these observations is that RCANs may facilitate loading iron ions into the active site of CnA or recycling of oxidized or otherwise damaged iron ions.

The results described above mostly were obtained from growth assays, mating assays, *in vitro* activity assays, β-galactosidase assays, and other population-based methods of measuring Cn activation. Using the GFP-CRZ1(ΔZF) probe described in Chapter 3, it was seen that Rcn1p is required for baseline Cn activity in non-stimulating conditions. The next step is to look at the response to stimulation. In this chapter, I directly observed the effect of Rcn1p on Cn activation dynamics in the initial minutes of exposure to elevated external calcium (Ca^{2+}) concentration ($[Ca^{2+}]_{ex}$) and during prolonged growth in this condition. Cn was more active when Rcn1p was present, supporting a role for Rcn1p as a positive regulator of Cn, possibly as a chaperone. Rcn1p increased the speed of Cn activation at the onset of signaling and allowed Cn to remain active longer during prolonged exposure to elevated $[Ca^{2+}]_{ex}$. This effect of Rcn1p was independent of transcriptional upregulation by Crz1p. Additionally, I saw a stimulatory effect of Crz1p on Cn activity that was independent of both *RCN1* and *PMC1*. These observations suggest that Rcn1p acts as a chaperone for

both Cn activation and reactivation and that Crz1p has other targets that can increase Cn activity.

MATERIALS AND METHODS

Yeast strains, plasmids, and media

All yeast strains were derived from parental strain W303-1A by standard transformations and mating crosses. Cells were grown in synthetic complete (SC) media, prepared as described (Sherman et al., 1986).

Strains TAY127-158, the full panel of mutants with all combinations of *pmc1Δ*, *vcx1Δ*, *crz1Δ*, and *rcn1Δ* containing *GFP-CRZ1(ΔZF)* and *HTB2-mCherry*, were created as described in Chapter 3.

Table 5-1. *Yeast strains used in Chapter 5.*

Strain	Genotype	Source
TAY133	*pmc1::LEU2 vcx1Δ GFP-CRZ1(ΔZF)::URA3 HTB2-mCherry::HIS3*	this study
TAY135	*crz1::G418 GFP-CRZ1(ΔZF)::URA3 HTB2-mCherry::HIS3*	this study
TAY141	*pmc1::LEU2 vcx1Δ crz1::G418 GFP-CRZ1(ΔZF)::URA3 HTB2-mCherry::HIS3*	this study
TAY149	*pmc1::LEU2 vcx1Δ rcn1::ADE2 GFP-CRZ1(ΔZF)::URA3 HTB2-mCherry::HIS3*	this study
TAY151	*crz1::G418 rcn1::ADE2 GFP-CRZ1(ΔZF)::URA3 HTB2-mCherry::HIS3*	this study
TAY157	*pmc1::LEU2 vcx1Δ crz1::G418 rcn1::ADE2 GFP-CRZ1(ΔZF)::URA3 HTB2-mCherry::HIS3*	this study

All strains are isogenic derivatives of strain K601/W303-1A (*MAT***a** *ade2-1 can1-100 his3-11,14 leu2-3,112 trp1-1 ura3-1*).

Microscopy

All samples were prepared and microscopy was done as described in Chapter 3.

Graphing and image quantification

Nuclear fluorescence of the probe over time was calculated as described in Chapter 3.

Response delay and response duration were calculated as described in Chapter 4.

Standard error of the median and Kruskal-Wallis p-values were calculated as described in Chapters 3 and 4.

RESULTS

Rcn1 increases Cn activity at early and late stages of the response to calcium

In previous chapters, the GFP-Crz1(ΔZF) fluorescent probe was imaged in yeast cells growing in standard medium before and after addition of high external calcium chloride ($CaCl_2$) to stimulate Cn activation. Using this method, time delay of initial activation of Cn and response duration of nuclear probe signal were determined. The effects of vacuolar transport on Cn activation were revealed by comparing these values in wild-type (WT) and *pmc1Δ vcx1Δ* single and double mutant strains. In order to study the role of Rcn1p, and when it has that role, the response delay and response duration were observed in *rcn1Δ* strains.

If Rcn1p has a positive effect on Cn activity before stimulation, as was seen in Chapter 3, deletion of *RCN1* should lead to a longer response delay since less Cn is available to be activated. If Rcn1p is needed for recycling or reactivation of Cn, deletion of *RCN1* should lead to a shorter response duration as Cn gets used up and cannot continue to activate the probe. Because response delay and response duration were strongly affected by Pmc1p and Vcx1p, a *pmc1Δ vcx1Δ rcn1Δ* strain was compared to a *pmc1Δ vcx1Δ* control strain to determine whether Rcn1p acts on Cn before or after stimulation.

As expected from the results in Chapter 3, comparison of response delay in control and *rcn1Δ* deletion strains showed a 3-fold increase in Cn activation time (Fig. 1 A). This indicates that Cn is less active in the absence of Rcn1, leading to the conclusion that Rcn1 is a chaperone that matures or primes Cn so

that it is ready to respond to an increase in cytosolic free Ca^{2+} concentration ($[Ca^{2+}]_{cyt}$).

Prolonged Cn stimulation may cause oxidation of active site metal ions, or of key amino acids, leading to activity-dependent inactivation (ADI) of Cn. ADI has been suggested to be a mechanism of inhibition of Cn by Ca^{2+} and oxidation that allows reduction of Cn activity during prolonged stimulation (Stemmer et al., 1995; Bito et al., 1996; Wang et al., 1996). If Rcn1p stimulates Cn by preventing or reversing ADI, *rcn1Δ* deletion strains should have a shorter response duration than control strains. Comparison of response duration in control and *rcn1Δ* deletion strains showed a significant decrease in prolonged Cn activity (Fig. 1 B). This indicates that Rcn1p may have a role in suppressing ADI of Cn.

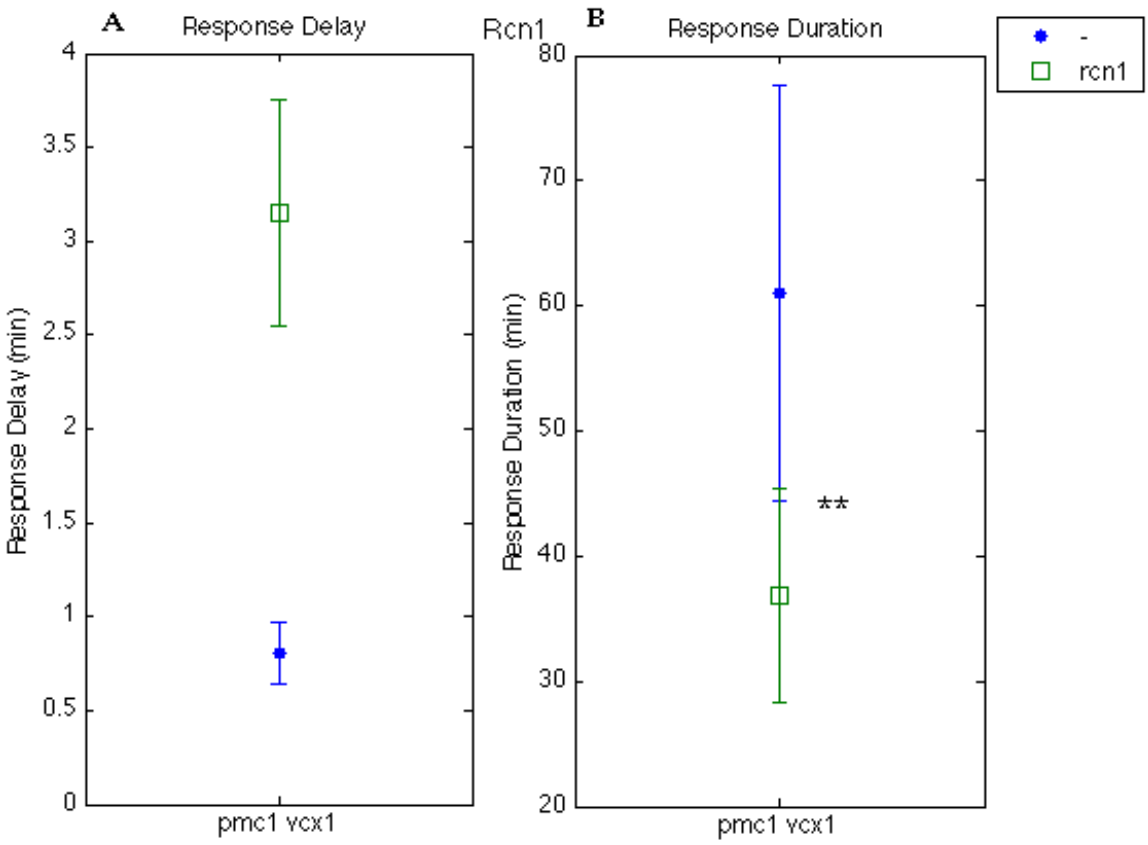

Figure 5-1. *Rcn1 increases Cn activity at early and late stages of the response to calcium.*

pmc1Δ vcx1Δ and *pmc1Δ vcx1Δ rcn1Δ* cells in continuously flowing ½X SC. Values of the (A) response delay and (B) response duration after switching to medium supplemented with 200 mM $CaCl_2$. Symbols are median values of delay and duration and bars represent standard error of the median. ** $p<0.01$

Rcn1 effect on Cn is independent of Crz1

The effect of Rcn1p on Cn activation in the absence of stimulation seen in Chapter 3 did not require Crz1p transcriptional upregulation. Since there is no time for a transcriptional effect in the immediate response to stimulation, it is hypothesized that the effect of Rcn1p on response delay will also be independent of Crz1p. Comparison of response delay between *pmc1Δ vcx1Δ crz1Δ* and *pmc1Δ vcx1Δ crz1Δ rcn1Δ* strains shows that response delay is still slower in the absence of Rcn1p even in the absence of Crz1p (Fig. 2 A). If there had been an effect of Crz1p on Rcn1p, the *pmc1Δ vcx1Δ crz1Δ* strain would have had a similarly long delay to the *pmc1Δ vcx1Δ crz1Δ rcn1Δ* strain.

Transcriptional upregulation could have an effect during the long response peak of the *pmc1Δ vcx1Δ* strain. If Crz1p is necessary for the effect of Rcn1p in reactivating Cn, knocking out *CRZ1* would shorten the peak by reducing the amount of Rcn1p available to reactivate Cn. Although both *crz1Δ* deletion strains have shorter response durations than the *CRZ1* strains, the difference is only significant in the *rcn1Δ* strain (Fig. 2 B). This indicates that Crz1p upregulation of Rcn1p is not needed for reactivation of Cn in the time frame observed.

Crz1 increases Cn activity in steady-state conditions

The effect of deleting *CRZ1* on the response delay was not significant (Fig. 2A). Deletion of *CRZ1* did have a significant effect on the duration of the response to prolonged high $[CaCl_2]_{ex}$ (Fig. 2 B). This effect is independent of Rcn1 and Pmc1, indicating that it is necessary for a different factor to positively

regulate Cn in this condition. A similar result was seen for Crz1p in the absence of stimulation, which is a steady-state condition, as is the response to prolonged stimulation. This may be evidence of a transcriptional effect that is too slow to have an effect on the immediate response to stimulation but is important for stimulating Cn over longer time scales.

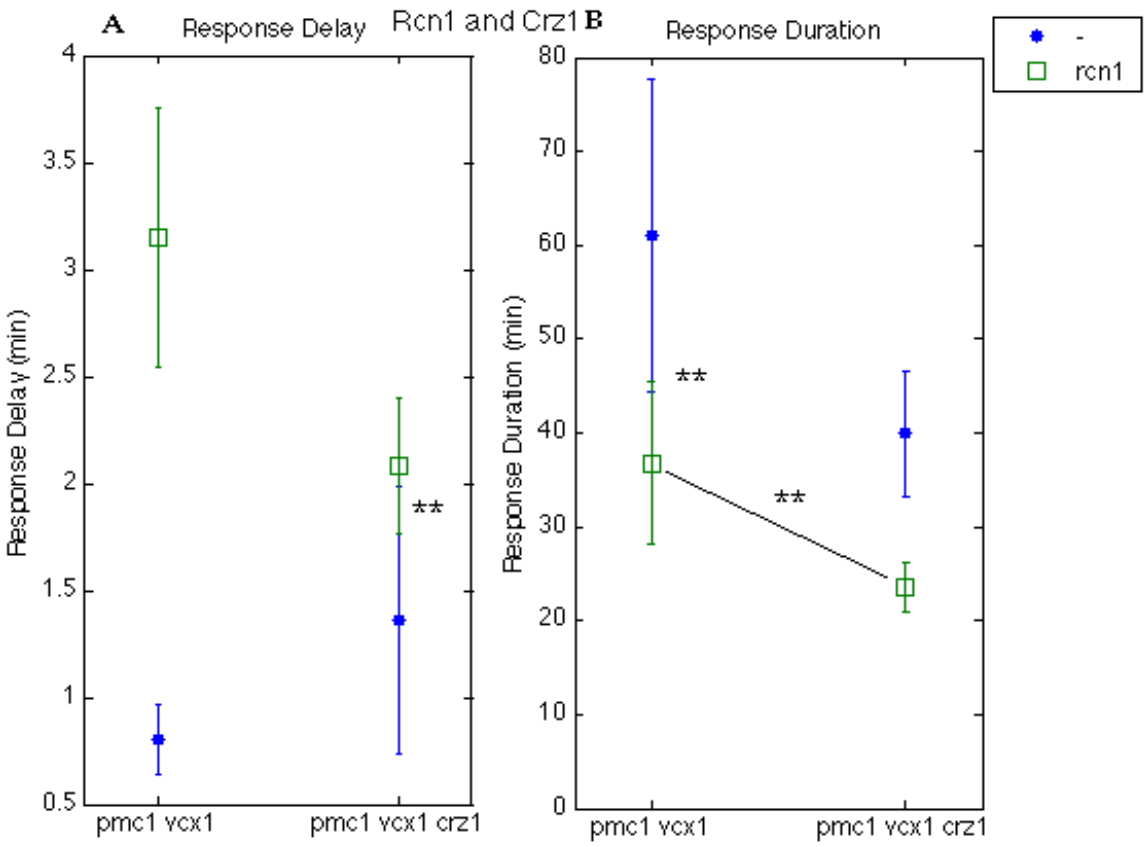

Figure 5-2. *Rcn1 effect on Cn is independent of Crz1.*

pmc1Δ vcx1Δ, *pmc1Δ vcx1Δ rcn1Δ*, *pmc1Δ vcx1Δ crz1Δ*, and *pmc1Δ vcx1Δ crz1Δ rcn1Δ* cells in continuously flowing ½X SC. Values of the (A) response delay and (B) response duration after switching to medium supplemented with 200 mM $CaCl_2$. Symbols are median values of delay and duration and bars represent standard error of the median. ** $p<0.01$

Activity dependent inactivation is not seen in yeast

It is possible that ADI, mentioned above, does not exist in yeast. To test this, response durations of strains with and without *RCN1* to varying concentrations of $CaCl_2$ were compared. If ADI of Cn does occur, increasing the stimulation would lead to faster decline of the response. In the previous chapter, the response durations of WT to varying concentrations of stimulus were compared and it was shown that increasing $[CaCl_2]_{ex}$ caused longer responses. This is assumed to be because higher $[CaCl_2]_{ex}$ induces higher $[CaCl_2]_{cyt}$, so $[CaCl_2]_{cyt}$ remains above the Cn activation threshold longer. In *pmc1Δ vcx1Δ crz1Δ*, response durations were similarly long at all concentrations. This may be because $[CaCl_2]_{cyt}$ is restored to baseline more slowly, so $[CaCl_2]_{cyt}$ remains above the Cn activation threshold for a long time regardless of the size of the initial stimulation. In both of these strains, Rcn1p is active, so it may be suppressing ADI, if ADI is happening. In *pmc1Δ vcx1Δ crz1Δ rcn1Δ*, higher $[CaCl_2]_{ex}$ again caused longer responses (Fig. 3). This is in contrast to what would be expected if ADI were occurring. Instead, Rcn1p may be increasing the sensitivity of Cn to $[CaCl_2]_{cyt}$. While $[CaCl_2]_{cyt}$ after stimulation with both 50 and 300 mM $CaCl_2$ may be different even in the *pmc1Δ vcx1Δ crz1Δ* strain, no difference in response duration was detected because in both cases it was above the Cn activation threshold. However, when Rcn1p is absent, the Cn activation threshold may be raised to a point where the difference in $[CaCl_2]_{cyt}$ after stimulation with both 50 and 300 mM $CaCl_2$ can be detected. This change in sensitivity could also explain the slower response delay in the *rcn1Δ* strain, since it would take longer for $[CaCl_2]_{cyt}$ to reach a higher threshold.

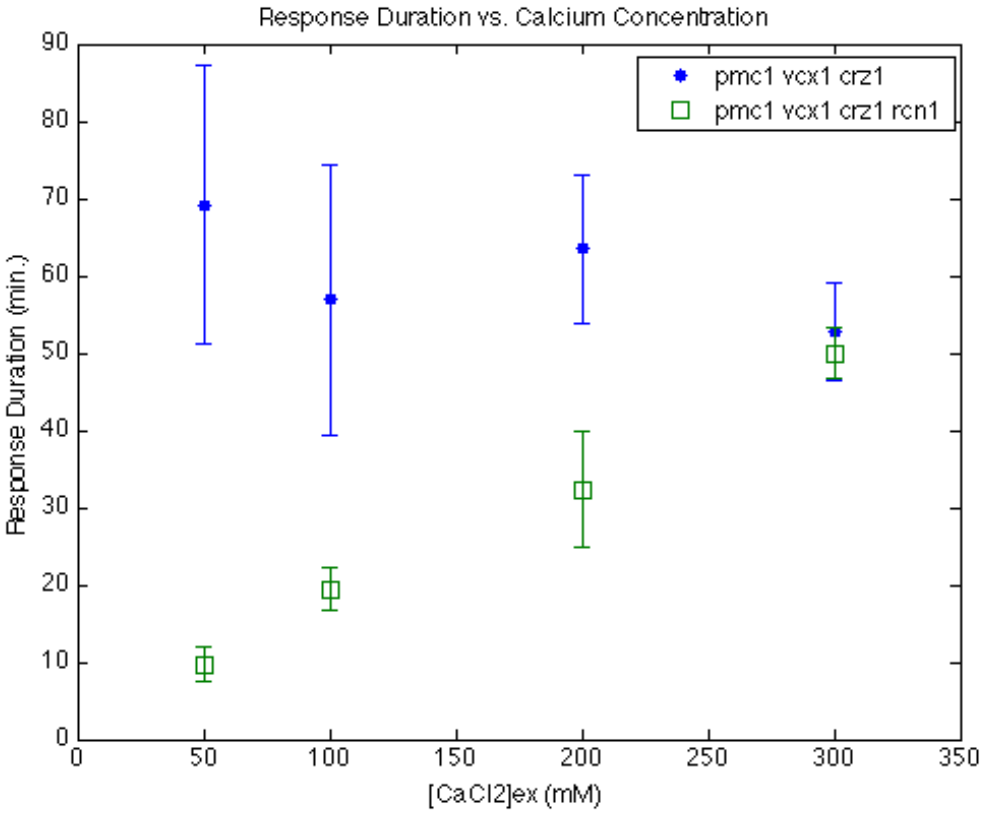

Figure 5-3. *Activity dependent inactivation is not seen in yeast.*

pmc1Δ vcx1Δ crz1Δ and *pmc1Δ vcx1Δ crz1Δ rcn1Δ* cells in continuously flowing ½X SC. Values of the peak width after switching to medium supplemented with 50, 100, 200, or 300 mM $CaCl_2$. Cells were imaged for at least 120 minutes after the addition of $CaCl_2$. Peak widths longer than the imaging time were determined by extrapolation. Symbols are median values of delay and duration and bars represent standard error of the median. Experiments with different concentrations were run separately.

Effect of Rcn1 is only seen in strains lacking vacuolar transporters

The above experiments were performed in strains lacking both vacuolar transporters, Pmc1 and Vcx1, because those strains have high Cn activity. The high level of Cn activity made it easy to see the reduction caused by lack of Rcn1p. The experiments were repeated in strains with functional Pmc1p and Vcx1p and therefore lower Cn activity. As above, Rcn1p prolonged the duration of Cn activity in the *crz1Δ pmc1Δ vcx1Δ* background. However, Rcn1p did not have an effect on signal duration in the *crz1Δ* background expressing the vacuolar transporters (Fig. 4). This may be due to the ability of the strains expressing the transporters to lower $[Ca^{2+}]_{cyt}$ quickly. $[Ca^{2+}]_{cyt}$ would not remain in the range between the WT Cn activation threshold and the higher Cn activation threshold of the *rcn1Δ* strain long enough to cause a detectable difference between the strains.

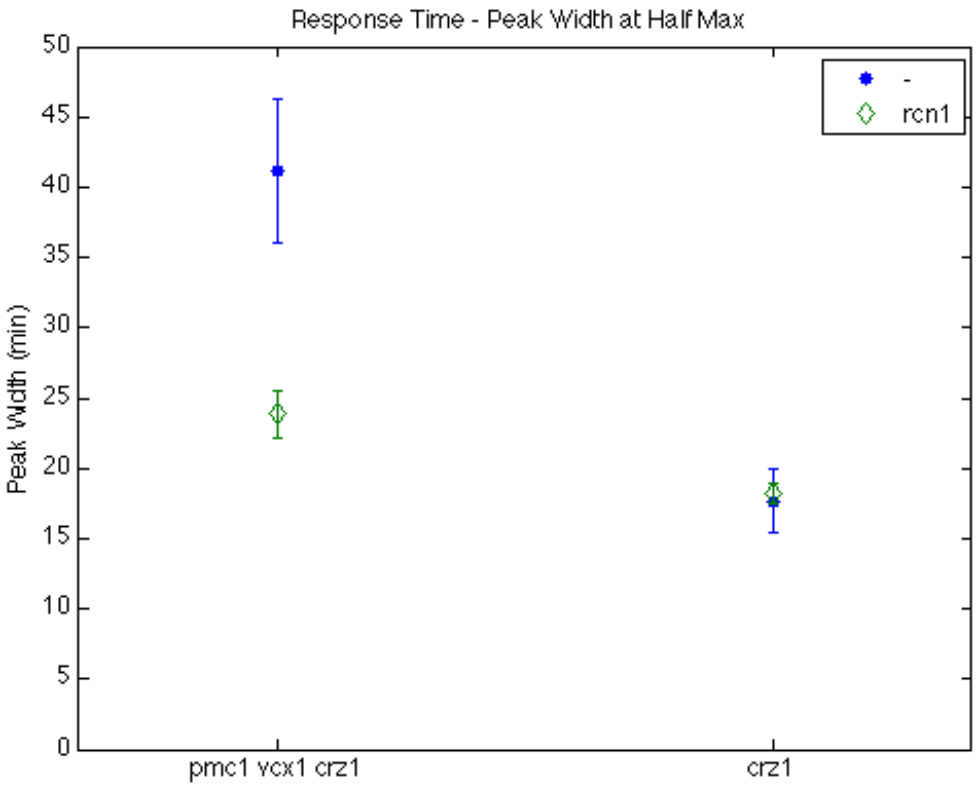

Figure 5-4. *Effect of Rcn1 is only seen in strains lacking vacuolar transporters.* *crz1Δ pmc1Δ vcx1Δ rcn1Δ*, *crz1Δ pmc1Δ vcx1Δ*, *crz1Δ rcn1Δ*, and *crz1Δ* cells in continuously flowing ½X SC. Values of the peak width after switching to medium supplemented with 200 mM $CaCl_2$. Cells were imaged for 140 minutes after the addition of $CaCl_2$. Symbols are median values of response duration and bars represent standard error of the median.

DISCUSSION

I have shown that Rcn1p at endogenous levels is stimulatory of Cn activity both before and after addition of elevated $[CaCl_2]_{ex}$. Rcn1p is necessary for the fast response of Cn to Ca^{2+} in strains lacking vacuolar transporters. Rcn1p is also necessary for sustained Cn signaling in these strains during prolonged exposure to elevated $[CaCl_2]_{ex}$. Neither of these functions of Rcn1p is dependent on Crz1p-induced transcription. The fact that this latter effect is independent of Crz1 is consistent with the fact that transcriptional upregulation takes on the order of one hour to have an effect (Stathopoulos and Cyert, 1997; Miseta et al., 1999). Imaging was continued for one and a half to two hours in 200 mM $[CaCl_2]_{ex}$ after activation of Cn. Transcriptional effects were not seen on response duration because the signal peaks were shorter than one hour. Examining the flickering of the probe after the end of peak would be informative in determining if there is an effect of transcriptional upregulation.

There was also an effect of Crz1p on Cn signaling duration that was independent of Pmc1p and Rcn1p. The experiments described in Chapter 3 to find the targets of Crz1p that increase flickering would also be able to find the targets of Crz1p that increase Cn response duration.

I did not study the effect of Rcn1p in a WT background, but it would be interesting to do so. Response delay is already slow in strains with functional vacuolar Ca^{2+} transport. Deleting *RCN1* would be expected to slow it further if Rcn1p is necessary for the initial activation of Cn. These experiments could be repeated in both the *crz1Δ* and WT strains to determine if Rcn1p has an effect in this condition. As in the *crz1Δ* strain, a reduction in the already short peak width

would not be expected when *RCN1* is deleted, but since the transcriptional feedback loop would be intact, more flickering might be seen after adaptation in the WT strain than the *rcn1Δ* strain during prolonged exposure to high $[CaCl_2]_{ex}$. This would indicate a low level of Cn signaling that requires Rcn1p for reactivation of Cn.

Mutations of Rcn1p have been described that can bind Cn but not stimulate its activity (Mehta et al., 2009). By expressing those variant *RCN1* genes in an *rcn1Δ* strain, I could further refine the role of Rcn1p in Cn activation. For instance, if Rcn1p is required for localization but not assembly, strains expressing these variants would be expected to have the same response delay as stains expressing the WT gene but shorter response duration. Other possible roles of Rcn1p would be seen by other differences in Cn activity.

CHAPTER SIX: CONCLUDING REMARKS

I have shown that the calcium (Ca^{2+})-responsive phosphatase calcineurin (Cn) is active in both stimulating – high external Ca^{2+} concentration ($[Ca^{2+}]_{ex}$) – and non-stimulating – low ($[Ca^{2+}]_{ex}$) – conditions. Activation of Cn is affected by vacuolar Ca^{2+} transporters Pmc1p and Vcx1p, the Cn chaperone Rcn1p, and the Cn-dependent transcription factor Crz1p in different ways in a variety of conditions.

Cn is important for regulating many cellular processes in response to changes in external conditions, including neurotransmitter release in neurons, T-cell activation, mitogen-activated protein kinase (MAPK) cascades, and transcription factor (TF) activation (Kumashiro et al., 2005; Clapham, 2007; Li et al., 2011). Additionally, a wide variety of pathological conditions have been shown to be caused by misregulation of Cn activity. These include Down Syndrome, Alzheimer's Disease (AD), some types of cancer, and certain types of heart disease (Li et al., 2011).

One of the most important and highly-conserved targets of Cn is the transcription factor (TF) NFAT, found in many cell types. NFAT is dephosphorylated by Cn and then translocated to the nucleus, where it regulates transcription in response to Ca^{2+} and Cn (Hogan et al., 2003). NFAT has many target genes that are regulated in very diverse ways. Yeast have an analogous TF, Crz1, which is also regulated by Cn (Matheos et al., 1997). Crz1-activated transcription can be used as a read-out of Cn activity.

I measured Cn-Crz1 dependent transcription from different synthetic promoters using the β-galactosidase activity assay. I found that increasing the number of binding sites for Crz1 within the promoter shifted the Ca^{2+}-

stimulation response curve to the left without changing its shape. This shows that the variety of response curve shapes seen among natural promoters is caused by more than just changes in the probability of Crz1 binding. Further investigation of the effect of disregulating cytosolic Ca^{2+} equilibrium showed that knockout of vacuolar Ca^{2+} transport did change the shape of the response curve. This indicates that increased basal Cn activity leads to changes in the Crz1 transcriptional response.

However, like many of studies of Cn activity, β-galactosidase activity is an imprecise assay. Many of the common assays look at many cells, or extract from many cells, in aggregate. This could mask differences in Cn activity within a population. Time resolution is also low in many of the common Cn assays. In order to better understand Cn dynamics, more precise and detailed assays are needed.

Some groups have studied Ca^{2+} signaling by a direct, single-cell, real-time readout of Cn activation utilizing a fluorescently tagged version of the yeast TF Crz1 (Stathopoulos-Gerontides et al., 1999; Kafadar et al., 2003; Cai et al., 2008; Bodvard et al., 2013). Among the many observations made using this system is the observation of all-or-none nuclear localization "bursts" of Crz1-GFP in constant stimulation seen by Cai *et al.* Other papers have reported seeing "pulsing" of other TFs into and out of the nucleus, which is similar to the "bursting" seen by Cai *et al.* (Levine et al., 2013; Petrenko et al., 2013; Dalal et al., 2014; Lin et al., 2015). A very interesting model of frequency-modulated gene expression coordination was developed based the characteristics of these bursts and measurements of gene expression.

Imaging of Crz1-GFP as just described offers an excellent opportunity to study how feedback regulation controls Cn activation. However, before I began using the system, I improved both the probe itself and the imaging conditions. I created an inert, overexpressed probe, GFP-CRZ1(ΔZF), which could be clearly seen and did not affect gene expression or Cn feedback regulation. I used this probe in conjunction with a nuclear label, to allow easy identification of nuclei, and a microfluidic flow system that constrained cells to the plane of focus and allowed fast switching of media. These improvements to the imaging system allowed for a more quantitative approach to measuring nuclear localization.

Using this new GFP-CRZ1(ΔZF) probe of Cn activity, I did not see the all-or-none "bursts" of nuclear localization seen by Cai *et al.* This could be due to the difference in expression level between their probe and mine. Instead, I saw partial localization "flickers" in constant conditions, both with and without stimulation of Cn. These flickers were caused by Cn activation of Crz1p, since they were suppressed by the addition of a Cn inhibitor to the medium. Flickers were increased when vacuolar Ca^{2+} transport was compromised, and cytosolic Ca^{2+} equilibrium was disrupted, by the deletion of either *PMC1* or *VCX1*. This effect is expected from the fact that disrupting vacuolar Ca^{2+} transport raises $[Ca^{2+}]_{cyt}$ and that raising $[Ca^{2+}]_{cyt}$ increases Cn activity (Miseta et al., 1999). The activity of Vcx1p in the absence of stimulation fits with previous findings that Vcx1p activity is high when Cn activity is low (Cunningham and Fink, 1996). The effect of Pmc1p is less expected, given that its expression is upregulated by Cn-Crz1, but previous studies have shown that there is Crz1-independent basal transcription of *PMC1* that could account for the effect of Pmc1p on flickering

(Stathopoulos and Cyert, 1997). To confirm that this effect is due to Crz1-independent Pmc1p expression, I showed that deleting *CRZ1* decreased flickering rather than increased it, as would be expected if Crz1p is necessary for the effect of Pmc1p.

This dependence of flickering on Crz1p reveals a positive feedback loop through Cn and Crz1p. Low Cn activity causes enough nuclear localization of Crz1p to activate expression of genes that stimulate Cn activity. One possible target of Crz1p that could increase Cn activity is Rcn1p.

Rcn1p is a small Cn-interacting protein. It is part of the highly conserved regulators of Cn (RCAN) family of proteins that has been observed to both stimulate and inhibit Cn activity (Shin et al., 2011). Growth assays in yeast with WT and mutant Rcn1 have shown Rcn1p to be stimulatory in endogenous conditions. Inhibition was only seen as a result of overexpression or incorrect phosphorylation (Mehta et al., 2009). In accord with this, I found that deletion of *RCN1* reduced flickering, implying that Rcn1p promotes Cn activity, even in the absence of stimulation. The effect of Rcn1p on flickering was independent of Crz1p. This suggests that Crz1p has other targets that increase flickering. These could be found by screening for Crz1p-dependent changes in flickering in strains lacking other targets of Cn-Crz1, of which over 150 have been identified (Yoshimoto et al., 2002).

The flickering described above is a phenomenon that has not been studied before and which needs to be confirmed in other systems. If flickering is broadly seen, it will be a new category of Cn activity: basal activity in the absence of a specific stimulus. Flickering could represent a way to maintain housekeeping

levels of transcription of certain genes by taking advantage of TF pulsing. Low levels of Crz1p in the nucleus could activate certain genes but not others, as seen by the difference in gene expression from variously sensitive promoters in Chapter 2. In support of this idea are two observations about the *pmc1Δ vcx1Δ* double mutant strain: it had more flickering than WT and it had higher normalized expression of the more-sensitive reporter construct in the absence of stimulation. Thus, increased flickering correlated with upregulated gene expression.

My experiments also showed some flickering during prolonged exposure to elevated $[CaCl_2]_{ex}$. Most of my data recordings ended shortly after recovery from the initial response to stimulation, however, so I did not quantify the later flickering. Recordings focused on that part of the response may provide insight into Cn activity in cells adapted to a stressful environment. Changes in baseline $[Ca^{2+}]_{cyt}$ have been observed in aging and AD (Berridge, 2011; Reese and Taglialatela, 2011). These changes lead to an increase in Cn activity. Factors that control the Cn response to extended stress could be found by measuring flickering in cells growing in high $[Ca^{2+}]_{ex}$.

In addition to using my new GFP-CRZ1(ΔZF) probe to study Cn activity in non-stimulating conditions, I also used it to study the response to stimulation and the effects of Cn regulators on that response. As in the case of flickering, I saw that vacuolar Ca^{2+} transport reduced Cn activity; deleting the transporters caused Cn both to be activated faster and to stay active longer than in wild type. This emphasizes the importance of cytosolic Ca^{2+} equilibrium in regulating Cn activation. These experiments not only confirm what has been observed for the

vacuolar Ca^{2+} transporters in other assays, they refine the time resolution of our understanding of the roles of these transporters.

Rcn1p acted as a stimulator of Cn during signaling as well as during flickering. The hyperactivation of Cn seen in the *pmc1Δ vcx1Δ* double deletion strains depended on the presence of Rcn1p. The effect of Rcn1p on Cn in the absence of stimulation and at its onset imply a role for Rcn1p as a chaperone that directs assembly, activation, or localization of Cn to ensure that Cn is ready to be turned on when needed. Since Rcn1p activity also increases Cn activity after stimulation, it seems to have a role in setting the sensitivity of Cn to $[Ca^{2+}]_{cyt}$. This dual role of Rcn1p, before stimulation and after, suggests that the effect of Rcn1p on Cn may be more complicated than a simple assembly chaperone, though it clearly has an effect on biogenesis or availability. I did not see any evidence of activity-dependent inactivation (ADI) of Cn in yeast, which argues against Rcn1p having a role in preventing or reversing ADI or in later effects on Cn, though my experiments do not rule this out. Further study is needed to continue to clarify the endogenous role of this conserved regulator of Cn. No effect was seen of Rcn1p in strains with wild-type vacuolar transport, but this may be because $[Ca^{2+}]_{cyt}$ was regulated quickly and was not in the range where Rcn1p affects sensitivity of Cn long enough to be detected.

Crz1p increased Cn activity in the steady-state conditions of no stimulation and prolonged stimulation, but not in the initial response to stimulation. Pmc1p and Rcn1p were not required for this effect. Crz1p likely participates in positive feedback on Cn activity through activation of transcription. This feedback is expected to be too slow to affect the immediate

response to stimulation but to increase Cn activation in steady-state conditions. Alternatively, the factor upregulated by Crz1p may be required only for long-term activation in steady-state conditions but not the large initial response to stimulation that uses a pool of available Cn. This new role of Crz1p highlights the complexity of the feedback loops that regulate Cn and its effectors.

All of the experiments described in this work were done with the addition of $CaCl_2$ to the medium as the method of stimulation. While it is effective at raising $[Ca^{2+}]_{cyt}$, it is not a physiological stimulus. In order to better understand Cn regulation, the GFP-CRZ1(ΔZF) probe could be used to observe the response to physiological stimuli. Changes in external conditions, such as addition of pheromone or salts, have been shown to activate Cn (Stathopoulos and Cyert, 1997). Fluorescently tagged Msn2, a yeast TF that also responds to stress, was recently shown to have unique nuclear localization patterns in response to different stimuli (Petrenko et al., 2013). Similar experiments with the GFP-CRZ1(ΔZF) probe would elucidate the way that Cn responds to different stressors.

The GFP-CRZ1(ΔZF) probe could be used to screen for previously unidentified elements of the Cn signaling pathway. These include Ca^{2+} influx pathways that have been proposed but not yet identified (Cui et al., 2009b). This probe could also be used to quickly screen for drugs or mutations that reduce Cn activity. Cn has been shown to promote virulence and survival of pathogenic fungi (Chen et al., 2012). Drugs such as tunicamycin and miconazole have been shown to kill cells only when Cn signaling is compromised by inhibition or mutation (Bonilla and Cunningham, 2002; Hilioti and Cunningham, 2004).

Targeted inhibitors of Cn are needed to combat infection and other pathological conditions associated with excess Cn activity.

Additionally, imaging the GFP-CRZ1(ΔZF) probe in the 4-chamber microfluidic device I used could allow for side-by-side comparison of Cn signaling in different conditions. Numerous yeast models have been created to study human diseases that have been linked to Cn misregulation (Voisset et al., 2014; Daniel and Moore, 2015). Basal Cn activity and the response to relevant stimuli could be observed over long periods to detect changes in the disease model strains compared to controls.

I have shown that Cn activation can be measured in real time in single cells. These measurements have revealed details of the timing of the action of Cn regulators. Despite the difference in their functions and regulation, I have shown that Pmc1p and Vcx1p are both needed to maintain cytosolic Ca^{2+} equilibrium in non-stimulating conditions and in the short-term response to stimulation. My experiments determined that Rcn1p is needed for activation of Cn both before and after a stimulus. I revealed a positive feedback loop through Crz1p on Cn in steady-state conditions, both with and without stimulation of Cn. These findings give us a greater understanding of how Cn is regulated. This understanding can be applied to the many clinical conditions which have implicated misregulation of Cn as a contributing factor. Future applications of the probe I developed have the potential to further elucidate this complex and crucial pathway.

REFERENCES

Ando A, Suzuki C. Cooperative function of the CHD5-like protein Mdm39p with a P-type ATPase Spf1p in the maintenance of ER homeostasis in Saccharomyces cerevisiae. Mol. Genet. Genomics. 2005 Jul;273(6):497–506.

Bakker AC, Webster P, Jacob WA, Andrews NW. Homotypic fusion between aggregated lysosomes triggered by elevated [Ca2+]i in fibroblasts. J. Cell. Sci. 1997 Sep;110 (Pt 18):2227–38.

Berna-Erro A, Redondo PC, Rosado JA. Store-operated Ca(2+) entry. Adv. Exp. Med. Biol. 2012;740:349–82.

Berridge MJ. Calcium signalling and Alzheimer's disease. Neurochem. Res. 2011 Jul;36(7):1149–56.

Berridge MJ. Calcium signalling remodelling and disease. Biochem. Soc. Trans. 2012 Apr;40(2):297–309.

Berridge MJ, Lipp P, Bootman MD. The versatility and universality of calcium signalling. Nat. Rev. Mol. Cell Biol. 2000 Oct;1(1):11–21.

Bers DM. Calcium cycling and signaling in cardiac myocytes. Annu. Rev. Physiol. 2008;70:23–49.

Bezprozvanny IB. Calcium signaling and neurodegeneration. Acta Naturae. 2010

Apr;2(1):72–82. PMCID: PMC3347543

Bito H, Deisseroth K, Tsien RW. CREB phosphorylation and dephosphorylation: a Ca(2+)- and stimulus duration-dependent switch for hippocampal gene expression. Cell. 1996 Dec 27;87(7):1203–14.

Bodvard K, Jörhov A, Blomberg A, Molin M, Käll M. The yeast transcription factor Crz1 is activated by light in a Ca2+/calcineurin-dependent and PKA-independent manner. PLoS ONE. 2013;8(1):e53404. PMCID: PMC3546054

Bonilla M, Cunningham KW. Calcium release and influx in yeast: TRPC and VGCC rule another kingdom. Sci. STKE. 2002 Apr 9;2002(127):pe17.

Bonilla M, Cunningham KW. Mitogen-activated protein kinase stimulation of Ca(2+) signaling is required for survival of endoplasmic reticulum stress in yeast. Mol. Biol. Cell. 2003 Oct;14(10):4296–305. PMCID: PMC207020

Bonilla M, Nastase KK, Cunningham KW. Essential role of calcineurin in response to endoplasmic reticulum stress. EMBO J. 2002 May 15;21(10):2343–53. PMCID: PMC126012

Bouillet LEM, Cardoso AS, Perovano E, Pereira RR, Ribeiro EMC, Trópia MJM, et al. The involvement of calcium carriers and of the vacuole in the glucose-induced calcium signaling and activation of the plasma membrane H(+)-ATPase in Saccharomyces cerevisiae cells. Cell Calcium. 2012 Jan;51(1):72–81.

Boyman L, Williams GSB, Khananshvili D, Sekler I, Lederer WJ. NCLX: The

mitochondrial sodium calcium exchanger. J. Mol. Cell. Cardiol. 2013 Jun;59:205–13.

Brini M, Carafoli E. Calcium pumps in health and disease. Physiol. Rev. 2009 Oct;89(4):1341–78.

Brochet DXP, Yang D, Cheng H, Lederer WJ. Elementary calcium release events from the sarcoplasmic reticulum in the heart. Adv. Exp. Med. Biol. 2012;740:499–509. PMCID: PMC3535270

Bultynck G, Heath VL, Majeed AP, Galan J-M, Haguenauer-Tsapis R, Cyert MS. Slm1 and slm2 are novel substrates of the calcineurin phosphatase required for heat stress-induced endocytosis of the yeast uracil permease. Mol. Cell. Biol. 2006 Jun;26(12):4729–45. PMCID: PMC1489119

Cai L, Dalal CK, Elowitz MB. Frequency-modulated nuclear localization bursts coordinate gene regulation. Nature. 2008 Sep 25;455(7212):485–90. PMCID: PMC2695983

Cai X, Lytton J. The cation/Ca(2+) exchanger superfamily: phylogenetic analysis and structural implications. Mol. Biol. Evol. 2004 Sep;21(9):1692–703.

Cao X, Kambe F, Miyazaki T, Sarkar D, Ohmori S, Seo H. Novel human ZAKI-4 isoforms: hormonal and tissue-specific regulation and function as calcineurin inhibitors. Biochem. J. 2002 Oct 15;367(Pt 2):459–66. PMCID: PMC1222895

Carafoli E, Brini M. Calcium pumps: structural basis for and mechanism of

calcium transmembrane transport. Curr Opin Chem Biol. 2000 Apr;4(2):152–61.

Chen Y-L, Konieczka JH, Springer DJ, Bowen SE, Zhang J, Silao FGS, et al. Convergent Evolution of Calcineurin Pathway Roles in Thermotolerance and Virulence in Candida glabrata. G3 (Bethesda). 2012 Jun;2(6):675–91. PMCID: PMC3362297

Clapham DE. Calcium signaling. Cell. 2007 Dec 14;131(6):1047–58.

Coen K, Flannagan RS, Baron S, Carraro-Lacroix LR, Wang D, Vermeire W, et al. Lysosomal calcium homeostasis defects, not proton pump defects, cause endo-lysosomal dysfunction in PSEN-deficient cells. J. Cell Biol. 2012 Jul 9;198(1):23–35. PMCID: PMC3392942

Connor JH, Frederick D, Huang HB, Yang J, Helps NR, Cohen PT, et al. Cellular mechanisms regulating protein phosphatase-1. A key functional interaction between inhibitor-2 and the type 1 protein phosphatase catalytic subunit. J. Biol. Chem. 2000 Jun 23;275(25):18670–5.

Cousin MA, Robinson PJ. The dephosphins: dephosphorylation by calcineurin triggers synaptic vesicle endocytosis. Trends Neurosci. 2001 Nov;24(11):659–65.

Crabtree GR, Graef IA. Bursting into the nucleus. Sci Signal. 2008;1(51):pe54. PMCID: PMC2713346

Cronin SR, Khoury A, Ferry DK, Hampton RY. Regulation of HMG-CoA

reductase degradation requires the P-type ATPase Cod1p/Spf1p. J. Cell Biol. 2000 Mar 6;148(5):915–24. PMCID: PMC2174543

Cronin SR, Rao R, Hampton RY. Cod1p/Spf1p is a P-type ATPase involved in ER function and Ca2+ homeostasis. J. Cell Biol. 2002 Jun 10;157(6):1017–28. PMCID: PMC2174042

Cui J, Kaandorp JA, Ositelu OO, Beaudry V, Knight A, Nanfack YF, et al. Simulating calcium influx and free calcium concentrations in yeast. Cell Calcium. 2009a Feb;45(2):123–32. PMCID: PMC3130064

Cui J, Kaandorp JA, Sloot PMA, Lloyd CM, Filatov MV. Calcium homeostasis and signaling in yeast cells and cardiac myocytes. FEMS Yeast Res. 2009b Dec;9(8):1137–47.

Cunningham KW. Acidic calcium stores of Saccharomyces cerevisiae. Cell Calcium. 2011 Aug;50(2):129–38. PMCID: PMC3137693

Cunningham KW, Fink GR. Calcineurin-dependent growth control in Saccharomyces cerevisiae mutants lacking PMC1, a homolog of plasma membrane Ca2+ ATPases. J. Cell Biol. 1994 Feb;124(3):351–63. PMCID: PMC2119937

Cunningham KW, Fink GR. Calcineurin inhibits VCX1-dependent H+/Ca2+ exchange and induces Ca2+ ATPases in Saccharomyces cerevisiae. Mol. Cell. Biol. 1996 May;16(5):2226–37. PMCID: PMC231210

Cyert MS. Genetic analysis of calmodulin and its targets in Saccharomyces cerevisiae. Annu. Rev. Genet. 2001;35:647–72.

Cyert MS. Calcineurin signaling in Saccharomyces cerevisiae: how yeast go crazy in response to stress. Biochem. Biophys. Res. Commun. 2003 Nov 28;311(4):1143–50.

Cyert MS, Philpott CC. Regulation of cation balance in Saccharomyces cerevisiae. Genetics. 2013 Mar;193(3):677–713. PMCID: PMC3583992

Dalal CK, Cai L, Lin Y, Rahbar K, Elowitz MB. Pulsatile dynamics in the yeast proteome. Curr. Biol. 2014 Sep 22;24(18):2189–94. PMCID: PMC4203654

Daniel G, Moore DJ. Modeling LRRK2 Pathobiology in Parkinson's Disease: From Yeast to Rodents. Curr Top Behav Neurosci. 2015;22:331–68.

Davies KJA, Ermak G, Rothermel BA, Pritchard M, Heitman J, Ahnn J, et al. Renaming the DSCR1 / Adapt78 gene family as RCAN: regulators of calcineurin. FASEB J. 2007 Oct;21(12):3023–8.

De Stefani D, Raffaello A, Teardo E, Szabò I, Rizzuto R. A forty-kilodalton protein of the inner membrane is the mitochondrial calcium uniporter. Nature. 2011 Aug 18;476(7360):336–40.

Demaegd D, Foulquier F, Colinet A-S, Gremillon L, Legrand D, Mariot P, et al. Newly characterized Golgi-localized family of proteins is involved in calcium and pH homeostasis in yeast and human cells. Proc. Natl. Acad. Sci. U.S.A.

2013 Apr 23;110(17):6859–64. PMCID: PMC3637739

Dolmetsch R. Excitation-transcription coupling: signaling by ion channels to the nucleus. Sci. STKE. 2003 Jan 21;2003(166):PE4.

Drerup MM, Schlücking K, Hashimoto K, Manishankar P, Steinhorst L, Kuchitsu K, et al. The calcineurin B-like calcium sensors CBL1 and CBL9 together with their interacting protein kinase CIPK26 regulate the Arabidopsis NADPH oxidase RBOHF. Mol Plant. 2013 Jan 18.

Dudgeon DD, Zhang N, Ositelu OO, Kim H, Cunningham KW. Nonapoptotic death of Saccharomyces cerevisiae cells that is stimulated by Hsp90 and inhibited by calcineurin and Cmk2 in response to endoplasmic reticulum stresses. Eukaryotic Cell. 2008 Dec;7(12):2037–51. PMCID: PMC2593186

Dunn T, Gable K, Beeler T. Regulation of cellular Ca2+ by yeast vacuoles. J. Biol. Chem. 1994 Mar 11;269(10):7273–8.

Ermak G, Harris CD, Davies KJA. The DSCR1 (Adapt78) isoform 1 protein calcipressin 1 inhibits calcineurin and protects against acute calcium-mediated stress damage, including transient oxidative stress. FASEB J. 2002 Jun;16(8):814–24.

Faas GC, Raghavachari S, Lisman JE, Mody I. Calmodulin as a direct detector of Ca2+ signals. Nat. Neurosci. 2011 Mar;14(3):301–4. PMCID: PMC3057387

Flory MR, Moser MJ, Monnat RJ, Davis TN. Identification of a human

centrosomal calmodulin-binding protein that shares homology with pericentrin. Proc. Natl. Acad. Sci. U.S.A. 2000 May 23;97(11):5919–23. PMCID: PMC18534

Fox DS, Heitman J. Calcineurin-binding protein Cbp1 directs the specificity of calcineurin-dependent hyphal elongation during mating in Cryptococcus neoformans. Eukaryotic Cell. 2005 Sep;4(9):1526–38. PMCID: PMC1214203

Fuentes JJ, Genescà L, Kingsbury TJ, Cunningham KW, Pérez-Riba M, Estivill X, et al. DSCR1, overexpressed in Down syndrome, is an inhibitor of calcineurin-mediated signaling pathways. Hum. Mol. Genet. 2000 Jul 1;9(11):1681–90.

Galione A, Chuang K-T. Pyridine nucleotide metabolites and calcium release from intracellular stores. Adv. Exp. Med. Biol. 2012;740:305–23.

Genazzani AA, Carafoli E, Guerini D. Calcineurin controls inositol 1,4,5-trisphosphate type 1 receptor expression in neurons. Proc. Natl. Acad. Sci. U.S.A. 1999 May 11;96(10):5797–801. PMCID: PMC21940

Gennaro R, Pozzan T, Romeo D. Monitoring of cytosolic free Ca2+ in C5a-stimulated neutrophils: loss of receptor-modulated Ca2+ stores and Ca2+ uptake in granule-free cytoplasts. Proc. Natl. Acad. Sci. U.S.A. 1984 Mar;81(5):1416–20. PMCID: PMC344846

Gilabert JA. Cytoplasmic calcium buffering. Adv. Exp. Med. Biol. 2012;740:483–98.

Goffeau A, Barrell BG, Bussey H, Davis RW, Dujon B, Feldmann H, et al. Life with 6000 genes. Science. 1996 Oct 25;274(5287):546–563–7.

Görlach J, Fox DS, Cutler NS, Cox GM, Perfect JR, Heitman J. Identification and characterization of a highly conserved calcineurin binding protein, CBP1/calcipressin, in Cryptococcus neoformans. EMBO J. 2000 Jul 17;19(14):3618–29. PMCID: PMC313974

Groth RD, Dunbar RL, Mermelstein PG. Calcineurin regulation of neuronal plasticity. Biochem. Biophys. Res. Commun. 2003 Nov 28;311(4):1159–71.

Guarente L. Yeast promoters and lacZ fusions designed to study expression of cloned genes in yeast. Meth. Enzymol. 1983;101:181–91.

Guiney EL, Goldman AR, Elias JE, Cyert MS. Calcineurin regulates the yeast synaptojanin Inp53/Sjl3 during membrane stress. Mol. Biol. Cell. 2015 Feb 15;26(4):769–85. PMCID: PMC4325846

Gwack Y, Feske S, Srikanth S, Hogan PG, Rao A. Signalling to transcription: store-operated Ca2+ entry and NFAT activation in lymphocytes. Cell Calcium. 2007 Aug;42(2):145–56.

Heath VL, Shaw SL, Roy S, Cyert MS. Hph1p and Hph2p, novel components of calcineurin-mediated stress responses in Saccharomyces cerevisiae. Eukaryotic Cell. 2004 Jun;3(3):695–704. PMCID: PMC420127

Heineke J, Wollert KC, Osinska H, Sargent MA, York AJ, Robbins J, et al.

Calcineurin protects the heart in a murine model of dilated cardiomyopathy. J. Mol. Cell. Cardiol. 2010 Jun;48(6):1080–7. PMCID: PMC2891089

Hersen P, McClean MN, Mahadevan L, Ramanathan S. Signal processing by the HOG MAP kinase pathway. Proc. Natl. Acad. Sci. U.S.A. 2008 May 20;105(20):7165–70. PMCID: PMC2386076

Hilioti Z, Cunningham KW. The RCN family of calcineurin regulators. Biochem. Biophys. Res. Commun. 2003 Nov 28;311(4):1089–93.

Hilioti Z, Cunningham KW. Calcineurin: Roles of the Ca2+/calmodulindependent protein phosphatase in diverse eukaryotes. Topics in Current Genetics. 2004 Oct 23;5:1–18.

Hilioti Z, Gallagher DA, Low-Nam ST, Ramaswamy P, Gajer P, Kingsbury TJ, et al. GSK-3 kinases enhance calcineurin signaling by phosphorylation of RCNs. Genes & Development. 2004 Jan 1;18(1):35–47. PMCID: PMC314273

Hill JA, Rothermel B, Yoo K-D, Cabuay B, Demetroulis E, Weiss RM, et al. Targeted inhibition of calcineurin in pressure-overload cardiac hypertrophy. Preservation of systolic function. J. Biol. Chem. 2002 Mar 22;277(12):10251–5.

Hogan PG, Chen L, Nardone J, Rao A. Transcriptional regulation by calcium, calcineurin, and NFAT. Genes & Development. 2003 Sep 15;17(18):2205–32.

Hurley TD, Yang J, Zhang L, Goodwin KD, Zou Q, Cortese M, et al. Structural basis for regulation of protein phosphatase 1 by inhibitor-2. J. Biol. Chem. 2007

Sep 28;282(39):28874–83.

Igarashi M, Watanabe M. Roles of calmodulin and calmodulin-binding proteins in synaptic vesicle recycling during regulated exocytosis at submicromolar Ca2+ concentrations. Neurosci. Res. 2007 Jul;58(3):226–33.

Iida H, Yagawa Y, Anraku Y. Essential role for induced Ca2+ influx followed by [Ca2+]i rise in maintaining viability of yeast cells late in the mating pheromone response pathway. A study of [Ca2+]i in single Saccharomyces cerevisiae cells with imaging of fura-2. J. Biol. Chem. 1990 Aug 5;265(22):13391–9.

Ingwall JS, Balschi JA. Energetics of the Na(+) pump in the heart. J. Cardiovasc. Electrophysiol. 2006 May;17 Suppl 1:S127–33.

Jang C, Lim JH, Park CW, Cho Y-J. Regulator of Calcineurin 1 Isoform 4 (RCAN1.4) Is Overexpressed in the Glomeruli of Diabetic Mice. Korean J. Physiol. Pharmacol. 2011 Oct;15(5):299–305. PMCID: PMC3222800

Jung M-S, Park J-H, Ryu YS, Choi S-H, Yoon S-H, Kwen M-Y, et al. Regulation of RCAN1 protein activity by Dyrk1A protein-mediated phosphorylation. J. Biol. Chem. 2011 Nov 18;286(46):40401–12. PMCID: PMC3220559

Kafadar KA, Zhu H, Snyder M, Cyert MS. Negative regulation of calcineurin signaling by Hrr25p, a yeast homolog of casein kinase I. Genes & Development. 2003 Nov 1;17(21):2698–708. PMCID: PMC280619

Kao S-C, Wu H, Xie J, Chang C-P, Ranish JA, Graef IA, et al. Calcineurin/NFAT signaling is required for neuregulin-regulated Schwann cell differentiation. Science. 2009 Jan 30;323(5914):651–4. PMCID: PMC2790385

Karlstad J, Sun Y, Singh BB. Ca(2+) signaling: an outlook on the characterization of Ca(2+) channels and their importance in cellular functions. Adv. Exp. Med. Biol. 2012;740:143–57. PMCID: PMC3316125

Kashir J, Jones C, Coward K. Calcium oscillations, oocyte activation, and phospholipase C zeta. Adv. Exp. Med. Biol. 2012;740:1095–121.

Katanosaka Y, Iwata Y, Kobayashi Y, Shibasaki F, Wakabayashi S, Shigekawa M. Calcineurin inhibits Na+/Ca2+ exchange in phenylephrine-treated hypertrophic cardiomyocytes. J. Biol. Chem. 2005 Feb 18;280(7):5764–72.

Kim Y, Lee Y-I, Seo M, Kim S-Y, Lee J-E, Youn H-D, et al. Calcineurin dephosphorylates glycogen synthase kinase-3 beta at serine-9 in neuroblast-derived cells. J. Neurochem. 2009 Oct;111(2):344–54.

Kingsbury TJ, Cunningham KW. A conserved family of calcineurin regulators. Genes & Development. 2000 Jul 1;14(13):1595–604. PMCID: PMC316734

Kishi T, Ikeda A, Nagao R, Koyama N. The SCFCdc4 ubiquitin ligase regulates calcineurin signaling through degradation of phosphorylated Rcn1, an inhibitor of calcineurin. Proc. Natl. Acad. Sci. U.S.A. 2007 Oct 30;104(44):17418–23. PMCID: PMC2077271

Krumpe K, Frumkin I, Herzig Y, Rimon N, Özbalci C, Brügger B, et al. Ergosterol content specifies targeting of tail-anchored proteins to mitochondrial outer membranes. Mol. Biol. Cell. 2012 Oct;23(20):3927–35. PMCID: PMC3469509

Kumashiro S, Lu Y-F, Tomizawa K, Matsushita M, Wei F-Y, Matsui H. Regulation of synaptic vesicle recycling by calcineurin in different vesicle pools. Neurosci. Res. 2005 Apr;51(4):435–43.

Lanner JT. Ryanodine receptor physiology and its role in disease. Adv. Exp. Med. Biol. 2012;740:217–34.

Laviña WA, Hermansyah, Sugiyama M, Kaneko Y, Harashima S. Functionally redundant protein phosphatase genes PTP2 and MSG5 co-regulate the calcium signaling pathway in Saccharomyces cerevisiae upon exposure to high extracellular calcium concentration. J. Biosci. Bioeng. 2012 Oct 11.

Lee JI, Dhakal BK, Lee J, Bandyopadhyay J, Jeong SY, Eom SH, et al. The Caenorhabditis elegans homologue of Down syndrome critical region 1, RCN-1, inhibits multiple functions of the phosphatase calcineurin. J. Mol. Biol. 2003 Apr 18;328(1):147–56.

Levine JH, Lin Y, Elowitz MB. Functional roles of pulsing in genetic circuits. Science. 2013 Dec 6;342(6163):1193–200. PMCID: PMC4100686

Li H, Rao A, Hogan PG. Interaction of calcineurin with substrates and targeting proteins. Trends Cell Biol. 2011 Feb;21(2):91–103. PMCID: PMC3244350

Li J, Jia Z, Zhou W, Wei Q. Calcineurin regulatory subunit B is a unique calcium sensor that regulates calcineurin in both calcium-dependent and calcium-independent manner. Proteins. 2009 Nov 15;77(3):612–23.

Li L, Guerini D, Carafoli E. Calcineurin controls the transcription of Na+/Ca2+ exchanger isoforms in developing cerebellar neurons. J. Biol. Chem. 2000 Jul 7;275(27):20903–10.

Lin Y, Sohn CH, Dalal CK, Cai L, Elowitz MB. Combinatorial gene regulation by modulation of relative pulse timing. Nature. 2015 Nov 5;527(7576):54–8.

Lissandron V, Podini P, Pizzo P, Pozzan T. Unique characteristics of Ca2+ homeostasis of the trans-Golgi compartment. Proc. Natl. Acad. Sci. U.S.A. 2010 May 18;107(20):9198–203. PMCID: PMC2889052

Locke EG, Bonilla M, Liang L, Takita Y, Cunningham KW. A homolog of voltage-gated Ca(2+) channels stimulated by depletion of secretory Ca(2+) in yeast. Mol. Cell. Biol. 2000 Sep;20(18):6686–94. PMCID: PMC86178

Lodygin D, Odoardi F, Schläger C, Körner H, Kitz A, Nosov M, et al. A combination of fluorescent NFAT and H2B sensors uncovers dynamics of T cell activation in real time during CNS autoimmunity. Nat. Med. 2013 Jun;19(6):784–90.

Longtine MS, McKenzie A, Demarini DJ, Shah NG, Wach A, Brachat A, et al. Additional modules for versatile and economical PCR-based gene deletion and modification in Saccharomyces cerevisiae. Yeast. 1998 Jul;14(10):953–61.

Lytton J. Na+/Ca2+ exchangers: three mammalian gene families control Ca2+ transport. Biochem. J. 2007 Sep 15;406(3):365–82.

Mackrill JJ. Ryanodine receptor calcium release channels: an evolutionary perspective. Adv. Exp. Med. Biol. 2012;740:159–82.

Maier LS. Ca(2+)/calmodulin-dependent protein kinase II (CaMKII) in the heart. Adv. Exp. Med. Biol. 2012;740:685–702.

Martin DC, Kim H, Mackin NA, Maldonado-Báez L, Evangelista CC, Beaudry VG, et al. New regulators of a high affinity Ca2+ influx system revealed through a genome-wide screen in yeast. J. Biol. Chem. 2011 Mar 25;286(12):10744–54. PMCID: PMC3060525

Matheos DP, Kingsbury TJ, Ahsan US, Cunningham KW. Tcn1p/Crz1p, a calcineurin-dependent transcription factor that differentially regulates gene expression in Saccharomyces cerevisiae. Genes & Development. 1997 Dec 15;11(24):3445–58. PMCID: PMC316804

Mehta S, Li H, Hogan PG, Cunningham KW. Domain architecture of the regulators of calcineurin (RCANs) and identification of a divergent RCAN in yeast. Mol. Cell. Biol. 2009 May;29(10):2777–93. PMCID: PMC2682025

Michailova A, McCulloch A. Model study of ATP and ADP buffering, transport of Ca(2+) and Mg(2+), and regulation of ion pumps in ventricular myocyte. Biophys. J. 2001 Aug;81(2):614–29. PMCID: PMC1301539

Minami T, Horiuchi K, Miura M, Abid MR, Takabe W, Noguchi N, et al. Vascular endothelial growth factor- and thrombin-induced termination factor, Down syndrome critical region-1, attenuates endothelial cell proliferation and angiogenesis. J. Biol. Chem. 2004 Nov 26;279(48):50537–54.

Miseta A, Kellermayer R, Aiello DP, Fu L, Bedwell DM. The vacuolar Ca2+/H+ exchanger Vcx1p/Hum1p tightly controls cytosolic Ca2+ levels in S. cerevisiae. FEBS Lett. 1999 May 21;451(2):132–6.

Miyakawa T, Mizunuma M. Physiological roles of calcineurin in Saccharomyces cerevisiae with special emphasis on its roles in G2/M cell-cycle regulation. Biosci. Biotechnol. Biochem. 2007 Mar;71(3):633–45.

Molkentin JD, Lu JR, Antos CL, Markham B, Richardson J, Robbins J, et al. A calcineurin-dependent transcriptional pathway for cardiac hypertrophy. Cell. 1998 Apr 17;93(2):215–28.

Montalvo GB, Artalejo AR, Gilabert JA. ATP from subplasmalemmal mitochondria controls Ca2+-dependent inactivation of CRAC channels. J. Biol. Chem. 2006 Nov 24;281(47):35616–23.

Muller EM, Locke EG, Cunningham KW. Differential regulation of two Ca(2+) influx systems by pheromone signaling in Saccharomyces cerevisiae. Genetics. 2001 Dec;159(4):1527–38. PMCID: PMC1461924

Muller EM, Mackin NA, Erdman SE, Cunningham KW. Fig1p facilitates Ca2+ influx and cell fusion during mating of Saccharomyces cerevisiae. J. Biol.

Chem. 2003 Oct 3;278(40):38461–9.

Muravyov A, Tikhomirova I. Role Ca(2+) in mechanisms of the red blood cells microrheological changes. Adv. Exp. Med. Biol. 2012;740:1017–38.

Müller B, Grossniklaus U. Model organisms--A historical perspective. J Proteomics. 2010 Oct 10;73(11):2054–63.

Müller MR, Sasaki Y, Stevanovic I, Lamperti ED, Ghosh S, Sharma S, et al. Requirement for balanced Ca/NFAT signaling in hematopoietic and embryonic development. Proc. Natl. Acad. Sci. U.S.A. 2009 Apr 28;106(17):7034–9. PMCID: PMC2678457

Nakamura TY, Jeromin A, Mikoshiba K, Wakabayashi S. Neuronal calcium sensor-1 promotes immature heart function and hypertrophy by enhancing Ca2+ signals. Circ. Res. 2011 Aug 19;109(5):512–23.

Neher E, Sakaba T. Multiple roles of calcium ions in the regulation of neurotransmitter release. Neuron. 2008 Sep 25;59(6):861–72.

Oda K. Calcium depletion blocks proteolytic cleavages of plasma protein precursors which occur at the Golgi and/or trans-Golgi network. Possible involvement of Ca(2+)-dependent Golgi endoproteases. J. Biol. Chem. 1992 Aug 25;267(24):17465–71.

Padhan K, Varma R. Immunological synapse: a multi-protein signalling cellular apparatus for controlling gene expression. Immunology. 2010 Mar;129(3):322–

8. PMCID: PMC2826677

Palmer CP, Zhou XL, Lin J, Loukin SH, Kung C, Saimi Y. A TRP homolog in Saccharomyces cerevisiae forms an intracellular Ca(2+)-permeable channel in the yeast vacuolar membrane. Proc. Natl. Acad. Sci. U.S.A. 2001 Jul 3;98(14):7801–5. PMCID: PMC35422

Palty R, Hershfinkel M, Sekler I. Molecular, Identity and Functional Properties of the Mitochondrial Na+/Ca2+ Exchanger. J. Biol. Chem. 2012 Jul 20. PMCID: PMC3442499

Palty R, Sekler I. The mitochondrial Na(+)/Ca(2+) exchanger. Cell Calcium. 2012 Jul;52(1):9–15.

Parys JB, De Smedt H. Inositol 1,4,5-trisphosphate and its receptors. Adv. Exp. Med. Biol. 2012;740:255–79.

Petrenko N, Chereji RV, McClean MN, Morozov AV, Broach JR. Noise and interlocking signaling pathways promote distinct transcription factor dynamics in response to different stresses. Mol. Biol. Cell. 2013 Jun;24(12):2045–57. PMCID: PMC3681706

Popa C-V, Dumitru I, Ruta LL, Danet AF, Farcasanu IC. Exogenous oxidative stress induces Ca2+ release in the yeast Saccharomyces cerevisiae. FEBS J. 2010 Oct;277(19):4027–38.

Pozos TC, Sekler I, Cyert MS. The product of HUM1, a novel yeast gene, is

required for vacuolar Ca2+/H+ exchange and is related to mammalian Na+/Ca2+ exchangers. Mol. Cell. Biol. 1996 Jul;16(7):3730–41. PMCID: PMC231369

Prins D, Michalak M. Organellar calcium buffers. Cold Spring Harb Perspect Biol. 2011 Mar;3(3). PMCID: PMC3039927

Ramsey IS, Delling M, Clapham DE. An introduction to TRP channels. Annu. Rev. Physiol. 2006;68:619–47.

Reese LC, Taglialatela G. A role for calcineurin in Alzheimer's disease. Curr Neuropharmacol. 2011 Dec;9(4):685–92. PMCID: PMC3263462

Resende RR, Adhikari A, da Costa JL, Lorençon E, Ladeira MS, Guatimosim S, et al. Influence of spontaneous calcium events on cell-cycle progression in embryonal carcinoma and adult stem cells. Biochim. Biophys. Acta. 2010 Feb;1803(2):246–60.

Roberts SK, McAinsh M, Widdicks L. Cch1p mediates Ca2+ influx to protect Saccharomyces cerevisiae against eugenol toxicity. PLoS ONE. 2012;7(9):e43989. PMCID: PMC3441571

Rodríguez A, Benito B, Cagnac O. Using heterologous expression systems to characterize potassium and sodium transport activities. Methods Mol. Biol. 2012;913:371–86.

Ronkainen JJ, Hänninen SL, Korhonen T, Koivumäki JT, Skoumal R, Rautio S, et

al. Ca2+-calmodulin-dependent protein kinase II represses cardiac transcription of the L-type calcium channel alpha(1C)-subunit gene (Cacna1c) by DREAM translocation. J. Physiol. (Lond.). 2011 Jun 1;589(Pt 11):2669–86. PMCID: PMC3112547

Rothermel B, Vega RB, Yang J, Wu H, Bassel-Duby R, Williams RS. A protein encoded within the Down syndrome critical region is enriched in striated muscles and inhibits calcineurin signaling. J. Biol. Chem. 2000 Mar 24;275(12):8719–25.

Rusnak F, Mertz P. Calcineurin: form and function. Physiol. Rev. 2000 Oct;80(4):1483–521.

Saftig P, Klumperman J. Lysosome biogenesis and lysosomal membrane proteins: trafficking meets function. Nat. Rev. Mol. Cell Biol. 2009 Sep;10(9):623–35.

Sanna B, Brandt EB, Kaiser RA, Pfluger P, Witt SA, Kimball TR, et al. Modulatory calcineurin-interacting proteins 1 and 2 function as calcineurin facilitators in vivo. Proc. Natl. Acad. Sci. U.S.A. 2006 May 9;103(19):7327–32. PMCID: PMC1464340

Saris N-EL, Carafoli E. A historical review of cellular calcium handling, with emphasis on mitochondria. Biochemistry Mosc. 2005 Feb;70(2):187–94.

Sasaki T, Takemori H, Yagita Y, Terasaki Y, Uebi T, Horike N, et al. SIK2 is a key regulator for neuronal survival after ischemia via TORC1-CREB. Neuron. 2011

Jan 13;69(1):106–19.

Saucerman JJ, Bers DM. Calmodulin mediates differential sensitivity of CaMKII and calcineurin to local Ca2+ in cardiac myocytes. Biophys. J. 2008 Nov 15;95(10):4597–612. PMCID: PMC2576378

Schaub MC, Heizmann CW. Calcium, troponin, calmodulin, S100 proteins: from myocardial basics to new therapeutic strategies. Biochem. Biophys. Res. Commun. 2008 Apr 25;369(1):247–64.

Schwaller B. Cytosolic Ca2+ buffers. Cold Spring Harb Perspect Biol. 2010 Nov;2(11):a004051. PMCID: PMC2964180

Schwaller B. The regulation of a cell's Ca(2+) signaling toolkit: the Ca (2+) homeostasome. Adv. Exp. Med. Biol. 2012;740:1–25.

Sherman F, Hicks JB, Fink GR. Methods in Yeast Genetics. Cold Spring Harbor, NY: Cold Spring Harbor Laboratory; 1986.

Shigekawa M, Katanosaka Y, Wakabayashi S. Regulation of the cardiac Na+/Ca2+ exchanger by calcineurin and protein kinase C. Ann. N. Y. Acad. Sci. 2007 Mar;1099:53–63.

Shin S-Y, Yang HW, Kim J-R, Heo WD, Cho K-H. A hidden incoherent switch regulates RCAN1 in the calcineurin-NFAT signaling network. J. Cell. Sci. 2011 Jan 1;124(Pt 1):82–90.

Siwek M, Henseler C, Broich K, Papazoglou A, Weiergräber M. Voltage-gated

Ca(2+) channel mediated Ca(2+) influx in epileptogenesis. Adv. Exp. Med. Biol. 2012;740:1219–47.

Skelding KA, Rostas JAP. The role of molecular regulation and targeting in regulating calcium/calmodulin stimulated protein kinases. Adv. Exp. Med. Biol. 2012;740:703–30.

Skupin A, Thurley K. Calcium signaling: from single channels to pathways. Adv. Exp. Med. Biol. 2012;740:531–51.

Stathopoulos AM, Cyert MS. Calcineurin acts through the CRZ1/TCN1-encoded transcription factor to regulate gene expression in yeast. Genes & Development. 1997 Dec 15;11(24):3432–44. PMCID: PMC316814

Stathopoulos-Gerontides AM, Guo JJ, Cyert MS. Yeast calcineurin regulates nuclear localization of the Crz1p transcription factor through dephosphorylation. Genes & Development. 1999 Apr 1;13(7):798–803. PMCID: PMC316598

Stemmer PM, Wang X, Krinks MH, Klee CB. Factors responsible for the Ca(2+)-dependent inactivation of calcineurin in brain. FEBS Lett. 1995 Oct 30;374(2):237–40.

Su Z, Zhou X, Loukin SH, Saimi Y, Kung C. Mechanical force and cytoplasmic Ca(2+) activate yeast TRPY1 in parallel. J. Membr. Biol. 2009 Feb;227(3):141–50.

Suzuki C, Shimma YI. P-type ATPase spf1 mutants show a novel resistance

mechanism for the killer toxin SMKT. Mol. Microbiol. 1999 May;32(4):813–23.

Sørensen DM, Møller AB, Jakobsen MK, Jensen MK, Vangheluwe P, Buch-Pedersen MJ, et al. Ca2+ induces spontaneous dephosphorylation of a novel P5A-type ATPase. J. Biol. Chem. 2012 Aug 17;287(34):28336–48. PMCID: PMC3436585

Takita Y, Engstrom L, Ungermann C, Cunningham KW. Inhibition of the Ca(2+)-ATPase Pmc1p by the v-SNARE protein Nyv1p. J. Biol. Chem. 2001 Mar 2;276(9):6200–6.

Tang F, Liu W. An age-dependent feedback control model of calcium dynamics in yeast cells. J Math Biol. 2010 Jun;60(6):849–79.

Thurley K, Skupin A, Thul R, Falcke M. Fundamental properties of Ca2+ signals. Biochim. Biophys. Acta. 2012 Aug;1820(8):1185–94.

Tipper DJ, Harley CA. Yeast genes controlling responses to topogenic signals in a model transmembrane protein. Mol. Biol. Cell. 2002 Apr;13(4):1158–74. PMCID: PMC102259

Tisi R, Baldassa S, Belotti F, Martegani E. Phospholipase C is required for glucose-induced calcium influx in budding yeast. FEBS Lett. 2002 Jun 5;520(1-3):133–8.

Ton V-K, Rao R. Functional expression of heterologous proteins in yeast: insights into Ca2+ signaling and Ca2+-transporting ATPases. Am. J. Physiol., Cell

Physiol. 2004 Sep;287(3):C580–9.

Uchida K, Aramaki M, Nakazawa M, Yamagishi C, Makino S, Fukuda K, et al. Gene knock-outs of inositol 1,4,5-trisphosphate receptors types 1 and 2 result in perturbation of cardiogenesis. PLoS ONE. 2010;5(9). PMCID: PMC2931702

Vashist S, Frank CG, Jakob CA, Ng DTW. Two distinctly localized p-type ATPases collaborate to maintain organelle homeostasis required for glycoprotein processing and quality control. Mol. Biol. Cell. 2002 Nov;13(11):3955–66. PMCID: PMC133606

Vega RB, Rothermel BA, Weinheimer CJ, Kovacs A, Naseem RH, Bassel-Duby R, et al. Dual roles of modulatory calcineurin-interacting protein 1 in cardiac hypertrophy. Proc. Natl. Acad. Sci. U.S.A. 2003 Jan 21;100(2):669–74. PMCID: PMC141054

Vega RB, Yang J, Rothermel BA, Bassel-Duby R, Williams RS. Multiple domains of MCIP1 contribute to inhibition of calcineurin activity. J. Biol. Chem. 2002 Aug 16;277(33):30401–7.

Voisset C, García-Rodríguez N, Birkmire A, Blondel M, Wellinger RE. Using yeast to model calcium-related diseases: example of the Hailey-Hailey disease. Biochim. Biophys. Acta. 2014 Oct;1843(10):2315–21.

Wang H, Du Y, Xiang B, Lin W, Li X, Wei Q. A renewed model of CNA regulation involving its C-terminal regulatory domain and CaM. Biochemistry. 2008 Apr 15;47(15):4461–8.

Wang X, Culotta VC, Klee CB. Superoxide dismutase protects calcineurin from inactivation. Nature. 1996 Oct 3;383(6599):434–7.

Wang Y, De Keulenaer GW, Weinberg EO, Muangman S, Gualberto A, Landschulz KT, et al. Direct biomechanical induction of endogenous calcineurin inhibitor Down Syndrome Critical Region-1 in cardiac myocytes. Am. J. Physiol. Heart Circ. Physiol. 2002 Aug;283(2):H533–9.

White PJ, Broadley MR. Calcium in plants. Ann. Bot. 2003 Oct;92(4):487–511.

Wiesenberger G, Steinleitner K, Malli R, Graier WF, Vormann J, Schweyen RJ, et al. Mg2+ deprivation elicits rapid Ca2+ uptake and activates Ca2+/calcineurin signaling in Saccharomyces cerevisiae. Eukaryotic Cell. 2007 Apr;6(4):592–9. PMCID: PMC1865649

Yamashita T. Ca2+-dependent regulation of synaptic vesicle endocytosis. Neurosci. Res. 2012 May;73(1):1–7.

Yang J, Rothermel B, Vega RB, Frey N, McKinsey TA, Olson EN, et al. Independent signals control expression of the calcineurin inhibitory proteins MCIP1 and MCIP2 in striated muscles. Circ. Res. 2000 Dec 8;87(12):E61–8.

Yáñez M, Gil-Longo J, Campos-Toimil M. Calcium binding proteins. Adv. Exp. Med. Biol. 2012;740:461–82.

Yoshimoto H, Saltsman K, Gasch AP, Li HX, Ogawa N, Botstein D, et al. Genome-wide analysis of gene expression regulated by the calcineurin/Crz1p

signaling pathway in Saccharomyces cerevisiae. J. Biol. Chem. 2002 Aug 23;277(34):31079–88.

Yu D-Y, Tong L, Song G-J, Lin W-L, Zhang L-Q, Bai W, et al. Tau binds both subunits of calcineurin, and binding is impaired by calmodulin. Biochim. Biophys. Acta. 2008 Dec;1783(12):2255–61.

Zaidi NF, Thomson EE, Choi E-K, Buxbaum JD, Wasco W. Intracellular calcium modulates the nuclear translocation of calsenilin. J. Neurochem. 2004 May;89(3):593–601.

Zhang N, Dudgeon DD, Paliwal S, Levchenko A, Grote E, Cunningham KW. Multiple signaling pathways regulate yeast cell death during the response to mating pheromones. Mol. Biol. Cell. 2006 Aug;17(8):3409–22. PMCID: PMC1525234

Zhou X-L, Batiza AF, Loukin SH, Palmer CP, Kung C, Saimi Y. The transient receptor potential channel on the yeast vacuole is mechanosensitive. Proc. Natl. Acad. Sci. U.S.A. 2003 Jun 10;100(12):7105–10. PMCID: PMC165837

TOVAH HONOR ARONIN

Tovah.Aronin@gmail.com • 443-928-4746

https://www.linkedin.com/in/TovahAronin

EDUCATION

Ph.D. in Biology Aug. 2006 - Jan. 2016

Johns Hopkins University, Baltimore, MD

Dissertation title: Imaging Calcineurin Dynamics in Yeast: Development and Application of a Novel Probe for Calcineurin Activity

None-degree coursework Aug. 2005 - June 2006

The Convervative Yeshiva in Jersusalem, Jerusalem, Israel

Subjects: Talmud, Bible, Midrash, Hebrew Language

B.S. in Biology Aug. 2001 - May 2005

Brandeis University, Waltham, MA

Cum laude

Minor in Mathematics

Senior Thesis, Highest Honors: Gold-binding by Metallothionein *in vitro*

RESEARCH EXPERIENCE

Graduate Research Assistant June 2007 - Jan. 2016

Lab of Kyle Cunningham, Johns Hopkins University

Designed, executed and documented research developing a new probe for calcineurin activity and using that probe to investigate the effects of four genes on calcineurin activity in three conditions.

Undergraduate Research Assistant Oct. 2002 - May 2005

Lab of David DeRosier, Brandeis University

Planned, conducted and presented research investigating the possible use of metallothionein as a label for electron microscopy.

FELLOWSHIPS

Nanotechonogy for Biology and Medicine Graduate Training Program, Institute for NanoBioTechnology, Johns Hopkins University and Howard Hughes Medical Institute

Included courses in Nanomaterials and Cell Biology, a NanoBio lab course, and an interdisciplinary journal club including engineering, physics, chemistry, and biology

Howard Hughes Undergraduate Summer Fellowship

Completed an independent research project

PRESENTATIONS

Oral presentations:

Aronin, T.H. and Cunningham, K.W. Imaging Calcim Dynamics. *Johns Hopkins Yeast Club*, Johns Hopkins School of Medicine, Baltimore, MD. Nov. 2011

Aronin, T.H. and Cunningham, K.W. Feedback Controls in the Calcium Signaling Network: Calcineurin and Crz1. *Johns Hopkins Yeast Club*, Johns Hopkins School of Medicine, Baltimore, MD. Nov. 2009

Poster presentations:

Aronin, T.H. and Cunningham, K.W. Imaging Calcium Dynamics in Yeast. *Johns Hopkins University Graduate Program in Cell, Molecular, and Developmental Biology and Biophysics Department Retreat*, St. Michael's, MD. Oct. 2011

Aronin, T.H. , van Dyk, D., Andrews, B., and Cunningham, K.W. Identifying Potential Calcium Influx Pathways in Yeast. *Yeast Cell Biology Meeting*, Cold Spring Harbor Laboratory, NY. Aug. 2009

Aronin, T.H. and Cunningham, K.W. Identifying Potential Calcium Influx Pathways in Yeast. *Symposium on Nanoscience for Neuroscience and Neurosurgery*, Johns Hopkins Institute for NanoBioTechonology, Baltimore, MD. May 2009

TEACHING EXPERIENCE

Teaching Assistant

Johns Hopkins University, Dept. of Biology

Genetics (Lecture only) Fall 2012

Instructors: Dr. Kyle W. Cunningham, Dr. M. Andrew Hoyt

Introduction to the Human Brain (Lecture) Spring 2012, 2011, 2010

Instructor: Dr. Ed Hedgecock

Advanced Cell Biology (Lecture) Fall 2011, 2010, 2009

Instructors: Dr. Kyle W. Cunningham, Dr. Beverly Wendland, Dr. Trina Schroer, Dr. Steve Farber, Dr. M. Andrew Hoyt, Dr. Haiqing Zhao

Cell Biology (Lecture and Laboratory) Spring 2008

Instructors: Dr. Beverly Wendland, Dr. Trina Schroer, Dr. Robert Horner

Genetics (Lecture and Laboratory) Fall 2007

Instructors: Dr. Kyle W. Cunningham, Dr. M. Andrew Hoyt, Dr. Beatrice Kondo

Graded exams and assignments, held office hours, guided the selection of topics for term papers, and guided laboratory experiments from set-up to analysis.

REFERENCES

Dr. Kyle Cunningham, Johns Hopkins University, kwc@jhu.edu, 410-516-7844

Dr. Elana Fertig, Johns Hopkins University, ejfertig@jhmi.edu, 301-801-0138

Mary Spiro, Johns Hopkins University Institute for NanoBioTechnology, mspiro@jhu.edu, 410-516-4802